



Grassland soil moisture utilising Sentinel 2 imagery and agricultural applications

Title	Grassland soil moisture utilising Sentinel 2 imagery and agricultural applications
Author(s)	Basu, Rumia
Publication Date	2024-06-12
Publisher	University of Galway



OLLSCOIL NA GAILLIMHÉ
UNIVERSITY OF GALWAY

Grassland soil moisture utilising Sentinel 2 imagery and agricultural applications

Rumia Basu

B.Sc., M.Sc.

A thesis submitted for the degree of doctor of philosophy to the

University of Galway, Ireland

Supervisors

Dr. Eve Daly, Earth and Ocean Sciences, School of Natural Sciences,
University of Galway

Dr. Patrick Tuohy, Animal & Grassland Research and Innovation Centre,
Teagasc, Moorepark

February 2024



Table of Contents

Table of Contents.....	i
List of Figures.....	iv
List of Tables.....	vii
Declaration.....	viii
Acknowledgements.....	ix
Abstract.....	xi
Chapter1. Introduction.....	1
1.1 What is Soil Moisture?.....	1
1.2 Soil Moisture and climate change.....	3
1.3 Soil Moisture and agriculture.....	4
1.4 Soil Moisture and Irish agriculture.....	5
1.5 Measurement of Soil Moisture.....	6
1.5.1 In-situ and laboratory measurement of Soil Moisture.....	7
1.5.2 Remote sensing of Soil Moisture.....	12
1.5.3 Measurement of Soil Moisture in Ireland.....	15
1.6 Basic Concepts.....	16
1.6.1 Enhanced Vegetation Index (EVI) for soil moisture estimation.....	16
1.6.2 Richard’s Equation.....	17
1.7 Aim of research.....	17
1.8 Summary of chapters.....	18
Chapter 2: Temporal Stability of Grassland Soil Moisture Utilising Sentinel-2 Satellites and Sparse Ground-Based Sensor Networks.....	19
2.1 Abstract.....	19
2.2 Introduction.....	20
2.3 Data and Methods.....	23
2.3.1 Study Area.....	23
2.3.2 Satellite and In Situ data.....	25
2.3.3 OPTRAM Basics.....	26
2.3.4 Relationships between VSM and nSSM.....	28
2.3.5 Considerations for Implementing OPTRAM.....	31
2.3.6 Temporal Stability (TS) Metrics.....	33
2.4 Results.....	34

2.4.1 Satellite and VSM Data.....	34
2.4.2 Choice of Vegetation Index	37
2.4.3 Fitting of Edge Curves	37
2.4.4 Relationships between Satellite and In Situ Sensor Soil Moisture	39
2.4.5 Maps of nSSM	40
2.4.6 Temporal Stability of nSSM	41
2.5 Discussion.....	43
2.5.1 Edge Curves and Vegetation Index.....	43
2.5.2 Variable Vegetation Cover and Soil Moisture	45
2.5.3 Time-Delayed VSM and nSSM	45
2.5.4 Satellite-Derived Surface Moisture TS for Land-Use Management.....	47
2.6 Conclusion	50
Chapter 3: Identifying favourable conditions for farm scale trafficability and grass growth using a combined Sentinel-2 and soil moisture deficit approach	52
3.1 Abstract.....	52
3.2 Introduction.....	53
3.3 Materials and Methods.....	56
3.3.1 Study Area	56
3.3.2 Satellite and in-situ data for estimation and validation of normalised surface soil moisture (nSSM).....	57
3.3.3 OPTRAM.....	58
3.3.4 Soil Moisture Deficit (SMD)	60
3.3.5 Development of optimal thresholds using nSSM and SMD	61
3.3.6 Calculation of proportion of farm area within the optimum category at a daily time step ..	63
3.4 Results.....	63
3.4.1 Optimal threshold range for nSSM	63
3.4.2 Spatial and temporal patterns of nSSM on the farm	64
3.4.3 Relationship between proportion of farm area in the optimum category and SMD	66
3.5 Discussion.....	69
3.5.1 Overall advantage of using optimal nSSM thresholds ranges over SMD alone	69
3.5.2 Future Research.....	71
3.6 Conclusion	74
Chapter 4: Retrospective examination of fertilizer application decisions on a heavy textured dairy farm using paddock specific management records, in-situ weather and soil moisture threshold maps	76
4.1 Abstract.....	76
4.2 Introduction.....	77
4.3 Materials and Methods.....	79

4.3.1 Study Area	79
4.3.2 Data collation for fertiliser application, associated moisture status of the soil and rainfall.	81
4.3.3 Development of SMT maps	81
4.3.4 Proportion of farm area in the favourable nSSM category	83
4.3.5 Data analysis	84
4.4 Results	84
4.4.1 Fertiliser application timing	84
4.4.2 Soil and rainfall conditions for fertiliser application dates	85
4.4.3 Fertiliser application dates with respect to favourable soil and crop conditions.....	89
4.5 Discussion	91
4.5.1 Insights into N application and probable consequences	91
4.5.2 Future work	93
4.6 Conclusion	94
Chapter 5: Discussion and Conclusion	96
5.1 Discussion	96
5.2 Highlights.....	96
5.2.1. Optical Trapezoid Model	96
5.2.2. Temporal Stability of soil moisture	98
5.2.3. Farm and nutrient management using the concept of nSSM and SMD.....	98
5.3 Future work.....	99
5.4 Conclusion	100
List of References	102
Appendix.....	120
Summary of Research Outputs	122
Journal Publications:.....	122
Conferences:	123
Other science communications:	123
Paper acknowledgements.....	124

List of Figures

Figure 1.1. 1: Representation of soil moisture in a soil column (adapted from Seneviratne et al.(2010)).....	2
Figure 1.5. 1: Diagrammatic representation of in-situ and satellite estimation of soil moisture. Note: figure is not to scale and is not exhaustive.....	7
Figure 2.3. 1: Locations of (a) Rossmore and (b) Stradone sites. Yellow polygons indicate zones of forests and water bodies excluded from the analysis. Note the different scales for each area. Background imagery from Google Earth.....	25
Figure 2.3. 2: Idealised representation of OPTRAM STR-VI scatter plot. The blue line represents the (saturated) wet edge, the black line represents the dry edge and red dots represent STR-VI couplets allocated to VI bins of width 0.01 and STR bins of height 0.01 multiplied by the range of STR.....	28
Figure 2.4. 1: (a) VSM and (b) daily rainfall and evapotranspiration for Rossmore; (c, d) equivalent time series for Stradone. Vertical lines date S-2 observations since the installation of the network. Stra1, Stra3 and Stra5 VSM sensors record values > saturated VSM after high rainfall/low ET events, indicating over-saturated conditions with free water at the surface. ET peaks and VSM is at its minimum in mid-summer (July); cumulative rainfall is higher in winter (October–March) than summer.....	36
Figure 2.4. 2: STR-EVI scatter plots. (a) Rossmore without land cover masks; (b) Rossmore with land cover masks; (c) Stradone without land cover masks; and (d) Stradone with land cover masks.....	38
Figure 2.4. 3: Scatter plots of STR-VI with land cover masks at each site. (a) Rossmore STR-MSAVI, (b) Stradone STR-MSAVI, (c) Rossmore STR-NDVI, (d) Stradone STR-NDVI, (e) Rossmore STR-NDREI, (f) Stradone STR-NDREI.....	39
Figure 2.4. 4: Correlations between VSM and nSSM for the two farm sites. Each circle corresponds to a sensor reading. The S-2 data that did not meet the conditions of drying (Section 2.5.4), i.e., during a period with an increase in VSM, were excluded from the regression (blue circles). The absolute differences in the means (MD m^3/m^3), the unbiased Root Mean Square Deviations (m^3/m^3) and Percent Bias (PB) between the predicted VSM and observed VSM are, respectively, (a) 0.001, 0.05 and 0.23, (b) 0.003, 0.06 and -1.25, (c) 0.001, 0.06 and 0.19, (d) 0.003, 0.06 and -0.96. The MD and PB between the predicted and observed VSM are insignificant in the limited range of $0.1 < nSSM < 0.5$	40

Figure 2.4. 5: nSSM maps for Rossmore for (a) high NWF and (b) low NWF, and Stradone for (c) high NWF and (d) low NWF. White areas are exclusion zones. Co-ordinates are in meters in the Irish Transverse Mercator (ITM) projection.41

Figure 2.4. 6: Temporal Stability for Rossmore (a) \hat{W} and (b) σ , and Stradone (c) \hat{W} and (d) σ . Farm boundaries shown by solid black lines. White areas are exclusion zones. Co-ordinates are in meters in the Irish Transverse Mercator (ITM) projection.42

Figure 2.4. 7: Median Relative Difference, \hat{W} , Median Absolute Deviation Relative Difference, σ , and Great Soil Groups for the two farm sites. (a) Rossmore \hat{W} , (b) Rossmore σ , (c) Rossmore Great Soil Groups, (d) Stradone \hat{W} , (e) Stradone σ , (f) Stradone Great Soil Groups. Numbers refer to areas discussed in the text.43

Figure 3.3. 1: (A) Study area is within the orange polygon (B) paddock boundaries and paddock drainage class distribution in the study area i.e. orange paddocks are poorly drained and white paddocks are well drained57

Figure 3.4. 1: Linear regression between SMD and mean nSSM for (A) poorly drained and (B) well drained soils.64

Figure 3.4. 2: Example of nSSM maps for negative, ~0, optimum category and positive SMD. Green regions represent soil in the “optimum” category, blue regions represent wetter than optimum conditions and red region represent drier than optimum conditions. Units of SMD are in mm.65

Figure 3.4. 3: (A) Proportion of farm area in the optimum category of nSSM.(B) Proportion of farm area in the drier and wetter than optimum category. Note: Dashed lines are the piecewise regression model between the variables.....66

Figure 3.4. 4: Daily estimates of farm area proportions (%) in the optimum nSSM category between 2017 and 2021, calculated using the piecewise regression function between nSSM and SMD.68

Figure 3.4. 5: (A) Monthly mean proportions of farm area in the optimum nSSM category from January-June of the time-series, (B) Monthly mean proportions of farm area in the optimum nSSM category from July-December of the time-series (C) Monthly mean proportions of farm area in the optimum nSSM category for the year 2018.68

Figure 4.3. 1: Paddocks on the study farm with locations of the weather station and soil moisture sensors. Red paddocks are poorly drained and blue paddocks are well drained. The white triangle shows the weather station on the farm and yellow crosses are the in-situ soil moisture sensors. Paddocks 9 and 10 are the focus of this study. 80

Figure 4.3. 2: Linear regression between mean normalised surface soil moisture (nSSM) and Soil Moisture Deficit (SMD) for the study farm. 83

Figure 4.3. 3: Piecewise linear regression model fitted between proportions of paddock area in the optimum/favourable nSSM category and corresponding SMD values for paddocks 9 and 10. 84

Figure 4.4. 1: Paddock area proportions in the favourable nSSM category compared with N applied for a) paddock 9 and b) paddock 10. Filled circles represent dates when rainfall for the 48-hour period after N application was less than 5 mm, squares represent rainfall between 5-10mm and inverted triangles represent rainfall greater than 10 mm.91

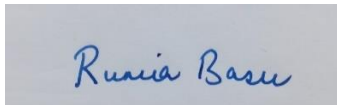
Figure A 1: Flowchart of methodology (Chapter 3) 121

List of Tables

Table 1.1. 1: Saturated and residual soil moisture values for different soil types. Note: Sand (includes sandy loam, loamy sand and sandy clay loam), Clay (includes sandy clay, silty clay and silty clay loam), Silt (includes silty loam) (Adapted from (Schaap and Leij, 2000))	3
Table 1.5. 1: Sentinel 2 bands with wavelength and pixel resolution.....	13
Table 1.5. 2: Common in-situ and RS techniques of soil moisture measurement (Babaeian et al., 2019a; Franz et al., 2012b; Rasheed et al., 2022)	14
Table 1.6. 1: Vegetation indices from band <i>B</i> in Sentinel 2 optical bands.....	16
Table 2.4. 1: Laboratory measurements of soil samples around sensors at the two sites. The measurement uncertainties are $<\pm 0.02 \text{ m}^3/\text{m}^3$. Ross = Rossmore, Stra = Stradone.	35
Table 2.4. 2: Distance correlation coefficient <i>dcor</i> and Spearman's rank correlation coefficient <i>ρcor</i> (in brackets) between STR and VIs for Rossmore (lower triangle with orange background) and Stradone (upper triangle with blue background). Coefficients are for data that have been masked to remove exclusion zones.	37
Table 3.4. 1: SMD values and farm area proportions (%) within the identified nSSM categories.	75
Table 4.4. 1: Date of N application and associated soil and rainfall conditions for paddock 9. Blue colour represents waterlogged conditions (SMD less than 0 mm), green colour represents SMD between 10-50 mm and red colour represents SMD greater than 50 mm.....	88
Table 4.4. 2: Date of N application and associated soil and rainfall conditions for paddock 10. Blue colour represents waterlogged conditions (SMD <0mm), green colour represents SMD between 10-50mm, yellow colour represents SMD between 0-10mm and red colour represents SMD greater than 50 mm.	88
Table A 1: All S-2 passes for Rossmore and Stradone used in the study. Dates in bold are those used in the validation with in situ VSM sensors	120

Declaration

I, Rumia Basu, declare that the work presented in this thesis is my own work and that it has not been used to obtain any other form of degree in this University or elsewhere. To the best of my knowledge and belief, the thesis contains no material previously published or written by another person except where due reference is made in the thesis itself.



Rumia Basu

Acknowledgements

A PhD is the culmination of years of hard work and determination, interspersed with successes and failures. I would first of all like to express my sincere gratitude towards my supervisors Dr. Eve Daly and Dr. Patrick Tuohy for giving me the opportunity to work on this project. They were always actively involved in my research, providing timely and valuable inputs and most importantly acting as mentors throughout, telling me to keep my “chin up” in every situation. I would also like to thank Prof. Colin Brown for helping me develop ideas for this thesis. The engaging discussions that I had with him made me think harder and come up with better outcomes that helped shape this thesis. My eternal thanks also go to Prof. Owen Fenton for his ideas and timely inputs on the manuscripts. He was available for discussions and his encouraging words helped me sail through. He helped me see the larger picture, especially during the final stages of this journey.

I would also like to thank the four members of my GRC committee, Dr Tiernan Henry, Prof. Mark Healy, Prof. Aaron Golden and Prof. Peter Croot. Our yearly meetings helped me be on time and their valuable inputs improved my research. Their friendly interactions made an otherwise tense yearly review relaxed.

I would also like to thank my “PhD friends” from Earth and Ocean Sciences in University of Galway, for making this journey enjoyable. Dave, Hilary, Celine, Ciara, Isuri- a big shout out to you guys for always being around. Thank you for listening to my rants and always coming up with just the right words to cheer me up. It helps to know that there are others who understand your situation. I will always cherish our dinner dates and walks through “shop street”.

I would also like to thank SFI and VistaMilk SFI Research Centre, Teagasc for providing the funding for this PhD. A special thanks to Dr. Donagh Berry, Director, Vista Milk, for giving

me the opportunity to participate in various outreach and science communication activities. These experiences will help me throughout my career.

To my friends and family, this PhD belongs to each one of you. My parents, for being my biggest source of strength and support, especially my mother who right from my childhood encouraged me to dream big and gave me the courage to chase my dreams. My father for being the greatest listener. A big thank you to my elder sister, Sonali, for being the best sibling ever. She has been my biggest cheerleader and always had my back. My niece, Aalina, for making me famous as a “scientist” even before I became one. I hope I have made her proud. A big thank you to my best friend, Dr. Panchali Bhattacharya. Having gone through the journey of a PhD herself, she encouraged me to move towards the finish line slowly each day. She became my sunshine during some of the darkest days. This PhD belongs to you too. I would also like to express my heartfelt gratitude to Dr. Bani Roy, my Chemistry professor in college who encouraged me to keep going and gave the best pieces of advice throughout this journey.

And finally, the biggest gratitude to my husband, Dr. Gourav Misra. It is because of his unflinching support that I was able to finish this PhD. He encouraged me and believed in my dreams, even when at times, I was unsure. Being from a similar field of study, his inputs helped shaped my ideas and this thesis better.

Abstract

Soil moisture is an essential climate variable that affects the climate system through its impact on evapotranspiration, which in turn affects, land, water and energy balances as these are coupled through evapotranspiration. At the surface, soil moisture controls the partitioning of incoming solar energy into latent and sensible heat fluxes, which affects the water and energy cycles. Additionally, soil moisture is also linked to biogeochemical cycles such as the carbon and nitrogen cycles through plant transpiration and photosynthesis. It is especially significant for agriculture and farm management. Information on soil moisture at high spatial and temporal resolution is crucial for an overall management of land and water resources. In this thesis, Sentinel-2 data was used to estimate normalised surface soil moisture (nSSM) at a high spatial resolution of 10 m for two Irish farms using a modified Optical Trapezoid Model (OPTRAM). These farms are dominated by soils that are poorly draining, remaining wet for large parts of the year and the major crop is grass. The modelled nSSM was validated against in-situ volumetric soil moisture data from sensors. Two applications were developed for farm management whereby, a) a proof of concept was developed for an improved decision support system using the concept of soil moisture deficit and nSSM safeguarding both soil and crop health and b) Nitrogen fertiliser application was analysed using high resolution soil moisture threshold maps and weather data suggesting that soil moisture should be considered an important variable for framing rules and policies around nutrient management. The methodology developed in this thesis can be applied globally for precision agriculture strategies and serves as an important starting point for application on other land cover categories.

Chapter1. Introduction

1.1 What is Soil Moisture?

Soil moisture or soil water content can be defined as the water present in the top 0-2m of the soil. It was recognised as an Essential Climate Variable (ECV) in 2010 (ESA, 2010; GCOS, 2020) and plays an important role in the environment and climate system through atmospheric feedback, governing crucial land-atmospheric processes such as infiltration, evaporation and run-off (Rasheed et al., 2022) at the local, regional and global scales (Seneviratne et al., 2010). There are many ways of defining and measuring soil moisture and these definitions can change depending on the context. A few popular definitions and terms are discussed here.

Soil moisture is often defined with respect to a given volume of soil measured in $\text{m}^3_{\text{water}} / \text{m}^3_{\text{soil}}$, known as volumetric water content. Soil moisture differs for different soil volumes because it is not homogeneously distributed vertically and horizontally in the soil (Seneviratne et al., 2010). The maximum volumetric soil moisture in a given volume of soil is known as the saturation soil moisture or the water holding capacity of soil, when all pore spaces are filled with water (University of Minnesota Extension, 2021). Residual soil moisture is defined as the moisture content present under dry conditions because it is impossible to achieve completely dry out soil (Babaeian et al., 2019a). Field capacity (FC) is the water remaining in the soil after natural drainage following a rainfall or irrigation event. At FC, the pore spaces in soil contain both water and air and it depends on the soil type. For example, at FC, a sandy soil may have only 5 or 10% volumetric water, while a clayey soil can have 50% volumetric water (Campbell, 2015; Kirkham, 2005). Permanent wilting point (WP) is defined as the point where the soil still contain some water but the plants cannot extract this water and at this point most plants die (Rai et al., 2017). For sandy soils, the WP could be 2% volumetric water content , while that

for clayey could be 20% volumetric water (Kirkham, 2005). WP is a good approximation for residual soil moisture in sandy soils, however, in clayey soils, there may be water present below WP (Kirkham, 2014). Plant available water (AW) or the allowable water holding capacity is the difference between FC and WP and this is the maximum water available to plants. AW for sandy soils is around 3% volumetric water and for clayey soils, it is around 30% volumetric water (Kirkham, 2005; Seneviratne et al., 2010). Another concept related to AW is that of allowable depletion. It is defined as the fraction of AW that is allowed to be used before commencing irrigation (Devine and O’Geen, 2019). For most crops and soil textures, allowable depletion corresponds to about 50% of AW (Hanson et al., 2000). Soil water tension (SWT) is also used to measure the wetness or dryness of soils and is defined as the force needed by plants to extract water from the soil. The drier the soil, higher is the SWT and vice-versa. Figure 1.1.1 below is a representation of the different soil moisture status in a column of soil.

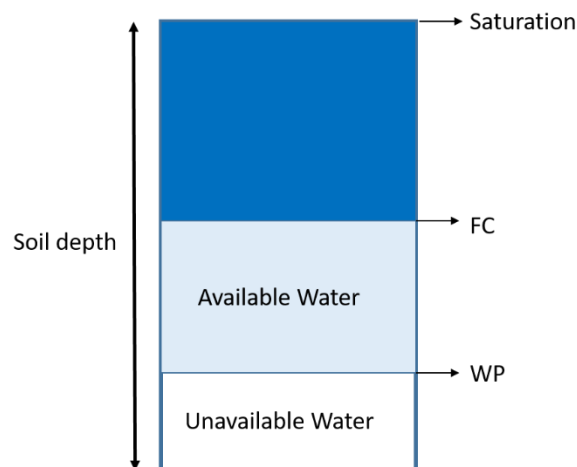


Figure 1.1. 1: Representation of soil moisture in a soil column (adapted from Seneviratne et al.(2010))

Table 1.1.1 below shows saturated and residual soil moisture values as per Schaap and Leij (2000). These values were found to be similar for Irish soils (Environmental Protection Agency Ireland, 2014).

Table 1.1. 1: Saturated and residual soil moisture values for different soil types. Note: Sand (includes sandy loam, loamy sand and sandy clay loam), Clay (includes sandy clay, silty clay and silty clay loam), Silt (includes silty loam) (Adapted from (Schaap and Leij, 2000))

Soil Type	Saturated soil moisture (m ³ /m ³)	Residual soil moisture (m ³ /m ³)
Sand	0.396	0.052
Loam	0.512	0.056
Silt	0.428	0.031
Clay	0.512	0.098

1.2 Soil Moisture and climate change

Soil moisture affects global climate by influencing the precipitation-evapotranspiration cycle and feedbacks (Zhou et al., 2021). A deficit in soil moisture can result in droughts (Wang et al., 2011), or an increase in the number of hot days in a region's hottest month resulting from a deficit in soil moisture due to decreased precipitation (Mueller and Seneviratne, 2012). Alternatively, saturated soils with surplus soil moisture can result in floods due to more discharge after precipitation (Yu et al., 2023). Alternatively prolonged periods of drought can also result in decreased soil moisture conditions (Ribeiro et al., 2021). Soil Moisture is also a governing factor in deciding soil's ability to act as a carbon source or sink, such that very high or very low soil moisture can increase organic carbon accumulation by reducing microbial activity (Rodrigues et al., 2023). On grassland fertilised soils, soil moisture is a major controlling factor for carbon dioxide (CO₂), nitrous oxide (N₂O) and methane(CH₄) fluxes (da Silva Cardoso et al., 2020), which in turn has effects on nutrient utilisation and the environment.

According to IPCC AR6 (IPCC 6th Assessment report, 2023), soil moisture is driven by changes in evapotranspiration (ET), precipitation and also irrigation. Such changes would alter the water balance by affecting infiltration and discharge and ultimately the change in soil moisture storage (change in storage = infiltration-discharge). Regional trends of satellite derived estimates of soil moisture reveal annual variation of up to $\pm 20\%$ across the globe between late 1970s and late 2010 and it does not always follow the regime of “wet getting wetter, dry getting drier”. The drier areas are primarily located in southeast North America, North Africa, southwest Europe, central Asia and Australia. The wetter areas are majorly located in North America, Northern Europe and Southeast Asia (Feng and Zhang, 2015).

1.3 Soil Moisture and agriculture

The agricultural sector uses 70 % of the world’s freshwater resources, being its largest consumer (IPCC 6th Assessment report, 2023; UN Water, 2022). Drought conditions in which soil moisture is low, can lead to decreased productivity, biomass and crop yields (Gałęzewski et al., 2021). The World Meteorological organisation defines drought as an extended dry period resulting from a lack of rainfall (World Meteorological Organisation, 2024). The Irish Meteorological Service (Met Eireann) defines meteorological drought as period of 15 days or more with less than 0.2mm rainfall on each day and agricultural drought as a period where the soil moisture deficit (SMD) exceeds 50 mm (Met Eireann, 2020). They are linked to low precipitation and dry soils (Qing et al., 2023). Similarly, excess surface soil moisture, with a probability of water logging on the surface can also lower crop (Champagne et al., 2019) and grass (Schulte et al., 2012) yields. Another way in which soil moisture impacts agriculture is through its effect on fertiliser or nutrient use efficiency. However, the effect of soil moisture on nutrient utilisation also depends on climatic conditions. For example, while nutrient absorption by crops and pastures is enhanced under high soil moisture conditions in Mediterranean and temperate climates (Chtouki et al., 2022; Pembleton et al., 2013), in Atlantic

climates such as in Ireland, excess soil moisture can lead to poor nutrient uptake and increased loss through run-off (Schulte et al., 2012). Additionally, when soil moisture exceeds that at FC, the pore spaces have less air leading to anoxic conditions which limits the rate of photosynthesis, thereby limiting crop growth (Schulte et al., 2012).

1.4 Soil Moisture and Irish agriculture

In Ireland, soil moisture conditions provide an interface between the agricultural sector and the environment through its controls on the grass growth rate, length of the growing season, nutrient uptake and therefore, the loss of nutrients to the environment (Schulte et al., 2005). Ireland has an Atlantic climate which is characterised by high precipitation, such that annual precipitation is higher than annual evapotranspiration (Schulte et al., 2012). Excess soil moisture is of particular concern here. This problem is exacerbated by the fact that 30% of Irish grasslands are composed of poorly draining or “heavy” soils (Teagasc, 2021a) that remain wet for long periods of time throughout the year and reach saturation (defined by SMD conditions in Ireland, such that at saturation $SMD = -10\text{mm}$) during rainfall. This negatively impacts the productivity and profitability on such farms due to shorter grazing seasons (Teagasc, 2021b). There is also risk of soil compaction on wetter soils such that compaction could be irreversible if the soil is trafficked close to the time of a rainfall event when the soil is saturated. This risk is lower on dry soils where the compaction occurs at the surface and gets naturally corrected. Similarly, at FC, compaction affects the top soil and can be reversed (Lepore et al., 2023; Teagasc, 2022). Ireland is primarily a grass based economy, with agriculture covering 67.6% of the total land cover, of which pasture land accounts for 55.1% (EPA, 2018). Other crops such as cereals and vegetables are mostly grown in South-East Ireland (Ireland Central Statistics Office, 2022). It is projected that with climate change, extended dry periods in Ireland will become more prevalent especially in the summer months (McGrath et al., 2023). This will be likely to cause a cohort of Irish farmers to resort to irrigation, with potato farmers already adopting targeted

irrigation (Teagasc, 2019). Thus, high-resolution spatial and temporal information on soil moisture would be imperative in Irish agriculture.

1.5 Measurement of Soil Moisture

Soil moisture can be categorised across multiple depth ranges. Water in the <10 cm depth profile of soil is referred to as surface or near-surface soil moisture, water stored in the plant-root zone (30-110 cm), is referred to as the root-zone soil moisture, and water in a zone that extends from the land surface to the unconfined groundwater table is the vadose zone soil moisture (Ahmadi et al., 2022; Babaeian et al., 2019). Soil moisture is expressed either in gravimetric (g/cm^3) or volumetric units (m^3/m^3) and also as a function of soil properties like WP and FC (Kerr, 2007). It is highly variable in space and time and can be measured across scales depending on the technique, from regional and global scale (1000s of km^2), to plot and field scale (100s m^2) using both in-situ instruments and satellites. Figure 1.5.1 is a representation of some of the in-situ instruments and satellites that are used to measure soil moisture. Soil moisture networks are being set up at catchment, regional and national scales (Cosh et al., 2021; Rosenbaum et al., 2012). The International Soil Moisture Network (ISMN) was established in 2009, funded by the European Space Agency (ESA) with the aim of being a central repository for all globally available in situ soil moisture measurements. Its existence is seen as essential in the validation and calibration of satellite based estimates of soil moisture (Al-Yaari et al., 2019). Through this network, all in situ soil moisture data (m^3/m^3), measured by different networks is made freely available through an open centralised web portal, in standardised units, sampling rates and advanced quality control at daily, hourly or some at even higher frequency intervals (Dorigo et al., 2021).

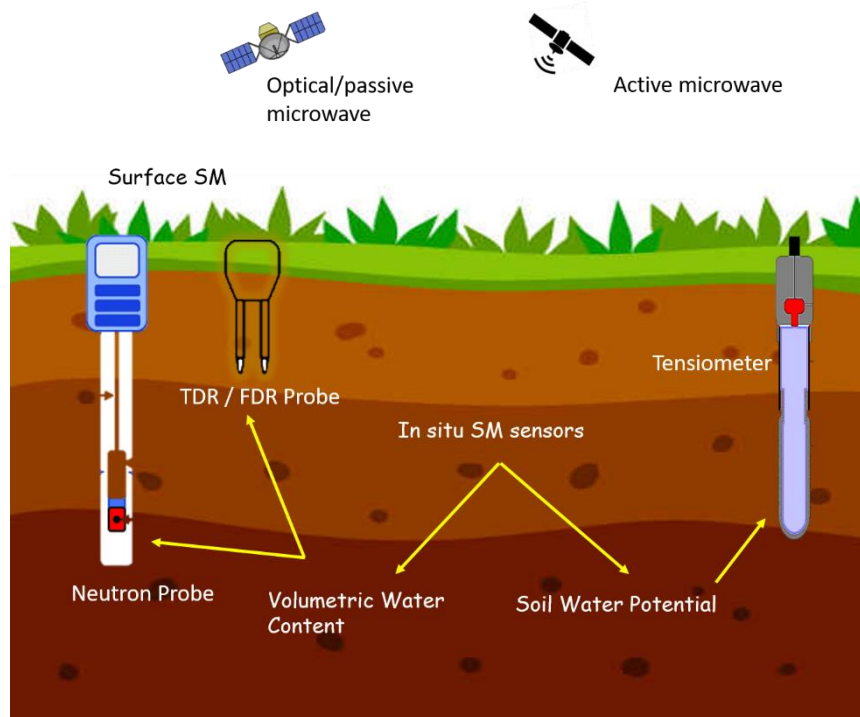


Figure 1.5. 1: Diagrammatic representation of in-situ and satellite estimation of soil moisture. Note: figure is not to scale and is not exhaustive.

1.5.1 In-situ and laboratory measurement of Soil Moisture

In situ techniques provide point based localised volumetric water content information. In in-situ or point based techniques, the instrument is placed in contact with the soil. These sensors can provide real time high resolution soil moisture information representative of the plot or field conditions and very useful for agricultural applications. Table 1.5.2 presents an overview of some of the popularly used in-situ methods of measuring soil moisture with their depth ranges and the type of soil moisture that each technique measures. In the following paragraphs, these methods are discussed in detail.

One of the most standard method of soil moisture measurement is the gravimetric method in which a known volume of a soil sample is weighed and oven dried at 105°C for 24 hours and re-weighed. The difference between the weights gives the amount of water present in soil that can be expressed in either gravimetric or volumetric units and is useful for calibration purposes.

Though being simple and highly accurate, this process is also time and labour intensive and cannot be repeated at the same sample location since it is damaging to the soil sample (Kashyap and Kumar, 2021; Walker et al., 2004). Another problem with this technique is the volatilisation of organic matter at high temperatures which may also account for the weight loss apart from evaporation of water and therefore the true amount of soil moisture may not be known (Susha Lekshmi et al., 2014). Calcium carbide technique is another way of measuring soil moisture in the laboratory, whereby the soil moisture content is determined by the measuring the gas pressure created as a result of the reaction between the soil moisture and calcium carbide (Susha Lekshmi et al., 2014).

The neutron probe or neutron scattering method is a very widespread method for volumetric soil moisture measurements as mentioned in Table 1.5.1. It was first introduced by Brunner and Mardock (1946) and uses the property of the hydrogen molecules to reduce the speed of neutrons (Babaeian et al., 2019a; Kashyap and Kumar, 2021). Neutron probes are widely used for agriculture and forestry applications. In this method, high energy neutrons are scattered into the soil using a radioactive source (radium-beryllium, americium-beryllium) such that the neutrons collide with the hydrogen molecule in the soil water, are slowed down and thermalized (Mukhlisin et al., 2021). The neutrons are captured on a detector and the measurements from the probes can be calibrated to represent the soil moisture content (Kashyap and Kumar, 2021; Rasheed et al., 2022). This technique is highly accurate, fast (response time of 1-2 minutes), can measure soil moisture at different depths and less dependent on soil temperature and salinity (Kashyap and Kumar, 2021; Rasheed et al., 2022). The biggest advantage of this technique is that it can measure soil moisture at the field scale at an hourly resolution (Bogena et al., 2015). However, this method also has several disadvantages like coarse spatial resolution, adverse health effects due to radiation exposure, cost intensive etc. (Rasheed et al., 2022). Additionally, in humid climates and woody regions, this method yields volumetric soil

moisture values that exceeds the soil porosity because it is influenced by other sources of water in these regions such as atmospheric water vapour and water content in the organic matter etc.(Babaeian et al., 2019a). Adjustments have since been made to correct for these effects by Franz et al. (2012) and Bogena et al. (2013). Lv et al. (2014) used Cosmic Ray Neutron Probe (CRNP) to measure soil moisture in a heterogeneous forest with and RSME of $0.011 \text{ m}^3/\text{m}^3$ and high correlation (R^2) of 0.97 with measurements from other in situ data. Neutron probe networks have been established at large scales and there are 194 permanent CRNP stations across the world (Babaeian et al., 2019a; Bogena et al., 2015).

Time Domain Reflectometry (TDR) was first introduced by Topp et al. (1980) to measure soil moisture. In this method, a high frequency electromagnetic signal is transmitted through the soil and its velocity is measured by TDR. The velocity is dependent on the dielectric constant which in turn is related to the soil moisture. TDR measures the volumetric water content and does not pose any health hazard. As mentioned in Table 1.5.1, this method can be used to measure volumetric soil moisture across different depths. Additionally, it does not require soil calibration and is independent of the soil texture and temperature, though it is an expensive instrument (Bhuyan et al., 2020; Mukhlisin et al., 2021; Rasheed et al., 2022). Another method similar to TDR is the Frequency Domain Reflectometry (FDR) which was first used for military applications (Mukhlisin et al., 2021). In this method an electromagnetic wave is transmitted through the soil along probes and the frequency of the reflected wave is recorded such that the oscillation frequency is inversely related to the soil moisture content (Guadalupe Ramos Hernández et al., 2019). This method measures the volumetric water content of soils based on their dielectric properties and is more sensitive towards dry soils, where the volumetric water content is less than 5% and performs better than TDR in case of soils with high salinity (Mukhlisin et al., 2021; Rasheed et al., 2022). Recently Chen et al. (2019) developed a method for calibration of FDR probes, taking into account the effect of temperature

on the measurement accuracy that resulted in a reduced Root Mean Square Error (RMSE) in measurements. Guadalupe Ramos Hernández et al. (2019) used a combination of TDR and FDR to study soil moisture and found that both techniques showed similar results after a depth of 10cm.

Gamma ray attenuation or gamma ray spectroscopy is a method to measure volumetric soil moisture based on the probability of interaction of gamma photons with the soil (Mukhlisin et al., 2021). This method measures the attenuation of gamma rays as it travels through the soil because the water in the soil is more effective in attenuating these rays as compared to the soil minerals (Filippucci et al., 2020; Mukhlisin et al., 2021). The depth up to which a gamma ray travels depends on the soil moisture content and soil density (Mukhlisin et al., 2021). It is a radioactive method that uses radio waves to measure soil moisture up to a depth of 25mm. Apart from being sensitive to surface soil moisture, this technique is also sensitive to the soil bulk density which is an important parameter of soil health (Rasheed et al., 2022). Some of the advantages of this technique is that it is fast, inexpensive, high resolution of a few millimetres (mm) and can measure temporal changes in the soil moisture content, though it is affected by soil salinity (Mukhlisin et al., 2021; Pires, 2018). However, its greatest advantage over other traditional methods is that being non-destructive it allows repeated measurements at the same location (Pires, 2018). Recently, Filippucci et al. (2020) used this method to track irrigation at the field scale and found that the gamma ray spectroscopy was very well correlated with irrigation events and was also sensitive to changes in soil moisture content. The disadvantage of this method includes high cost of instrument, sensitivity to thickness of soil and variations due to bulk density of soil (Rasheed et al., 2022).

Tensiometer is also an in situ instrument used to study the soil matric potential or soil water tension based on the principle of soil water suction (Rasheed et al., 2022) and can be used across a range of soil depths as shown in Table 1.5.2. This instrument mimics the behaviour of

plant roots and measures the tension/pressure with which water travels from the soil to the plant (Kashyap and Kumar, 2021). It is an indirect method of estimation of soil moisture content as it measures the amount of tension required to eliminate water from the soil (Hardie, 2020), is only sensitive to a very small range of soil moisture content and is destructive to the soil (Rasheed et al., 2022). Recently, Gaddikeri et al. (2022) used a tensiometer to study soil moisture at depths of 15 and 30 cm. A correlation of 0.72 and 0.71 was obtained between the tensiometer and gravimetric measurements for the two depths respectively.

These methods have the advantage of representing field conditions by being in contact with the soil. Techniques like TDR do not require any calibration and are unaffected by soil temperature or texture (Bhuyan et al., 2020; Rasheed et al., 2022). There may be differences in soil moisture values as measured through TDR for different soil types and textures due to difference in electrical properties.

However, limitations of these methods include high temperatures that can be damaging to the soil sample, or volatilization of organic compounds (produced by microorganisms in soils) or in case of gravimetric methods (Insam and Seewald, 2010; Susha Lekshmi et al., 2014). TDR is also an expensive instrument and does not function well in highly saline or clayey soils (Rasheed et al., 2022). FDR sensors have low accuracy due to the dependence on soil texture and soil temperature (Babaeian et al., 2019a). Tensiometers can capture only a very small amount of the available soil moisture and can result in an inaccurate estimation of wilting point for most crops (Rasheed et al., 2022). The point-based measurements are also likely to be affected by soil heterogeneity and can lead to misinterpretations especially in hydrological applications (Stevanato et al., 2019). Additionally, these methods are prone to errors and uncertainties which can arise due to soil salinity, loss of sensor contact with soil due to biological activity and calibration errors (Babaeian et al., 2019a). These methods cannot be used to capture spatial soil moisture dynamics over large areas as they are time and labour

intensive and can also be destructive to the study site and for reliable measurements, the heterogeneity of the study area would have to be considered even for a dense network of ground sensors. (Petropoulos et al., 2013).

1.5.2 Remote sensing of Soil Moisture

Remotely sensed soil moisture generally refers to surface soil moisture (few millimetres from optical and thermal remote sensing) ,near-surface soil moisture (few centimetres with microwave sensors) (Li et al. 2021). Remote Sensing (RS) techniques are able to overcome the aforementioned limitations of in-situ sensors and allow global observations of soil moisture, with higher accuracies (Zhuang et al., 2023) as they can produce spatio-temporal maps of surface soil moisture at varying resolutions, as compared to in-situ sensors, which lack spatial information.

RS of soil moisture relies on the premise that any variation in soil moisture is reflected in the corresponding electromagnetic response from the land cover on the ground, recorded at the sensor (Zhuang et al., 2023).

Many studies have used optical and thermal RS to estimate soil moisture across a wide range of spatial scales using Vegetation Indices (VI) and models. Two popularly used VIs for soil moisture estimation are discussed in section 1.6. Sensors such as Landsat (Foroughi et al., 2020; Wang et al., 2020) and MODIS (Khellouk et al., 2021; Xu et al., 2018) have been popularly used to estimate surface soil moisture. With the launch of Sentinel-2 satellites in 2015, it is now possible to obtain estimates of surface soil moisture at a higher spatial resolution of 10m (Ambrosone et al., 2020) as compared to MODIS or Landsat. Sentinel 2 is a high-resolution multispectral satellite launched in 2015 by the European Space Agency (ESA).It has 13 spectral bands of varying spatial resolutions (pixel-size) as shown in Table 1.5.1 below.

Table1.5. 1: Sentinel 2 bands with wavelength and pixel resolution

Sentinel 2 bands	Central Wavelength (nm)	Pixel Resolution (m)
Band 1 (aerosol)	443	20
Band 2 (blue)	490	10
Band 3 (green)	560	10
Band 4 (red)	665	10
Band 5 (red edge)	705	20
Band 6 (red edge)	740	20
Band 7 (red edge)	783	20
Band 8 (NIR)	842	10
Band 8a (red edge)	865	20
Band 9 (water vapour)	945	60
Band 10 (SWIR-cirrus cloud)	1375	60
Band 11 (SWIR)	1610	20
Band 12 (SWIR)	2190	20

A number of machine learning algorithms such as random forest, gradient boosting etc. have also been developed using optical data and is becoming increasingly popular for soil moisture retrievals (Acharya et al., 2022; Nguyen et al., 2022).

The resolution requirements of satellites for measuring soil moisture, however, depends on specific applications. Applications related to precision agriculture or targeted nutrient application and other farm management decision support tools may benefit from a higher

spatial resolution as compared to temporal resolution. In such scenarios, global and regional scale soil moisture maps may not suffice for farm scale applications, particularly in Ireland where the farms are small with an average size of 32.4 ha (Teagasc, 2017). Similarly, for hydrological applications that require information of root zone soil moisture and for validation of modelled soil moisture from satellites, in- situ sensors remain indispensable.

Though optical remote sensing provides opportunities for high resolution mapping of soil moisture in tens of metres, they cannot be operated in all weather conditions and are mostly affected by clouds. This is a huge problem in regions of high cloud cover such as Ireland. This limitation is overcome by microwave satellites such as Soil Moisture and Ocean Salinity (SMOS) (Kerr et al., 2010), Soil Moisture Active Passive (SMAP) (Entekhabi et al., 2010; Pandey et al., 2020) and Advanced Scatterometer (ASCAT) (Wagner et al., 2013), that have the advantage of operating in all weather conditions as they are unaffected by cloud or solar illumination. Spatial and temporal resolution of these sensors is coarse as compared to optical sensors, active radars have spatial resolution of around 100m while that for passive is much coarser (tens of kilometres) (Edokossi et al., 2020; Roberts et al., 2022; Wu et al., 2021) with the exception of Sentinel-1. Sentinel -1 synthetic aperture radar (SAR) satellites have been very popular in high resolution soil moisture estimation (Bhogapurapu et al., 2022), providing data at 10m spatial resolution. However, radar data is affected by speckle and needs to be resampled to coarse resolutions even with Sentinel-1 to reduce complexities in image interpretation (Bauer-Marschallinger et al., 2019). Another popular approach is the synergetic use of Sentinel-1 and 2 datasets (Tripathi and Tiwari, 2022; Zhuo et al., 2019). Table 1.5.2 presents an overview of some of the in situ and RS techniques of soil moisture measurement.

Table 1.5. 2: Common in-situ and RS techniques of soil moisture measurement (Babaeian et al., 2019a; Franz et al., 2012b; Rasheed et al., 2022)

Method	What it measures	Depth
--------	------------------	-------

Gravimetry	Gravimetric moisture	Any depth
Neutron probe	Volumetric moisture	Less than 30 cm
TDR	Volumetric moisture	30 – 60 cm/deeper with new sensors
Gamma ray attenuation	Volumetric moisture	2.5 cm
Tensiometer	Soil metric potential	15-60 cm
CNRS	Volumetric moisture	12 -70 cm
Optical and thermal RS	Surface soil moisture	A few mm from the surface
Microwave (active/passive radar)	Surface soil moisture	Top few (1-10 cm) from the surface, top 1-m with P-band radar

1.5.3 Measurement of Soil Moisture in Ireland

In Ireland, soil moisture is mostly expressed as Soil Moisture Deficit (SMD) using the hybrid model of Schulte et al., (2015), which is a measure of dryness/wetness of soil. Using this model, daily SMD is obtained using rainfall, ET and drainage data for farms as inputs. All advice regarding farming activities such as nutrient or slurry application, trafficability etc. are generated based on SMD conditions. However, there is a need for in-situ soil moisture measurements and to integrate these measurements with satellite observations of soil moisture to be able to produce high-resolution soil moisture maps both at the national and farm scale. Recently, the Irish Soil Moisture Observation Network (ISMON) was launched in 2021 for real-time VSM at the field scale (Finkele et al., 2022). The network consist of ten sites covering major soil types, climate regimes and land use classes in Ireland. Measurements are made using a network of TDR probes and Cosmic-Ray Neutron Sensors (CRNS).

1.6 Basic Concepts

1.6.1 Enhanced Vegetation Index (EVI) for soil moisture estimation

Soil moisture is related to vegetation structure and dynamics and there exists a positive feedback between vegetation and soil water content (D’Odorico et al., 2007). Though there exists a time lag between changes in soil moisture and subsequent vegetation response (Zhang et al., 2011), vegetation indices have been successfully used to estimate soil moisture because the vegetation water content changes with changing soil moisture conditions and this is reflected by vegetation indices. Normalised Difference Vegetation Index (NDVI) and Enhanced Vegetation Index (EVI) are two of the most popularly used vegetation indices to study soil moisture on a variety of land cover types including grasslands (Krishnan and Indu, 2023; Zhang et al., 2011). NDVI is calculated using red and NIR bands of the electromagnetic spectrum, while EVI uses an additional blue band and soil correction parameters to adjust for canopy reflectance and atmospheric scattering effects. It has been shown that EVI is better correlated to measured soil moisture over NDVI because unlike NDVI, EVI is less likely to saturate at high vegetation cover (Qiu et al., 2019). This study also used different vegetation indices to estimate soil moisture. Table 1.6.1 below shows the vegetation indices used in this study and their calculation (B refers to the specific Sentinel 2 band, the wavelengths have been mentioned in section 1.5.2).

Table 1.6. 1: Vegetation indices from band B in Sentinel 2 optical bands

Vegetation index	Equation
Normalised Difference Vegetation Index (NDVI)	$\frac{B_8 - B_4}{B_8 + B_4}$
Enhanced Vegetation Index (EVI)	$\frac{2.5(B_8 - B_4)}{B_8 + 6B_4 - 7.5B_2 + 1}$

Modified Soil Adjusted Vegetation Index (MSAVI)	$0.5\{2B_8 + 1 - [(2B_8 + 1)^2 - 8(B_8 - B_4)]^{0.5}\}$
Normalised Difference Red Edge Index (NDREI)	$\frac{B_8 - R_5}{B_8 + B_5}$

1.6.2 Richard's Equation

The Richard's equation is used to describe the flow of water through a porous unsaturated medium by the action of gravity and capillary action. It is a non-linear partial differential equation (Farthing and Ogden, 2017). Sadeghi et al. (2017b) obtained a simplified analytical solution to this equation using soil hydraulic functions to obtain root zone soil moisture from P band radar data. This thesis discusses the benefit of Richard's equation in improving the relationship between modelled and observed values of soil moisture for the study sites. Details about the equation are outlined in Chapter 2.

1.7 Aim of research

In order to develop farm level agricultural and management applications, information on high resolutions spatial and temporal variability of soil moisture is crucial and this information is currently missing in Ireland at the farm level. Additionally, soil moisture measurements and corresponding farm management advisory for Irish farms are based on SMD values, which provide temporal information only and lack spatial information about soil moisture variability. To address this research gap and to develop a proof of concept for an improved farm management decision support system, this thesis derived surface soil moisture from Sentinel-2 data for Irish farms at a high spatial resolution of 10m and developed proof of concept for two agricultural applications. Given the small size of Irish farms, the spatial resolution is appropriate for developing farm level management applications. The overall aim and objective of this thesis was to improve the understanding of soil moisture variations on Irish farms at a

high spatial resolution and use this knowledge to analyse farm decisions related to trafficability and nutrient application. The following outcomes were achieved:

- Developed a modified Optical Trapezoid Model (OPTRAM) for estimating satellite derived soil moisture at the farm level.
- Developed a threshold for surface soil moisture for safe trafficability and optimum grass growth on the farm using SMD thresholds and provided a proof of concept for an improved decision support tool for farmers.
- Combined these thresholds with nitrogen (N) application and weather data to analyse decisions regarding fertiliser application on Irish farms.

1.8 Summary of chapters

Chapter 2 deals with developing a modified OPTRAM for estimating surface soil moisture at the farm level using Sentinel-2 data and this is validated using in situ VSM data from sensors installed on the farms.

Chapter 3 highlights the problems of using a single value of SMD for generating advice on farm management and addresses this research gap by taking into account spatial variability of the soil moisture regime and defining thresholds in satellite derived soil moisture corresponding to literature based SMD thresholds for safe trafficability and optimum grass growth.

Chapter 4 deals with the problem of environmental degradation in Ireland through nutrient losses to the environment. It introduces the nitrate directive in Ireland and present scenarios and rules for application of nutrients on farms. This chapter follows from the proof of concept developed in Chapter 3 and applied the thresholds obtained in Chapter 3 for analysing decisions around nitrogen application on the farm.

Chapter 5 presents an overall discussion about the methods and applications developed in this thesis, the concluding remarks and highlights future work that this thesis can support.

Chapter 2: Temporal Stability of Grassland Soil Moisture Utilising Sentinel-2 Satellites and Sparse Ground-Based Sensor Networks

Rumia Basu ^{1,2}, Eve Daly ^{2,*}, Colin Brown ², Asaf Shnel ¹ and Patrick Tuohy ¹

¹VistaMilk, Teagasc Moorepark, Fermoy, P61 C996, Ireland; r.basu1@universityofgalway.ie (R.B.); asaf.shnel@teagasc.ie (A.S.); patrick.tuohy@teagasc.ie (P.T.)

²Earth and Ocean Sciences, School of Natural Sciences, University of Galway, Galway, H91 TK33, Ireland; colin.brown@universityofgalway.ie (C.B.)

*Correspondence: eve.daly@universityofgalway.ie (E.D.)

Accepted for publication in Remote Sensing **2024**, *16*(2), 20;
<https://doi.org/10.3390/rs16020220>

2.1 Abstract

Soil moisture is important for understanding climate, water resources, water storage, and land use management. This study used Sentinel-2 (S-2) satellite optical data to retrieve surface soil moisture at a 10 m scale on grassland sites with low hydraulic conductivity soil in a climate dominated by heavy rainfall. Soil moisture was estimated after modifying the Optical Trapezoidal Model to account for mixed land cover in such conditions. The method uses data from a short-wave infra-red band, which is sensitive to soil moisture, and four vegetation

indices from optical bands, which are sensitive to overlying vegetation. Scatter plots of these data from multiple, infrequent satellite passes are used to define the range of surface moisture conditions. The saturated and dry edges are clearly non-linear, regardless of the choice of vegetation index. Land cover masks are used to generate scatter plots from data only over grassland sites. The Enhanced Vegetation Index demonstrated advantages over other vegetation indices for surface moisture estimation over the entire range of grassland conditions. In poorly drained soils, the time lag between satellite surface moisture retrievals and in situ sensor soil moisture at depth must be part of the validation process. This was achieved by combining an approximate solution to the Richards' Equation, along with measurements of saturated and residual moisture from soil samples, to optimise the correlations between measurements from satellites and sensors at a 15 cm depth. Time lags of 2–4 days resulted in a reduction of the root mean square errors between volumetric soil moisture predicted from S-2 data and that measured by in situ sensors, from $\sim 0.1 \text{ m}^3/\text{m}^3$ to $< 0.06 \text{ m}^3/\text{m}^3$. The surface moisture results for two grassland sites were analysed using statistical concepts based upon the temporal stability of soil water content, an ideal framework for the intermittent Sentinel-2 data in conditions of persistent cloud cover. The analysis could discriminate between different natural drainages and surface soil textures in grassland areas and could identify sub-surface artificial drainage channels. The techniques are transferable for land-use and agricultural management in diverse environmental conditions without the need for extensive and expensive in situ sensor networks.

Keywords: soil moisture; temporal stability; remote sensing; agriculture; vegetation

2.2 Introduction

Soil moisture is an Essential Climate Variable (Global Climate Observing System, 2020). It is highly variable in space with scales ranging from centimetres to kilometres, and time scales

from minutes to years (Vereecken et al., 2014). It impacts the exchange of water, carbon and energy (Berg and Sheffield, 2018; Seneviratne et al., 2010) and influences the distribution of rainwater between run-off, evapotranspiration and infiltration (Mimeau et al., 2021). Soil moisture provides input into models for crop growth and grassland production (Krueger et al., 2021), and it dictates the management of cattle grazing (Tuohy et al., 2015).

Soil moisture can be directly measured in the laboratory using thermogravimetric techniques on field samples or in the field using ground-based methods, such as electromagnetic sensors (Robinson et al., 2008). The availability of low-cost sensors has driven the development of regional soil moisture networks, allowing measurements at many sites and at several depths (Babaeian et al., 2019a). These measurements, however, have uncertainties due to salinity variations, variable local contact with the soil and site-specific calibration and they only provide measurements at depths > 5 cm in the soil, with a few exceptions (Sheng et al., 2017); moreover, local (~ 10 cm) sampling around the sensor is not always representative of the surrounding area (Petropoulos et al., 2013). Nevertheless, networks with systematic observations of soil moisture have long been useful to support agricultural decision making (Robock et al., 2000).

Satellite remote sensing technology provides a solution to measure soil moisture across scales such as a field (100s of m^2), catchment ($0.1\text{--}1$ km^2), sub-watershed ($1\text{--}80$ km^2) and beyond. Reviews of recent satellite soil moisture products have summarised the different methods of estimation, the limitations, the advantages/disadvantages, the trends in the evolution of thermal and optical sensors (Zhang and Zhou, 2016) or microwave sensors (Mohanty et al., 2017), and the potential synergies from multi-sensor fusion (Petropoulos et al., 2015). Most of the currently employed techniques have been deployed at relatively coarse scales (>3 km) in the optical (Sadeghi et al., 2017a), thermal (Shafian and Maas, 2015) and microwave (Entekhabi et al., 2010) parts of the electromagnetic spectrum. Microwave sensors, on satellite missions

such as Soil Moisture and Ocean Salinity (SMOS) (Kerr et al., 2010) , Soil Moisture Active Passive (SMAP) (Entekhabi et al., 2010) and Advanced Scatterometer (ASCAT) (Wagner et al., 2013), have the advantage of operating in all weather conditions as they are not affected by cloud or variable solar illumination. Sentinel-1 synthetic aperture radar satellites have been used for higher resolution soil moisture estimation (Bhogapurapu et al., 2022; Singh et al., 2020), but are sensitive to fine-scale features and (currently) need fusion with other microwave sensors and resampling to ~1 km scale to reduce the complexity in the interpretation of their data (Bauer-Marschallinger et al., 2019; Das et al., 2019). The use of satellite radar soil moisture products for field-scale agricultural decision support is therefore limited but is an active area of research (Peng et al., 2021).

In situ soil moisture networks are invaluable for validating satellite soil moisture retrievals (Bogena et al., 2015; Dorigo et al., 2021). The comparison of in situ and satellite measurements with different spatial and temporal resolutions is complicated (Gruber et al., 2020), and its investigation is partially driven by requirements for datasets at sub-daily temporal and <1 km spatial resolutions, at multiple soil depths and with consistent error information.

The objective of this study was to investigate high-resolution (10 m to 20 m) normalised Surface Soil Moisture (nSSM) at depths < 0.2 cm from Sentinel-2 (S-2) data using a modification of the Optical Trapezoid Model (OPTRAM; (Sadeghi et al., 2017a)) and very sparse soil moisture networks over grassland sites. The sites are in Ireland, a country which typifies a temperate, high-rainfall climate (Cui et al., 2021) with intensive agriculture. OPTRAM has been used to estimate soil moisture from Landsat (Sadeghi et al., 2017a), S-2 (Acharya et al., 2022; Mananze and Pôças, 2019) and MODIS (Babaeian et al., 2018; Chen et al., 2020; Sun et al., 2021). These studies were conducted in crop fields in arid or semi-arid climates, which are quite different from the climatic conditions in this study. They tend to follow the original OPTRAM formulation of (Sadeghi et al., 2017a) which incorporates the

Normalised Difference Vegetation Index (NDVI). This study explored the use of other vegetation indices appropriate for temperate climate and poorly draining soil conditions. Previous studies (Babaeian et al., 2019b; Chen et al., 2020; Sadeghi et al., 2017a) have obtained typical correlations between in situ VSM measurements and satellite-derived SSM (~0.2–0.8) but they did not take into account the sensor depths beneath the surface. This study combined laboratory measurements of saturated and residual VSM in representative soil samples with an approximate solution to the Richards' Equation (Farthing and Ogden, 2017; Sadeghi et al., 2017b) to establish relationships between optically derived nSSM and in situ sensor VSM. This deals with the time lag between a satellite pass and a sensor measurement to reduce uncertainties in the validation process (Urraca et al., 2017), especially in poorly draining soils. This study also introduced an analysis of temporal stability (TS) (Vachaud et al., 1985) to the S-2 nSSM. TS studies have been used for improving hydrological models, filling of missing in situ data and some limited environmental management (Vanderlinden et al., 2012) but tend to be based upon in situ sensor networks (Fry and Guber, 2020). This study is the first to use the TS of S-2 nSSM to explore 10 m scale variations in grassland to identify locations where the soil is consistently wetter or dryer than the average; this could be useful in decisions for targeted irrigation and drainage. We recognise that grassland occupies one third of the global land surface area and plays an important role in carbon sequestration, food production and other ecosystem services (Sollenberger et al., 2019).

2.3 Data and Methods

2.3.1 Study Area

The Republic of Ireland in North-West Europe borders the Atlantic Ocean which results in humid weather all year round with abundant rainfall: ~1000–1400 mm/year in the west and ~750–1000 mm/year in the east (MetEireann, 2022). The CORINE Land Cover 2018 inventory shows agriculture as the dominant type in Ireland, accounting for ~67% of the national land

cover. Within agriculture, pastureland (grassland) is the major class (~55%) followed by pastureland interspersed with other natural vegetation (6.9%) and arable land (4.5%). The other major land cover categories include wetlands (14.9%) and forests (9.5%) (EPA, 2018).

The study focuses on two areas (Figure 2.3.1) ~7.5 km² and 16 km² in size surrounding two farms, Rossmore (52°N, 8°W) and Stradone (53°N, 7°W), respectively. Both farms are part of the Teagasc Heavy Soils Programme (Teagasc, 2021b) and are ~50 ha. The objective of this programme is to improve the sustainability of grassland farms dominated by poorly drained soils used for grazing livestock. Rossmore is flat and contains loam and sandy loam soils, the dominant soil sub-group being surface water gley while Stradone has elevation differences less than ~ 3 metres and is comprised of loam and clay loam soils, and the dominant soil sub group is brown earth. A high-resolution soil survey of each farm was carried out following the protocol of the Irish Soil Information System (Environmental Protection Agency, 2014). The soils are classified (Schulte et al., 2015; Tuohy et al., 2018) as poorly drained (those that reach saturation during rainfall events and hold excess water for multiple days following rainfall events) or moderately drained (those that hold excess water during rainfall events but not afterwards). The farms are equipped with in situ soil moisture sensors providing daily measurements of VSM and a weather station recording daily measurements of rainfall, evapotranspiration (ET) and wind speed.

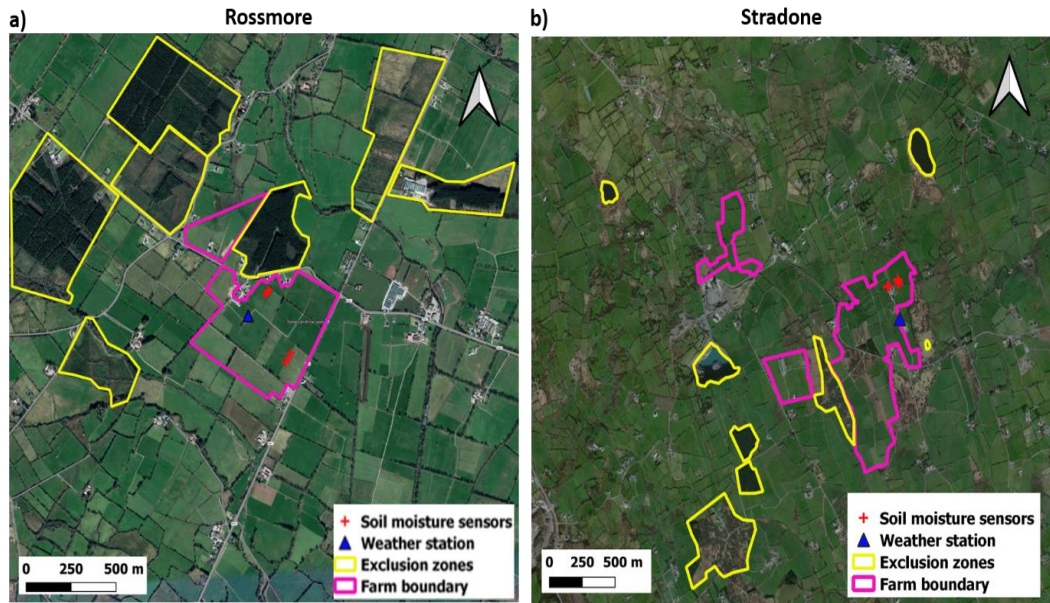


Figure 2.3. 1: Locations of (a) Rossmore and (b) Stradone sites. Yellow polygons indicate zones of forests and water bodies excluded from the analysis. Note the different scales for each area. Background imagery from Google Earth.

2.3.2 Satellite and In Situ data

The S-2 mission comprises two satellites (2A and 2B) that offer global coverage from 56°S to 84°N. The S-2 level 1C product (ESA, 2013) was downloaded from the United States Geological Survey (USGS) Earth Explorer platform. All the data were atmospherically corrected in QGIS using the Semi-automatic Classification Plugin (SCP) and the Dark Object Subtraction (DOS) algorithm (Gilmore et al., 2015). S-2 band 12 (centred at a wavelength of 2190nm) is resampled from 20 m to 10 m using the nearest neighbour algorithm in the SCP tool (Congedo, 2021) and as suggested by other studies (Asam et al., 2022). The cloudy S-2 data were masked using a cloud mask available with the S-2 Level-1C product as part of the quality information (Coluzzi et al., 2018). The method in this study requires two S-2 datasets. The first dataset consists of cloud-masked images of the two sites, available since the launch of the S-2 satellites in 2015. A total of 30 S-2 images for Rossmore are available, out of which 17 are cloud free; for Stradone, 25 images are available, out of which 23 are cloud free (Table A1). The second dataset consists of S-2 data, resampled onto 12 windows of 3 by 3 10 m pixels,

with each window covering an area of 900 m² and centred on each in situ sensor since the start of VSM monitoring; the centre of the central pixel in each window is therefore directly above its corresponding in situ sensor. This dataset is only used to establish relationships between OPTRAM nSSM estimates and in situ VSM for the validation of the model; it consists of 13 and 12 S-2 images from January 2021 to the end of 2022 for Rossmore and Stradone, respectively (Table A1).

Two fields in each of the two farm sites are each equipped with three Sensoterra (Sensoterra, n.d.) in-situ sensors (vertically aligned according to the manufacturer's instructions), which were placed in representative of the soil types at the sites and measure volumetric soil moisture (VSM). The in situ VSM (m³/m³) sensor data are acquired at a depth of ~15 cm to avoid disturbing the high-intensity dairy farms. Four soil samples representative of the two sites were used to calibrate the sensors. The samples were saturated in a laboratory and allowed to dry at room temperature over several weeks during which VSM was measured using the gravimetric technique (Robinson et al., 2008). This allowed a calibration of sensor readings from saturated to residual VSM for each sample.

2.3.3 OPTRAM Basics

The OPTRAM method (Sadeghi et al., 2015) estimates nSSM from optical satellite data based upon the Kubelka–Munk radiative transfer theory and vegetation indices (VI) which are spectral imaging transformations of two or more satellite image bands. OPTRAM represents a linear relationship between normalised surface soil moisture, W over bare soil, and short wavelength infrared (SWIR) transformed reflectance, STR :

$$W = (\theta - \theta_{res})/(\theta_{sat} - \theta_{res})$$

$$= (STR - STR_{dry})/(STR_{wet} - STR_{dry}) \text{ Equation 1}$$

$$STR = (1 - R_{SWIR})^2/2R_{SWIR} \text{ Equation 2}$$

where $0 \leq W \leq 1$, θ is the VSM at the surface (<0.2 cm), θ_{res} is the residual VSM, θ_{sat} is the saturated VSM, R_{SWIR} is the reflectance at an SWIR wavelength, and STR_{dry} and STR_{wet} are the STRs in soils with θ_{res} and θ_{sat} , respectively. θ_{res} is the VSM measured in the lab for the soil sample after saturation and drying of soil at room temperature (not the WP), whereas θ_{sat} is the VSM when all pores are filled with water, and is not equal to the FC. Equation (1) is valid for vegetated soil if there is also a linear relationship between root zone VSM and vegetation volumetric water content (Sadeghi et al., 2017a). This assumption is based on studies which suggest that SWIR reflectance is sensitive to vegetation water content (and leaf internal structure), and that STR reflectance is linearly correlated with vegetation water content. In this study, following (Sadeghi et al., 2017a), SWIR Band 12 was used to compute STR.

The water content of vegetation, and therefore vegetation spectral characteristics, is dependent on soil moisture status (Santos et al., 2014). Such changes can be captured by a VI required in OPTRAM. If the VI does not change, Equation (1) assumes that a change in the STR is a linear function of nSSM. If the value of a VI changes due to a change in water content or fractional surface area of vegetation in a pixel, the values of STR_{dry} and STR_{wet} will change. Therefore, the estimation of nSSM over vegetated soil requires a close assessment of how time-varying rainfall, evapotranspiration and infiltration has different effects on the changes in the amplitude of the STR for changes in the VI and associated VSM. This is partly achieved in OPTRAM

using a scatter plot in the STR-VI space based on many different hydro-meteorological conditions to estimate STR_{dry} and STR_{wet} (Figure 2.3.2).

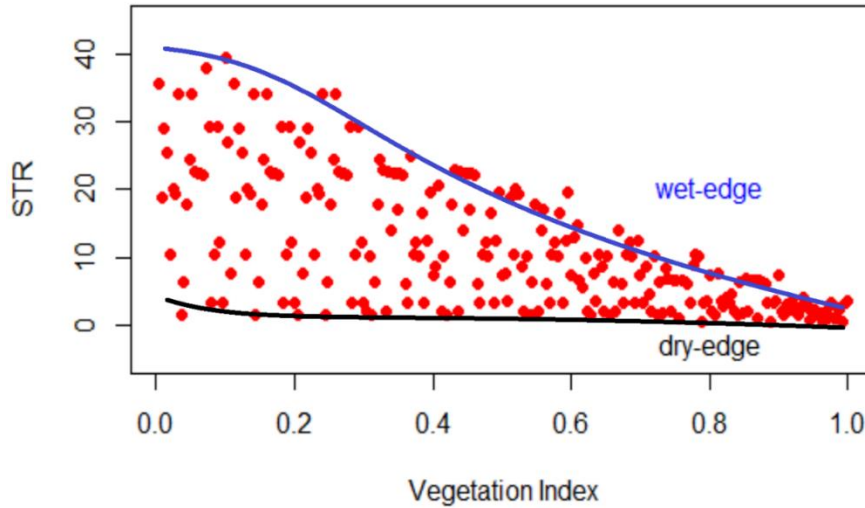


Figure 2.3. 2: Idealised representation of OPTRAM STR-VI scatter plot. The blue line represents the (saturated) wet edge, the black line represents the dry edge and red dots represent STR-VI couplets allocated to VI bins of width 0.01 and STR bins of height 0.01 multiplied by the range of STR.

Optical scenes may include oversaturated pixels (e.g., due to standing surface water after heavy precipitation) above the wet edge which will increase the STR. As nSSM is only valid for partially and fully saturated soils ($0 \leq W \leq 1$) and VSM cannot increase beyond θ_{sat} , all pixels on and above the wet edge are assumed to be saturated ($W = 1$). The dry edge represents pixels with θ_{res} . Equation (1) demonstrates that the nSSM for a pixel with an STR value is equivalent to the fractional distance between the two edges at the coincident VI. The geometry of the two edges changes with the choice of VI.

2.3.4 Relationships between VSM and nSSM

Linear correlations between a VI and its associated VSM from multiple in situ sensors within the root zone (<1 m) beneath a pixel can be optimised if the VSM has a time-delay after the VI acquisition date. (Santos et al., 2014) attribute this delay to the time required by plants to adjust their biological processes to match the surface conditions and water availability in the soil.

Correlations between nSSM and VSM from sensors within the root zone used to investigate uncertainties in the satellite retrievals must therefore account for time delays between the surface signal and the sensor response. These could be days depending upon, e.g., vegetation and soil hydraulic conductivity. This study addresses this problem using a solution to a model based on a 1-dimensional Richards' Equation, originally developed to retrieve root zone VSM from NASA's AirMOSS mission (Sadeghi et al., 2017b). This establishes the relationship between satellite-derived nSSM and in situ sensor VSM at depth. The solution is:

$$\theta(z) = [c_1 z + c_2 \exp(z/h_{cM}) + c_3]^{1/P} \quad \text{Equation 3}$$

$$K = K_{sat} \left(\frac{\theta - \theta_{res}}{\theta_{sat} - \theta_{res}} \right)^P = K_{sat} S^P \quad \text{Equation 4}$$

$$\exp\left(\frac{-h}{Ph_{cM}}\right) = \left(\frac{\theta - \theta_{res}}{\theta_{sat} - \theta_{res}}\right) \quad \text{Equation 5}$$

where z is the depth; P is related to the soil pore size distribution and is an empirical parameter that defines a relationship between saturated hydraulic conductivity, K_{sat} , and unsaturated conductivity, K ; h_{cM} is the effective capillary drive; c_1 , c_2 and c_3 are time-invariant constants; S is the effective saturation; and h is the pressure head. The solution is most accurate during soil drying, i.e., concurrent evapotranspiration and infiltration after a rainfall event. It represents a common scenario for acquiring optical satellite data above persistent cloud cover.

First, we estimate the VSM at the surface $z \sim 0$ from the nSSM, W :

$$\theta = \theta_{res} + (\theta_{sat} - \theta_{res}) W \quad \text{Equation 6}$$

For VSM measured at a sensor at depth z_S , Equation (6) can be written as:

$$\theta^{z_S} = [c_1 z_S + c_2 \exp(z_S/h_{cM}) + c_3]^{1/P} \quad \text{Equation 7}$$

and at $z = 0$:

$$\theta = [c_2 + c_3]^{1/P} \quad \text{Equation 8}$$

$$\theta^{z_s} = \{[a_1 z_s + a_2 \exp(z_s/h_{cM}) + a_3]^{1/P}\} \theta \quad \text{Equation 9}$$

$$\theta^{z_s} = A^{z_s}[\theta_{res} + (\theta_{sat} - \theta_{res}) W] = \theta_{min} + g W \quad \text{Equation 10}$$

Therefore,

where θ_{min} is the intercept, g is the gradient and A^{z_s} is a positive scalar calibration constant to transform nSSM to VSM at the sensor. This establishes the relationship between satellite-derived nSSM and in situ sensor VSM at depth. In principle, if θ_{res} and θ_{sat} are known, A^{z_s} can be estimated using Equation (10) from a nSSM-VSM plot for multiple satellite estimates of nSSM and coincident VSM measurements under different hydro-meteorological conditions. In practice, this still requires some winnowing of data (Section 2.5) to guarantee that the VSM measurements are responding to infiltration at the S-2 acquisition date. In these scenarios, $A^{z_s} > 1$, i.e., the VSM at the sensor depth z_s is greater than the VSM at the surface at the time of the S-2 data acquisition. This implies that the soil reaches saturation at z_s , when the nSSM $W^{z_s} < 1$ so that:

$$\theta_{sat} = A^{z_s}[\theta_{res} + (\theta_{sat} - \theta_{res}) W^{z_s}] \quad \text{Equation 11}$$

which is only true when

$$W^{z_s} = (\theta_{sat} - A^{z_s} \theta_{res}) / A^{z_s} (\theta_{sat} - \theta_{res}) \quad \text{Equation 12}$$

For a value of nSSM such that $W^{z_s} < W \leq 1$, the soil reaches saturation at a depth z_{sat} , where $z_s > z_{sat} \geq 0$. The volumetric soil moisture at depths $\geq z_{sat}$ is constant (θ_{sat}). The model is like Case B in ((Sadeghi et al., 2017b); Figure 7). The approach is sufficient to predict VSM at a sensor from nSSM and requires no knowledge of P or h_{cM} .

2.3.5 Considerations for Implementing OPTRAM

2.3.5.1 Choice of Vegetation Index

Alongside the most popularly used Normalised Difference Vegetation Index (NDVI), we evaluated a suite of other VIs: Enhanced Vegetation Index (EVI), Modified Soil Adjusted Vegetation Index (MSAVI) and, since the S-2 satellite provides the only freely available optical dataset containing the red-edge band, Normalised Difference Red-Edge Index (NDREI). Their computation is summarised in Table S2. The aim was to determine which VI is least correlated with its concurrent and coincident STR to maximise the sensitivity of the soil moisture estimate from the STR in the presence of vegetation water content which influences the VI. The choice for optimum VI was quantified through Spearman's and distance correlations between STR and VI, and the smoothness, shape, and practical range of the wet and dry edges.

2.3.5.2 Determination of Edge Curves and Calculation of nSSM

The original OPTRAM was developed with linear edge curves and recent studies have explored the use of non-linear edges. Some studies have shown that the VI-STR relationship with high vegetation cover may be non-linear (Hassanpour et al., 2020; Mananze and Pôças, 2019) and that non-linear parametrization of OPTRAM leads to better accuracies in soil moisture estimates compared to linear parametrization (Ambrosone et al., 2020). After the choice for an appropriate VI, the STR-VI couplets were allocated to an appropriate bin with a width of 1% of the range in the VI and STR. We used a numerical method which sweeps over the STR bins and then across the VI bins in the scatter plot to guide our selection of the dry and wet edges. A double logistic function (Equation (14); (Lipovetsky, 2010)) was fitted to each empirically determined edge, defined as the curves below and above which 1% of the couplets are regarded

as noise (e.g., man-made features or over-saturated pixels beyond the wet edge). Each edge was fitted using ‘trial and error’ forward modelling with the 7 free parameters in the function:

$$STR^j = STR_{min}^j + \frac{STR_{mid}^j - STR_{min}^j}{1 + \exp(-aVI + b)} + \frac{STR_{max}^j - STR_{mid}^j}{1 + \exp(-cVI + d)} \quad \text{Equation 13}$$

The free parameters in the double logistic function are flexible to approximate linear, exponential, or sigmoidal behaviour that is sufficiently complex to characterise the observed edge curves. The nSSM for each pixel was calculated as a linear distance between the dry and wet edges.

2.3.5.3 Land Cover Masks

Vegetation growth and root water uptake play an important role in soil moisture temporal dynamics at the field scale (Hupet and Vanclooster, 2002). An application of OPTRAM at the field scale needs to focus on classes within a complex land cover, e.g., grassland, forests, and water bodies, to minimise soil moisture variations associated with distinct types of vegetation or stages of growth. Therefore, a mask was created for forests and water bodies to identify ‘exclusion zones’ (Figure 2.3.1). Other land cover classes were not considered since they represent less than 1% of the areas and do not influence the scatter between the VI and STR significantly.

2.3.5.4 Normalised SSM and Time-Delayed VSM Data

For validation of satellite-derived nSSM and in situ VSM, the nSSM was estimated at the central pixel over a window of 3×3 pixels, centred above each sensor, by fitting a second order polynomial over the window to minimise any local spatial heterogeneity at a scale of 10 m. This becomes the variable W (Equation (10)). A coincident VSM can be chosen if the time series of daily sensor readings for δt ($0 \leq \delta t \leq 5$) days after the date of the S-2 acquisition shows a monotonic decrease in VSM implying consistent drying conditions which are the most

suitable for the model. The VSM, θ^{z_s} (Equation (10)), is a weighted average of any two consecutive daily VSM observations delayed by δt days to capture infiltration times from the surface to the sensor. The weights on the two VSM values represent the proportion of the day contributing to the weighted average.

The time-delay, δt , and calibration constant, A^{z_s} , for each field can then be estimated from a linear regression of θ^{z_s} vs. W for the three sensors at depth z_s by iteratively adjusting their values so that $\theta_{min} = \theta_{res}$ when $W = 0$, and $\theta_{max} = \theta_{sat}$ at W^{z_s} ; this is the nSSM which results in saturation at the sensor depth (Equation (12)). The final values are those which minimise the Root Mean Square Error (RMSE), maximise the coefficient of determination (R^2) and are consistent with Equation (9 and 10) and laboratory measurements of VSM from the soil samples.

2.3.6 Temporal Stability (TS) Metrics

Temporal stability is traditionally used in hydrology (Vereecken et al., 2014). It is based on a statistical approach to analyse any time-varying dataset. This study used TS equations to analyse the nSSM dataset. TS is a result of complex interactions among local (<30 m) and nonlocal weather, soil properties, vegetation, surface topography, sub-surface hydrology and agricultural practices (Vereecken et al., 2014). The grassland sites have minimal topographic variations, so the prima facie assumption is that TS is primarily controlled by time-invariant soil properties. The Mean Relative Difference (MRD) and the Standard Deviation Relative Difference (SDRD) are the most popular metrics to evaluate the TS of soil (Vanderlinden et al., 2012):

$$RD_{ij} = (W_{ij} - W_j)/W_j \quad \text{Equation 14}$$

$$MRD_i = (1/J) \sum_{j=1}^{j=J} RD_{ij} \quad \text{Equation 15}$$

$$SDRD_i = \sqrt{1/(J - 1) \sum_{j=1}^{j=J} (RD_{ij} - MRD_i)^2} \quad \text{Equation 16}$$

where RD_{ij} is the relative difference between the nSSM, W , at pixel i , satellite pass j and J is the number of passes. We modified these equations to obtain the Median Relative Difference (\hat{W}_i) and Median Absolute Deviation Relative Difference (σ_i).

2.4 Results

2.4.1 Satellite and VSM Data

The nSSM interpolated onto the centres of the central pixels in each of the 3×3 windows (Section 2.5.4) surrounding each sensor showed minor differences (~ 0.01) from nSSM values at each pixel in the corresponding window. This indicates that (1) interpolation of the 10–20 m optical data onto a 10 m grid does not introduce significant uncertainties, and (2) surface moisture conditions are homogeneous over 30 m scales. For the validation exercise only, the nSSM value was calculated for the centre of the central pixel and is directly located above the in situ VSM measurement.

The laboratory calibrations (Table 2.4.1) indicate that the soils have higher than average values for saturated VSM (e.g., [37]; Table 2.4.1), consistent with the characteristics of poorly drained soils which dominate these sites. The hydro-meteorological time series (Figure 2.4.1) showed that the VSM ranged from 0.03 to 0.49 m^3/m^3 for Rossmore and 0.10 to 0.67 m^3/m^3 for Stradone. Although the normalised linear correlations for the six sensors at both sites were >0.96 , some sensors had significantly different amplitudes from the other sensors in the same field. The differences ($\lesssim 0.2 \text{ m}^3/\text{m}^3$) in concurrent VSM values are explained by heterogeneity

in soil hydraulic properties and a possible systematic difference between laboratory calibration and field observations.

Table 2.4. 1: Laboratory measurements of soil samples around sensors at the two sites. The measurement uncertainties are $<\pm 0.02 \text{ m}^3/\text{m}^3$. Ross = Rossmore, Stra = Stradone.

Sensors	Soil Type	Soil Texture	Saturated VSM (m^3/m^3)	Residual VSM (m^3/m^3)
Ross 1–3	Brown Earth	Loam	0.64	0.06
Ross 4–6	Surface Water Gley	Sandy Loam	0.50	0.04
Stra 1–3	Luvisol	Loam	0.59	0.09
Stra 4–6	Stagnic Brown Earth	Clay Loam	0.57	0.08

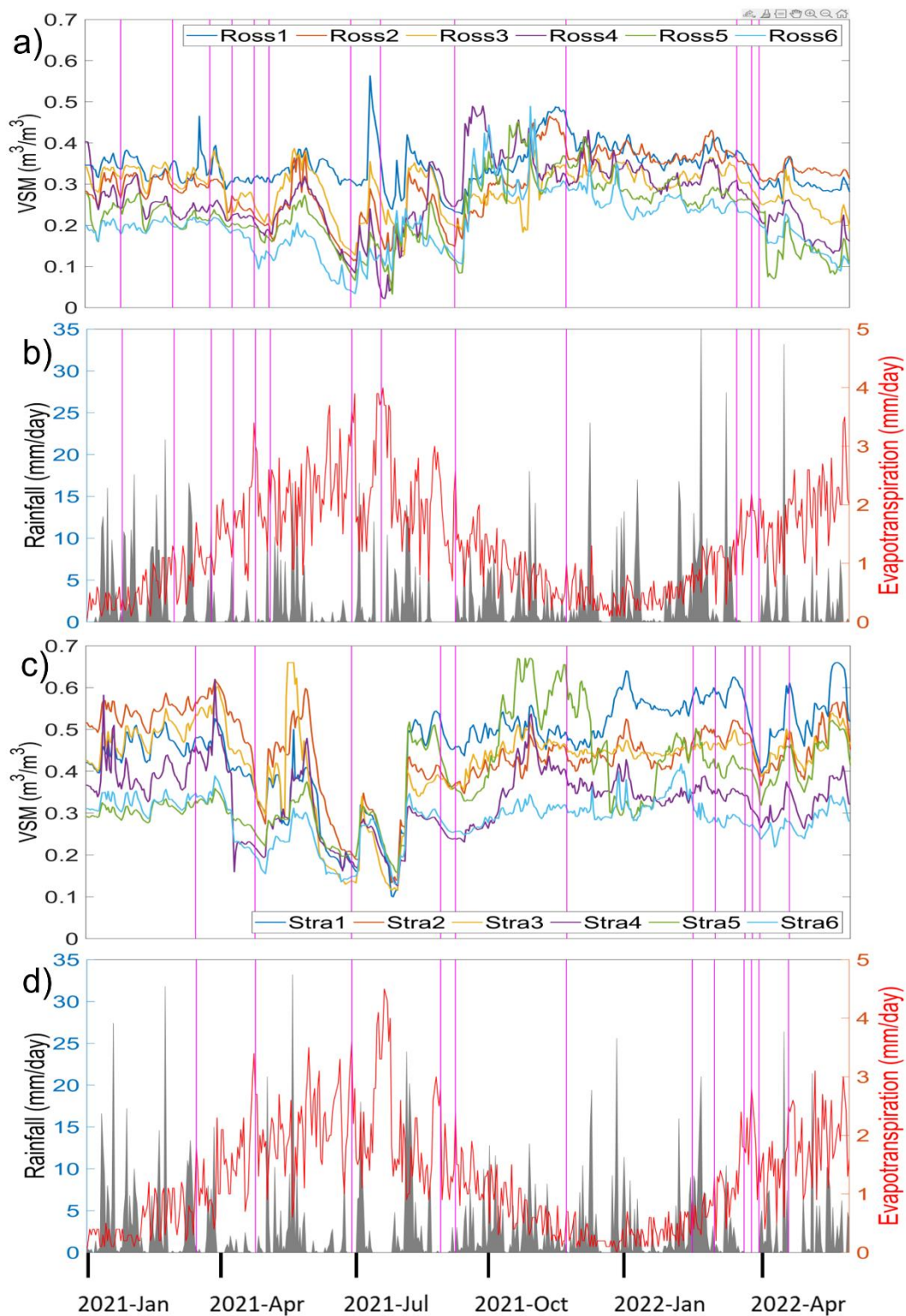


Figure 2.4. 1: **(a)** VSM and **(b)** daily rainfall and evapotranspiration for Rossmore; **(c, d)** equivalent time series for Stradone. Vertical lines date S-2 observations since the installation of the network. Stra1, Stra3 and Stra5 VSM sensors record values > saturated VSM after high rainfall/low ET events, indicating over-saturated conditions with free water at the surface. ET peaks and VSM is at its minimum in mid-summer (July); cumulative rainfall is higher in winter (October–March) than summer

2.4.2 Choice of Vegetation Index

The results (Table 2.4.2) of the pair-wise correlations between STR and VIs show that the STR-EVI Spearman's coefficients for Rossmore and Stradone were consistently negative and had lower values compared to the MSAVI and NDREI. STR was negatively correlated with NDVI and NDREI at Stradone and positively at Rossmore. The difference in scatter plots between the two sites is responsible for the change in sign in the Spearman's coefficients (Section 4.1). The average STR-EVI distance correlation coefficient from the two sites was consistently at the low end.

Table 2.4. 2: Distance correlation coefficient d_{cor} and Spearman's rank correlation coefficient ρ_{cor} (in brackets) between STR and VIs for Rossmore (lower triangle with orange background) and Stradone (upper triangle with blue background). Coefficients are for data that have been masked to remove exclusion zones.

	NDREI	MSAVI	EVI	NDVI	STR	
STR	1.00 (1.00)	0.89 (0.92)	0.58 (0.87)	0.96 (0.95)	0.27 (-0.07)	NDREI
NDVI	0.23 (0.17)	1.00(1.00)	0.69 (0.93)	0.90 (0.96)	0.36 (-0.29)	MSAVI
EVI	0.26 (-0.13)	0.51 (0.53)	1.00 (1.00)	0.57 (0.90)	0.30 (-0.08)	EVI
MSAVI	0.32 (-0.18)	0.79 (0.83)	0.80 (0.83)	1.00 (1.00)	0.30 (-0.15)	NDVI
NDREI	0.31 (0.34)	0.88 (0.89)	0.51 (0.53)	0.71 (0.73)	1.00 (1.00)	STR
	STR	NDVI	EVI	MSAVI	NDREI	

2.4.3 Fitting of Edge Curves

The STR-EVI scatter plots (Figure 2.4.2) for both sites show that the edges are non-linear. The double logistic function defined the wet and the dry edges well. For both sites, a bulge in the scatter was seen around an EVI of 0.7 and STR of 20 and 15 for Rossmore and Stradone (Figure 2.4.2a,c), respectively, indicating the effect of water bodies and forests. After masking these land cover classes, the bulges in the EVI-STR scatter plots were removed (Figure 2.4.2b,d).

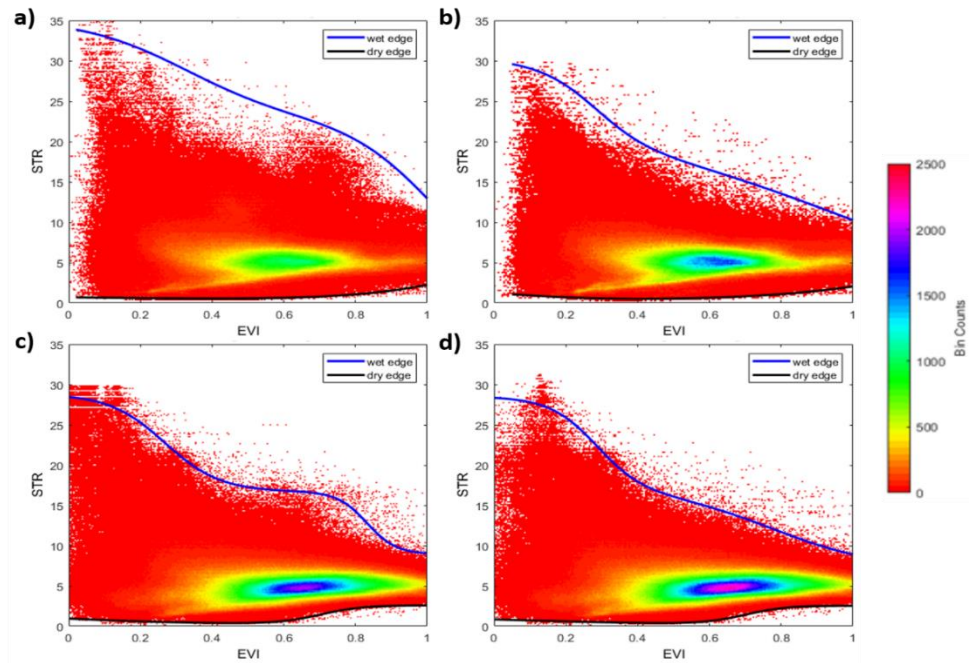


Figure 2.4. 2: STR-EVI scatter plots. **(a)** Rossmore without land cover masks; **(b)** Rossmore with land cover masks; **(c)** Stradone without land cover masks; and **(d)** Stradone with land cover masks.

The STR-VI scatter plots for the other VIs (Figure 2.4.3) demonstrated complicated behaviour at the wet edges for NDVI and NDREI; it is difficult to meaningfully fit edge curves. The STR-MSAVI scatter plots are comparable to the STR-EVI scatter plots, as expected from the correlations in Table 2. We noted that the maximum values of MSAVI and EVI were ~ 0.85 and ~ 1.0 , respectively. The low STR-EVI correlations, the smoothness, shape, and full range of the edge curves for the EVI scatter plots led us to choose EVI as the preferred VI for further analyses.

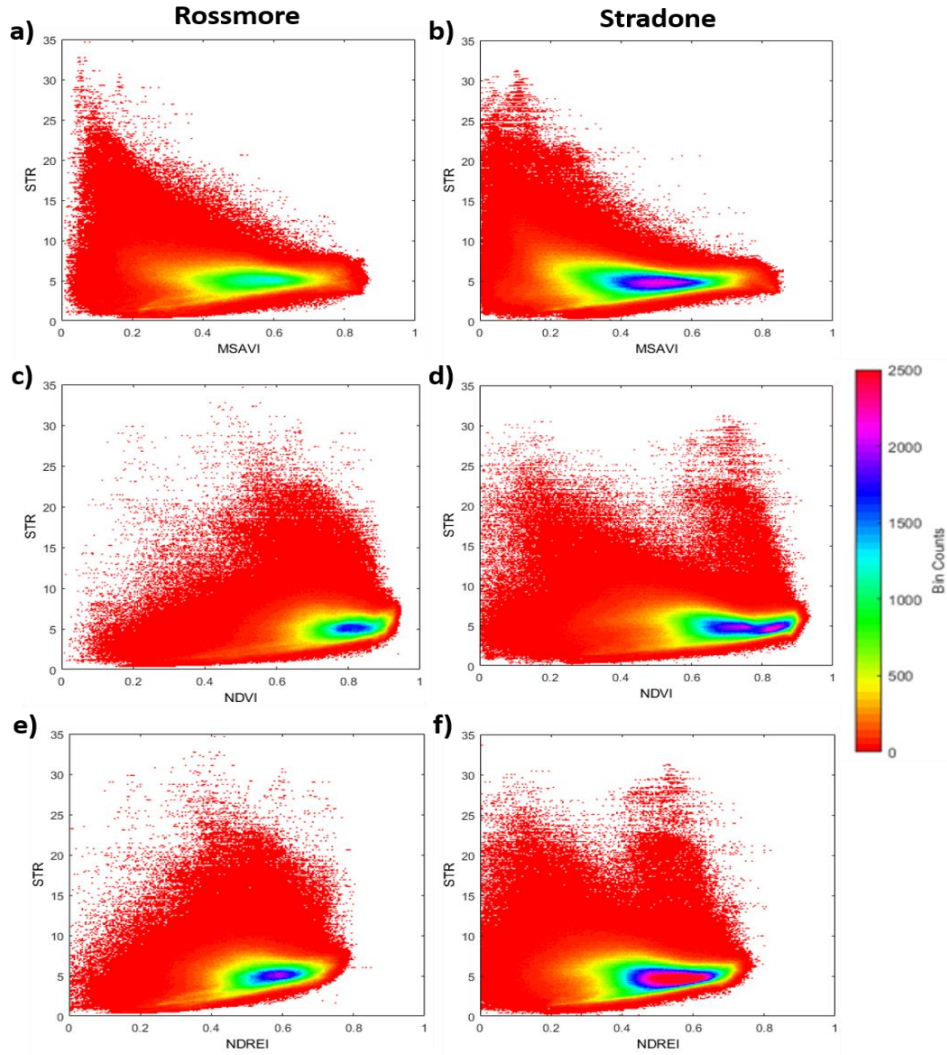


Figure 2.4. 3: Scatter plots of STR-VI with land cover masks at each site. (a) Rossmore STR-MSAVI, (b) Stradone STR-MSAVI, (c) Rossmore STR-NDVI, (d) Stradone STR-NDVI, (e) Rossmore STR-NDREI, (f) Stradone STR-NDREI.

2.4.4 Relationships between Satellite and In Situ Sensor Soil Moisture

Regressions between VSM and normalised SSM after choosing an A^{Zs} consistent with Equation (6) and the laboratory measurements of θ_{res} and θ_{sat} were used to make a quantitative judgement on uncertainties in the relationship between S-2 estimates and in situ VSM measurements. The results (Figure 2.4.4) suggest that a linear transformation of nSSM to VSM is associated with RMSE uncertainties of $\sim 0.06 \text{ m}^3/\text{m}^3$ for regressions limited to $nSSM < 0.5$. Without the introduction of time lags, the RMSE uncertainties were $\sim 0.1 \text{ m}^3/\text{m}^3$. The best fit line started at the residual VSM and finished at the saturated VSM determined from the

laboratory measurements of the soil sample in each of the four fields. The calibration constants were $1.0 \leq A^{Z_s} < 1.65$.

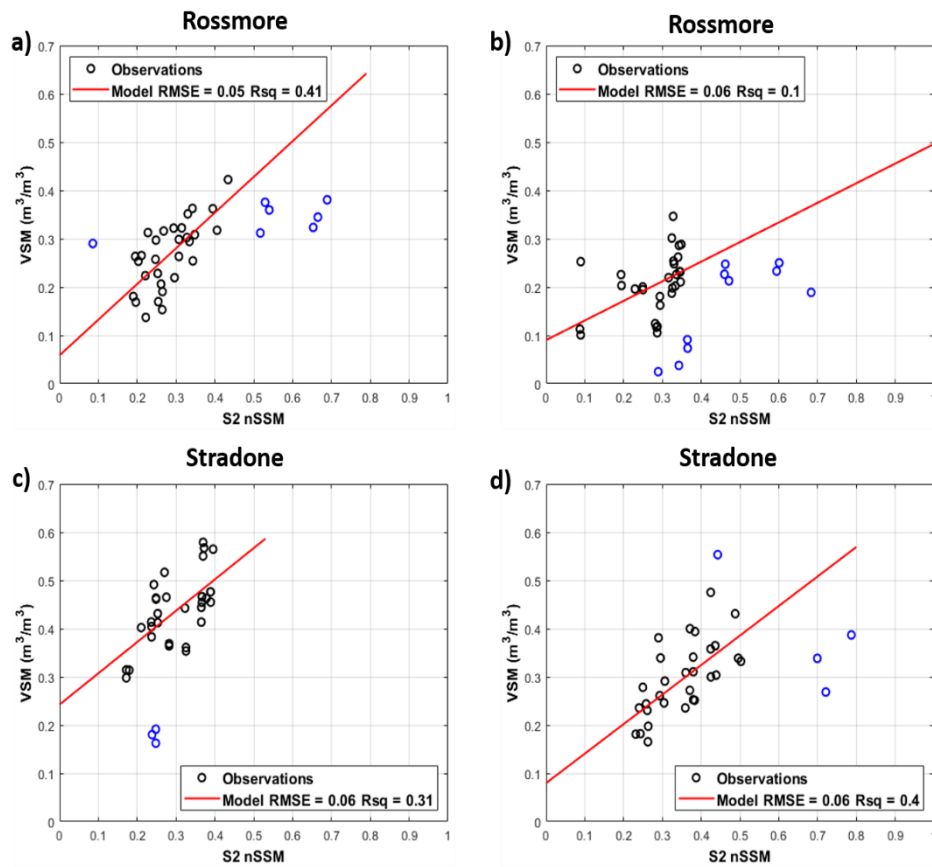


Figure 2.4. 4: Correlations between VSM and nSSM for the two farm sites. Each circle corresponds to a sensor reading. The S-2 data that did not meet the conditions of drying (Section 2.5.4), i.e., during a period with an increase in VSM, were excluded from the regression (blue circles). The absolute differences in the means (MD m^3/m^3), the unbiased Root Mean Square Deviations (m^3/m^3) and Percent Bias (PB) between the predicted VSM and observed VSM are, respectively, (a) 0.001, 0.05 and 0.23, (b) 0.003, 0.06 and -1.25 , (c) 0.001, 0.06 and 0.19, (d) 0.003, 0.06 and -0.96 . The MD and PB between the predicted and observed VSM are insignificant in the limited range of $0.1 < \text{nSSM} < 0.5$.

2.4.5 Maps of nSSM

Figure 2.4.5 shows examples of nSSM values derived from the STR-EVI scatter plots with land cover masks after events of high and low net water flux (NWF; the difference between cumulative infiltration and evapotranspiration) over 5 days prior to and including the day of the S-2 pass. The maps show the overall differences in nSSM and a spatial variability in nSSM that was correlated strongly with high and low NWF conditions within farm areas.

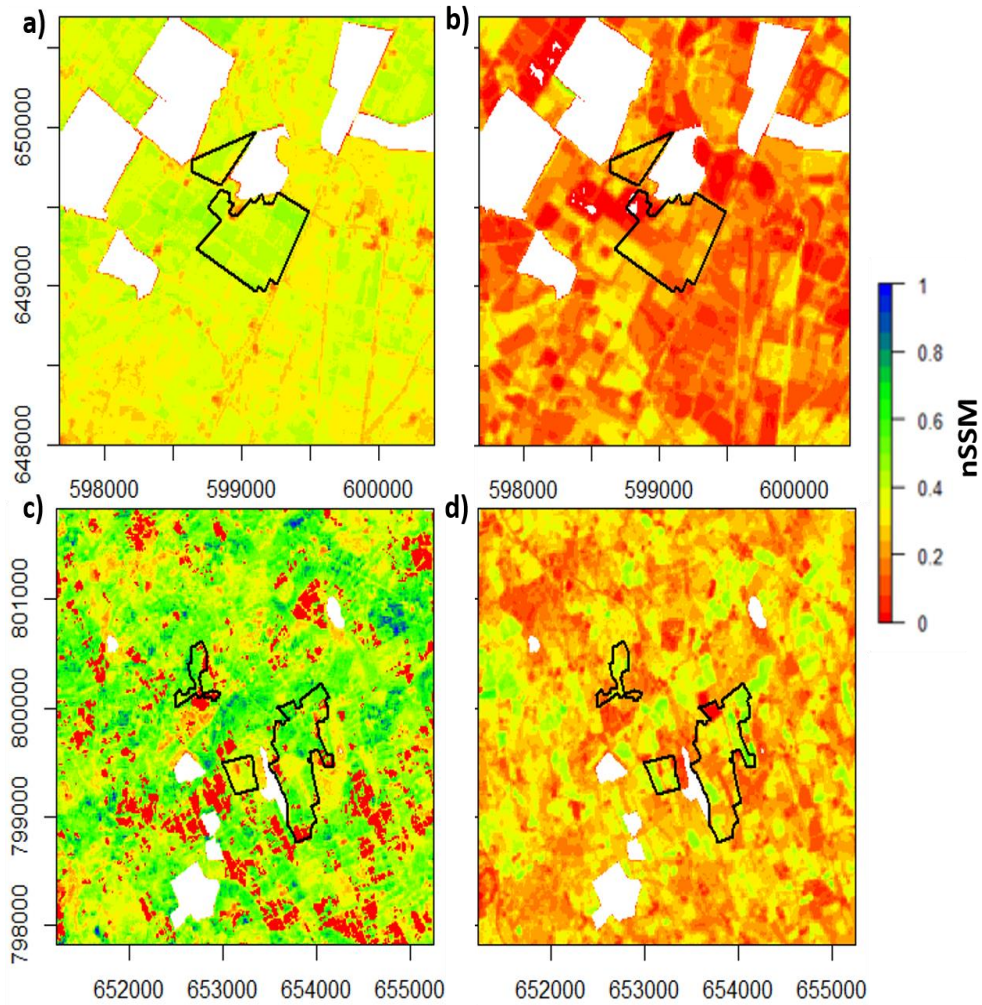


Figure 2.4. 5: nSSM maps for Rossmore for (a) high NWF and (b) low NWF, and Stradone for (c) high NWF and (d) low NWF. White areas are exclusion zones. Co-ordinates are in meters in the Irish Transverse Mercator (ITM) projection.

2.4.6 Temporal Stability of nSSM

The maps of Median Relative Difference, \hat{W} , and Median Absolute Deviation Relative Difference, σ , showed spatial variations (Figure 2.4.6) that were less noisy than the maps of MRD and SDRD. Linear features (roads and field boundaries) and buildings could be identified, and variations within fields were visible.

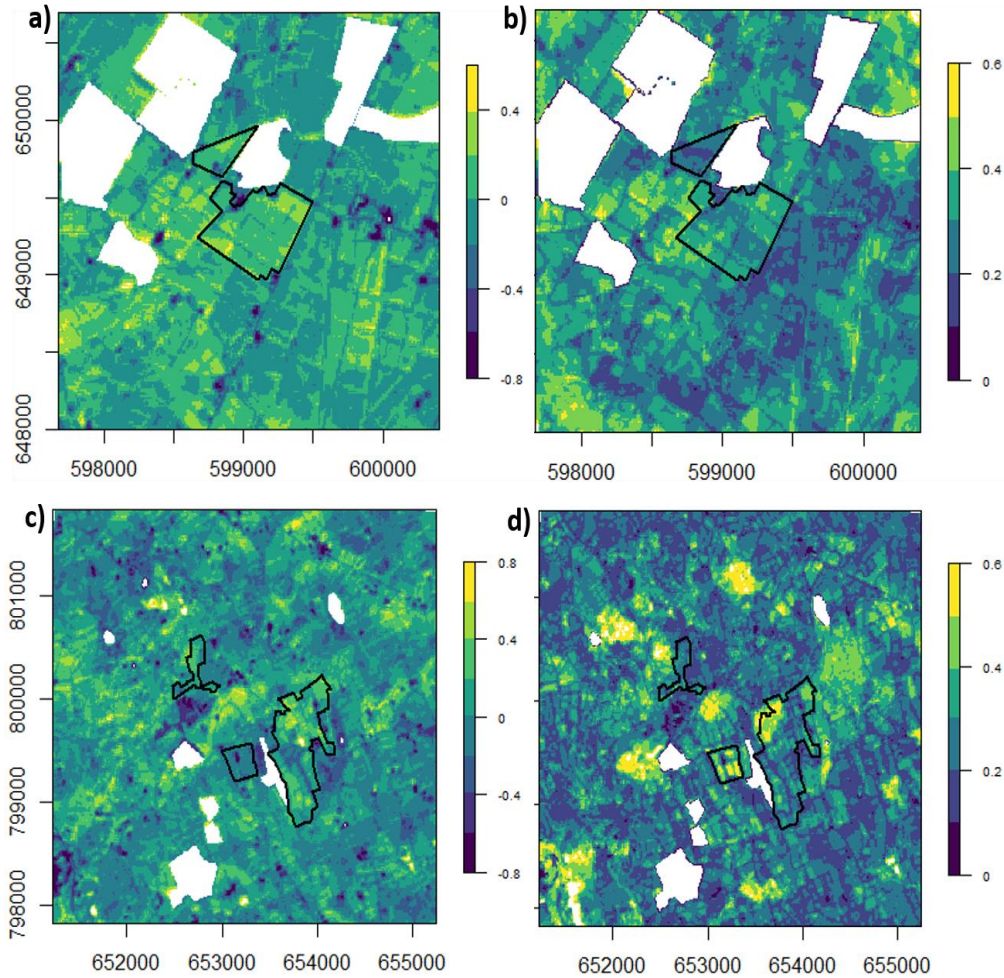


Figure 2.4. 6: Temporal Stability for Rossmore (a) \hat{W} and (b) σ , and Stradone (c) \hat{W} and (d) σ . Farm boundaries shown by solid black lines. White areas are exclusion zones. Co-ordinates are in meters in the Irish Transverse Mercator (ITM) projection.

The distinctive patterns in the TS behaviour can be better appreciated by focusing on the farm sites with \hat{W} and σ , shown with Great Soil Groups (GSGs) based on the extrapolation of data from auger points and soil pits, and local expert knowledge (Figure 2.4.7). In Rossmore, features 2 (Figure 2.4.7a) and 4 (Figure 2.4.7b) represent areas of high TS ($\hat{W} \sim 0$ and $\sigma \sim 0$), associated with roads and a sub-surface artificial drain, respectively. Feature 1 (Figure 2.4.7b) with $\sigma \sim 0.2$ represents one of the driest areas on this farm over moderately drained soil, while feature 3 (Figure 2.4.7b) with $\sigma \sim 0.5$ represents an area of low TS over poorly drained soil. In Stradone (Figure 2.4.7d), feature 1 with $\hat{W} \sim -0.1$ was associated with a dry area on this farm, feature 2 with $\hat{W} \sim -0.7$ was associated with a building, feature 4 with $\hat{W} > 1$ was associated

with a wet area around small tree patches which were not excluded by masking, and feature 5 with $\hat{W} \sim 0$ was associated with sparse vegetation (scrub) and/or bare soil. Feature 3 (Figure 2.4.7e) with $\sigma \sim 0.5$ is in an area of low TS over poorly drained soil. In both sites, individual fields could be identified from \hat{W} and σ , and variations in TS could be observed within the presumed Great Soil Groups.

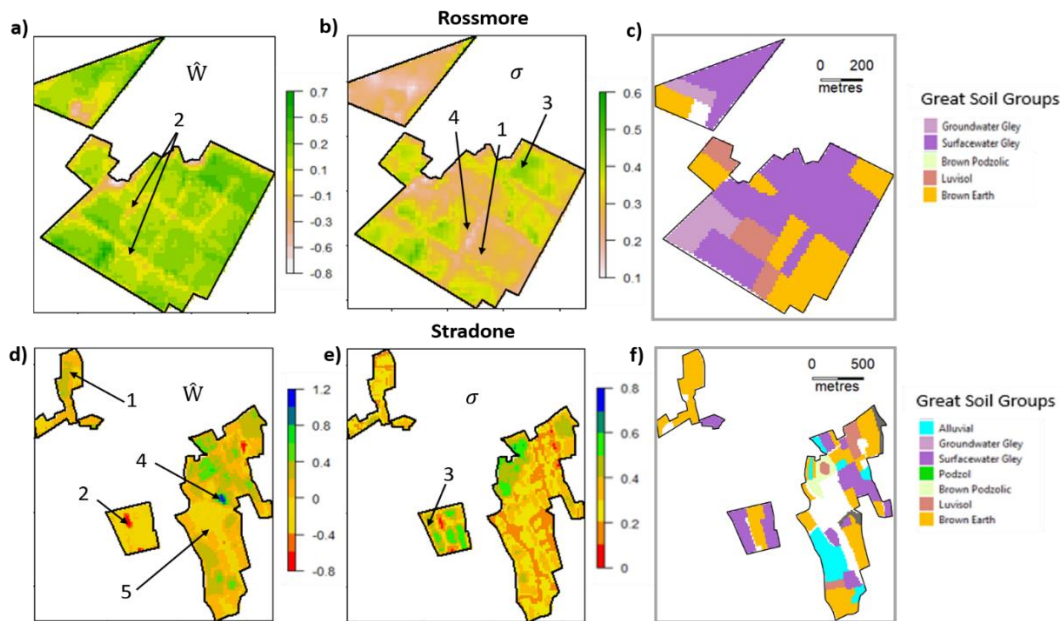


Figure 2.4. 7: Median Relative Difference, \hat{W} , Median Absolute Deviation Relative Difference, σ , and Great Soil Groups for the two farm sites. (a) Rossmore \hat{W} , (b) Rossmore σ , (c) Rossmore Great Soil Groups, (d) Stradone \hat{W} , (e) Stradone σ , (f) Stradone Great Soil Groups. Numbers refer to areas discussed in the text.

Features or areas that are moderately- to well-drained were associated with a high TS of surface moisture whereas poorly drained areas had a low TS, although there is insufficient evidence to rigorously quantify these associations.

2.5 Discussion

2.5.1 Edge Curves and Vegetation Index

The choice of the most appropriate VI for our study sites, EVI, was based on correlation analyses between STR and the selected VIs (Table 2.4.2) and the simplicity of the shape of the edge curves over the largest range of the VI (Figure 2.4.2).

If the edge curves are approximately linear, a non-zero Spearman's or distance correlation would result from a non-zero algebraic sum of the (signed) slopes of the two edge curves, e.g., if the wet edge has a negative slope whose magnitude is greater than the positive slope of the dry edge, the STR is negatively correlated with the VI in proportion to the difference. Electromagnetic radiative transfer theory requires a non-zero correlation between STR and a VI due to interactions with a vegetated canopy over soil. The reflectance from soil increases monotonically with wavelengths from ~500–900 nm (the range encompassing the VIs considered here), plateaus, dips and then peaks at ~2200 nm (Lobell and Asner, 2002) in the S-2 SWIR Band 12 used to compute the STR. Vegetation with increasing leaf water content is associated with increasing canopy reflectance, particularly at wavelengths > 700 nm, which increases the VI values (Gao, 1996) and decreases the SWIR band reflectance (Yilmaz et al., 2008); the canopy reflectance can even exceed that from the soil at a high VI (Yang et al., 2017). The negative STR-EVI (and STR-MSAVI) Spearman's correlation coefficients are therefore consistent with theory. As EVI increased (e.g., in the growing season), the reduced transmittance through the canopy lowered the sensitivity of the STR to soil conditions. The reduced STR difference between the wet and dry edges in an STR-EVI scatter plot is therefore also consistent with theory.

Other studies (Ojha et al., 2021) have documented the limitations of NDVI (it plateaus over areas with high vegetation density, it is influenced by soil in sparsely vegetated areas and is affected by atmospheric noise) and the benefits of EVI, which was developed to mitigate against these shortcomings. Our study showed that there was no improvement using NDREI within OPTRAM. A comparison of Figures 2.4.2 and 2.4.3 also demonstrates that there is little practical difference between the scatter plots of STR-EVI and STR-MSAVI at low values of vegetation cover, probably because grass is present at all stages of the agricultural/cattle grazing cycle for the study areas. The study also corroborates results from Sentinel-1 and S-2

imagery which indicate that EVI is optimum for the classification of Irish grassland (Saadeldin et al., 2022).

2.5.2 Variable Vegetation Cover and Soil Moisture

The use of land cover masks to exclude water bodies and forests demonstrates that STR values associated with forests are higher than those over grassland with the same EVI (Figure 2.4.2). A previous study on peatlands (Burdun et al., 2023) concluded that OPTRAM is insensitive to water table depth, especially for high (>50%) tree-cover areal density. This result also implies insensitivity to soil moisture in tree-covered areas and justifies the use of land masks to focus the analysis on grassland. Where data from small tree patches were included in the analysis (e.g., feature 4 in Figure 2.4.7d), they showed high values of soil moisture TS. This is consistent with observations which demonstrate that soil moisture below trees is higher than that below grassland in pasture landscapes because of reduced soil evaporation, greater soil infiltrability and groundwater recharge, and preferential water flow under trees (Benegas et al., 2021).

In grassland with high vegetation cover at high values of EVI, there was stronger coupling of soil moisture to vegetation water content; in these conditions, it was more accurate to categorise ‘normalised surface soil moisture’ estimated from OPTRAM as ‘normalised surface moisture’.

2.5.3 Time-Delayed VSM and nSSM

Previous studies have identified the problem of deriving soil moisture at depth from (near-) surface remote sensing data (Collow et al., 2012; Peng et al., 2021; Wagner et al., 1999). At present, there are limitations in our understanding of water fluxes in near-surface, variably saturated, porous soil. These are due to complex interactions among wetting and drying which can create large transient downward and upward water fluxes, respectively (Brutsaert, 2014; Salvucci and Entekhabi, 1994), bioturbation and water uptake by plant roots (Santos et al., 2014)) and time-varying pore structure dynamics of, e.g., soil bulk density, pore size

distribution and connectivity (Schwen et al., 2014). In agricultural regions, tillage, compaction due to animal and vehicle traffic, freeze/thaw events, periods of bare soil, etc., are common (Meurer et al., 2020) and can exacerbate changes in soil structure dynamics. The theory underpinning numerical models for relationships between soil moisture in the upper few cm and the deeper root zone is lacking and while classical approaches (e.g., Richards' Equation) can deal with variable soil hydraulic parameters, they are limited when dealing with root water (Verrot et al., 2019), an important mechanism for controlling VSM in the top 15 cm and deeper. This study demonstrated that there is a (weak) statistical correlation between nSSM satellite retrievals with in situ VSM measurements at a depth of 15 cm. It can provide reasonably accurate estimates of the time lags introduced to account for vertical flow of water between the surface and the in situ sensor. In general, time lags may be considerable, e.g., 15 to 20 days at depths of 20 cm to 100 cm, respectively (Wagner et al., 1999), or 5–10 days depending on chlorophyll content, growth rate and previous weather conditions (Santos et al., 2014). In our study with sensors at a depth of 15 cm, the optimal choice of time lags was ~2–3 days and ~3–4 days for the fields in Rossmore and Stradone, respectively. These lags correspond to an effective unsaturated hydraulic conductivity of ~4–7 cm/day. The resulting uncertainties in the correlations between nSSM and VSM are comparable with those from the agriculture study (Babaeian et al., 2019b) and regional studies in the United States (Babaeian et al., 2018) and China (Chen et al., 2020). The maximum reliable value of nSSM in our dataset to establish the nSSM–VSM relationships was ~0.5 because of the unavailability of S-2 data due to persistent cloud cover during and after heavy rainfall events when the soil approaches saturation. This is a source of bias in the linear regressions which can only be remedied by additional data. The permanent wilting point and field capacity are also critical reference points for soil moisture, but we have no data on these variables.

2.5.4 Satellite-Derived Surface Moisture TS for Land-Use Management

Whilst most land-use managers would probably prefer to work with temporal stability of volumetric soil moisture, this is not practical for high spatial resolution temporal stability analysis over large areas. VSM is the time-varying volumetric soil moisture that exists at a point in the soil. Satellite-derived VSM, predicted using correlations in Figure 2.4.4, are estimates of VSM at specific times and at specific locations/pixels of the in situ sensors. A map of predicted VSM for an area would have the same pattern of colours as the map of nSSM if (a) there is a perfect correlation, and (b) the residual and saturated VSM is constant over the whole area; the only difference would be in the values allocated to the colours in the colour bar. In OPTRAM, residual and saturated VSM are assumed to have the same value in every pixel with the same VI because vegetation is a major contributor to soil moisture in the top few cm. The OPTRAM's use of nSSM is attractive because it is based only on satellite data and its assumptions are transparent. The predicted VSM contains soil hydraulic parameters of residual and saturated VSM which are only appropriate for the limited number of pixels that contain the observed in situ VSM used in the validation. It is practically not feasible to create a map of VSM from nSSM without residual and saturated VSM observations at every pixel. Without these observations, spatial variations in residual and saturated VSM due to soil texture variations will not be captured over a broad study area. Any subsequent analysis of temporal stability based on the predicted VSM will be corrupted by introducing noise associated with spatial variations in hydraulic and soil texture properties over the area.

This study therefore used satellite-based normalized surface soil moisture temporal stability. It focused on areas of moderately- to poorly-drained soil within a pastoral system where surface moisture is closely linked to soil drainage and grass productivity (Tuohy et al., 2018). The deployment of livestock and machinery can be severely compromised in poorly draining soil (e.g., associated with ~ 50% of Irish farms) that can be saturated for prolonged periods of the

year, resulting in economic impacts on production. Forecasts of the most likely areas with saturated soils within a farm can support management strategies to locate artificial drainage, reduce the risk of soil compaction from grazing cattle (Paul et al., 2018) and minimise parasite infection of cattle (Naranjo-Lucena et al., 2018).

We suggest that the dominant factor leading to the \hat{W} patterns (Figure 2.4.7) is the near-surface soil texture, which controls soil hydraulic properties and the spatial distribution of soil moisture, particularly in wet conditions (Baroni et al., 2013). Terrain variations, which could drive sub-surface water flow are minimal, and time-varying net water flux patterns over two years are both unlikely to influence \hat{W} over these km-scale areas. A combination of seasonal changes, weather and time-varying management intervention of grass production is probably responsible for σ patterns.

The meteorological data (Figure 2.4.1) demonstrate that cumulative rainfall is higher in winter, and evapotranspiration peaks around the end of June in mid-summer and is minimum around the end of December in mid-winter; the mid-summer peak is inversely correlated with VSM at depth. Seasonal variation in nSSM probably follows this pattern, especially as the evapotranspiration is most active in the top few cm. Without claiming that these are representative of long-term (> 10 years) seasonal variations, they are probably the main causes of seasonal changes in net water flux, illustrated in Figure 2.4.5, e.g., by high net water flux at Rossmore in winter (1st March 2020) and low net water flux in summer (30th June 2018). The temporal stability maps (Figure 2.4.6) are based on 30 and 25 S-2 passes, respectively, over Rossmore and Stradone. Table A1 (supplementary information) shows that there are 19 S-2 passes in the 2 months either side of mid-winter and 14 S-2 passes in the 2 months either side of mid-summer. This is not substantial, but it is probable that there are unquantifiable biases in temporal stability statistics due to the limited period over which the data have been acquired.

More generally, surface moisture TS derived from S-2 optical data has implications for land use scenarios which require information on local areas that are significantly drier or wetter than the surroundings. These include indications for the onset of fires, drought, and flood risks, modelling hydrological processes, managing water resources, agricultural plant production and productivity, and sustaining ecosystem services (Vereecken et al., 2014).

TS analyses at sub-field level have mainly been confined to ground-based techniques (Abdu et al., 2017; Fry and Guber, 2020). Whilst other studies have used satellite radar to estimate soil moisture TS, mostly at coarser spatial scales (Mohanty and Skaggs, 2001; Rötzer et al., 2014; Wagner et al., 2008; Zhang and Shao, 2017), we have demonstrated that surface moisture TS derived from S-2 optical data can identify distinct natural areas at 10 m spatial scale. We note however that its efficacy at broader spatial scales (~ 500 m) is degraded due to an increase in vegetation mixtures with different water contents, and the reduction of variance in the data (Burdun et al., 2020b). The complexity of soil moisture TS results in agricultural fields over many scales and environmental conditions is well-summarised in Fry and Guber (2020).

The approach in this paper may have implications as global grassland systems are monitored for irrigation design and land use intensity (Lange et al., 2022; Reinermann et al., 2020). It is relevant for rewetting efforts in the European Union (EU, 2022) where member states are committed to restoring 20% of degraded ecosystems, including grassland and drained peatlands under agricultural use, after centuries of wetland loss due to artificial drainage (Fluet-Chouinard et al., 2023). Soil moisture information at ~10 m scale can also help target the rewetting of peatlands for carbon sequestration (Burdun et al., 2023; Ojanen and Minkkinen, 2020; Schwieger et al., 2021) which require assessments of soil moisture and drainage status prior to, during and after re-wetting efforts.

2.6 Conclusion

The paper demonstrated the potential of Sentinel-2 satellite optical data to provide meaningful retrievals of normalised surface soil moisture at a 10 m resolution in a region with persistent cloud cover. The study was conducted on moderately to poorly drained soil within a pastoral system where soil moisture is linked to soil drainage. The data were analysed using OPTRAM but required a re-assessment of the model to suit the wet conditions associated with heterogeneous land cover overlying soil with low hydraulic conductivity. The modification and validation of OPTRAM, and interpretation of the results are summarised below.

1. An exploration of four vegetation indices used in scatter plots of STR-VI identified EVI as the index which provided upper and lower boundaries (wet and dry edges, respectively) best suited to estimate normalised surface soil moisture. The wet and dry edges in the STR-VI space were clearly non-linear and could be characterised, for example, using a double logistic function.
2. The introduction of a time lag for the responses of in situ volumetric soil moisture sensors improved correlations with the normalised soil moisture by a factor of ~ 2 but only if S-2 data were used at the start of a dry-down period. The time lag was estimated from a semi-empirical solution to the Richards' Equation and measurements of residual and saturated soil moisture from field soil samples. The results are comparable with other validation studies despite the sparse sensor networks in this study.
3. Retrievals of OPTRAM normalised surface soil moisture are most suited to temporal stability analyses, given the absence of regular time series of satellite optical data in cloudy regions.
4. An interpretation of the surface soil moisture temporal stability, where local topographic controls on subsurface-water flow are negligible and the vegetation type is uniform, suggest that local areas are systematically wetter or dryer than their

surroundings. This is associated with local drainage, hydraulic conductivity and soil texture.

These techniques are useful for any grassland sites in temporal climates and may be extended to other applications for agricultural and land-use management, including the identification of areas at risk from extreme natural events (drought, flooding), soil compaction, parasite infection associated with ruminant grazing, land rewetting for carbon sequestration and input into crop growth models.

Chapter 3: Identifying favourable conditions for farm scale trafficability and grass growth using a combined Sentinel-2 and soil moisture deficit approach

Rumia Basu^{1,3}, Owen Fenton², Eve Daly³, Patrick Tuohy^{1*}

¹ *Vista Milk SFI Research Centre, Teagasc, Moorepark, Fermoy, Co. Cork, Ireland*

² *Environmental Research Centre, Teagasc, Johnstown Castle, Wexford, Co. Wexford, Ireland*

³ *Earth and Ocean Sciences, School of Natural Sciences, University of Galway, Ireland*

***Correspondence:**

Patrick Tuohy

patrick.tuohy@teagasc.ie

Accepted for publication in *Frontiers in Environmental Sciences* **2024**,
<https://doi.org/10.3389/fenvs.2024.1331659> (in press)

3.1 Abstract

In Atlantic Europe, on poorly drained grasslands soils, compaction negatively affects soil health when trafficked in wet conditions, while optimum grass growth cannot be achieved in excessively dry conditions. In Ireland, daily soil moisture deficit (SMD) information is forecasted at regional scale for all soil drainage classes. Optimal paddock conditions can occur between trafficking (10 mm) and optimum grass growth (50 mm) SMD thresholds for an identified drainage class. The objective of this farm scale study is to improve the identification of optimum conditions in time and space by combining high resolution spatial soil moisture estimates with soil drainage class specific SMD data. For that purpose, Sentinel-2 (S-2) data was used in a modified Optical Trapezoid Model (OPTRAM) to derive normalised surface soil moisture (nSSM) estimates at farm level. In-situ soil moisture sensors providing daily estimates of volumetric soil moisture were used for validation of OPTRAM with an RMSE of 0.05. Cumulative 7-day SMD prior to the date of each S-2 image was analysed for each year from 2017-2021 to select nSSM maps corresponding to negative, 0 or ~0 and positive SMD. Results

established a relationship between nSSM and SMD indicating optimal conditions changed spatially and temporally. The months of April, May, August and September always presented at least 35% of the farm area available for optimum management operations. Future refinement of this methodology utilising daily high resolution remote sensing data could provide near real-time information for farmers.

Keywords: Grassland, Heavy Soils, Remote Sensing, Decision support, OPTRAM

3.2 Introduction

Globally, grasslands are one of the major ecosystems, covering one-third of the earth's landmass (Bengtsson et al., 2019; Lemaire et al., 2011). In Europe, permanent grasslands cover 34% of the agricultural area and provide a wide variety of ecosystem services (Habel et al., 2013; Schils et al., 2022). They are also diverse due to natural factors such as climate and soil, but also due to varying intensities of management practices resulting in gradients of fertilisation and grazing intensities (Blüthgen et al., 2012). Permanent grasslands in Europe have been the main source of livestock production and nutrient cycling on farms for centuries (Hejcman et al., 2013; Schils et al., 2022). Grass remains the cheapest source of high-quality feed for meat and dairy production (Schils et al., 2022).

In Atlantic Europe, excess of soil moisture is the main biophysical constraint to farm management (Schulte et al. 2012) and one of the main grassland soil threats is compaction induced by animals and machinery traffic, especially when the soil is excessively wet (Lepore et al., 2023; Newell-Price et al., 2013; Piwowarczyk et al., 2011; Tuohy et al., 2015). Over 90% of the agricultural land in Ireland consist of grasslands, pasture or hay which are an important source of feed for Irish livestock (Bondi et al., 2021). In Ireland, 56% of the livestock farms contain land classified as Less Favourable Area (areas that are difficult for cultivation

because of natural factors such as steep slopes, soil productivity, etc.) (Schulte et al. 2012) and 30% of grasslands are on poorly drained soils (Teagasc, 2021b)

Soil moisture is commonly expressed in terms of soil moisture deficit (SMD), which is the amount of rainfall (mm) required to return the soil to field capacity (FC) i.e., the volume of water that can be present in the soil against gravity. SMD is independent of pore space or rooting depth and can be used as a proxy for volumetric water (VW) content and requires fewer variables for measurement as compared to VW (Herbin et al. 2011; Schulte et al. 2012). In Ireland, Schulte et al. (2005,2015) developed the hybrid SMD model for grassland capable of predicting daily SMD applicable to five soil drainage classes. At present, Met Éireann (National Meteorological Service) utilises this model and publishes daily SMD values across all soil drainage classes at regional scale. Daily SMD values can vary between -10 mm to 110 mm. For the farmer, this regional scale information can inform paddock scale decisions when the paddock soil drainage class is known. In terms of management decisions at -10 mm the soil is sub-optimal and saturated, between 10 and 50 mm the soil presents as optimal while drought like conditions are evident around 75 mm and the wilting point is reached at 110 mm (Schulte et al. 2012). The 10 mm and 50 mm thresholds are important from a farm management perspective and can be observed for any paddock of known drainage class. Although thresholds exist for SMD conditions related to soil and crop health, no such thresholds have been defined for soil moisture content.

Satellite remote sensing technology provides a mechanism to measure soil moisture at sub-field (100's m²), sub-catchment (0.1–1 km²) and catchment (1–80 km²) scales. Many optical satellites such as Landsat , Sentinel-2 etc. offer high resolution data that has been used to estimate soil moisture (Urban et al., 2018; Wang et al., 2020; West et al., 2018). High resolution microwave sensors such as Sentinel 1 have the added advantage of operating in all weather conditions and have been used to estimate high resolution soil moisture (Bhogapurapu

et al., 2022; Chaudhary et al., 2022; Singh et al., 2020). Such technologies can help bridge the gap in existing decision support systems (e.g. hybrid SMD model coupled with farmer knowledge of paddock specific soil drainage class) by providing real or near real time spatial and temporal information to farmers about on-farm optimal operational conditions. However, both optical and radar satellites have limited penetration capabilities (Mohanty et al., 2017) and have been evaluated for soil moisture estimation at coarser spatial scales, especially with microwave sensors (Wang and Fu, 2023). Thus, they have restricted abilities at finer spatial and temporal scales, and therefore cannot be used for precision-agricultural applications (Babaeian et al., 2019b). This is especially true for Ireland where persistent cloud cover is a reality.

The objective of the present study is to develop a methodology and application at high spatial resolution, whereby areas of a farm that are indicative of optimal/favourable trafficable and grass growth conditions can be identified both spatially and temporally. This is achieved by using a combination of daily SMD data which gives temporal information and Sentinel-2 derived normalised surface soil moisture (nSSM) which provides high resolution spatial information (10 m) on soil moisture conditions on the farm. The focus of the study is a dairy grassland farm in Ireland dominated by poorly drained heavy textured soils which tend to remain wet for very long periods especially after a rainfall event. Existing models for farm management are based on SMD thresholds alone and advisories for farm management in Ireland are based on these SMD thresholds (Met Eireann, 2023). Since SMD values do not have a spatial component/spatial information, any decision support tool based on SMD alone does not include spatial information crucial for decision making on the ground. To address this knowledge gap and to improve existing forecasts based on SMD estimates, this study uses optical satellite data from Sentinel-2 to estimate high-resolution normalised surface soil moisture (nSSM) using the Optical Trapezoid Model (OPTRAM) in conjunction with existing

SMD based models. Estimates of nSSM are combined with an SMD model to define specific soil moisture thresholds for grass growth and trafficability on this farm to develop a decision support tool for farmers for designing targeted paddock-based management intervention. This study is aimed at developing soil moisture thresholds for defining favourable farm management conditions using a combined nSSM and SMD approach. The results are validated using in situ soil moisture data and through regular monitoring of farm conditions.

3.3 Materials and Methods

3.3.1 Study Area

The study farm (40 hectare (Ha)) is located in Rossmore, Co. Tipperary (52° 36'N, 8° 01'W) and is part of the Teagasc Heavy Soils Programme (HSP) (Teagasc, 2021b). The farm mostly has a flat terrain and receives approximately 980 mm of rainfall annually. Annual grass production on this farm in 2022 was 13178 kg DM/Ha, being 11608 kg DM grazed and 1570 kg DM as silage conserved (Dry matter (DM) is the grass/silage remaining after removal of water content).

A soil survey at paddock scale was conducted on the farm in 2015, with every paddock assigned to a soil subgroup and associated drainage class in accordance with protocols developed for the Irish Soil Information System (ISIS) project. The ISIS project was established in 2008 with the objective of constructing a national soil map at 1:25,000 scale to provide spatial and quantitative information about the soil type in Ireland. All the soils belong to one of the 11 soil Great Group and can be further classified into sub-groups (Environmental Protection Agency, 2014; Simo et al., 2008). Mapping of the soil type for each paddock on the farm was carried out using an auger and test pit survey. For every Ha (0.01 km²), an auger bore was driven into the soil to a depth of 1m and soil features such as colour, texture, mottling etc. were recorded and soil type and drainage class (as shown in Figure 3.3.1(B)) assigned. Additionally, 3-4 soil pits, each at depth of 1-2m were dug on the farm to further analyse the dominant soil type

(Teagasc, 2021b). The dominant soil subgroup is Surface-Water Gley, which are wet, acidic soils and have gleying within 40cm (Teagasc, 2014). The soil texture is mostly sandy loam and the paddocks are generally poorly drained (i.e., those that are saturated during a rainfall event and continue to hold excess water for multiple days after such events), except for paddocks 8,10 and 21 (Figure 3.3.1(B)) which are well drained (i.e., those that hold excess water during a rainfall event but not afterwards) (Schulte et al. 2015; Tuohy et al. 2018). Knowledge of the paddock drainage class enabled the correct SMD values to be assigned to each paddock.

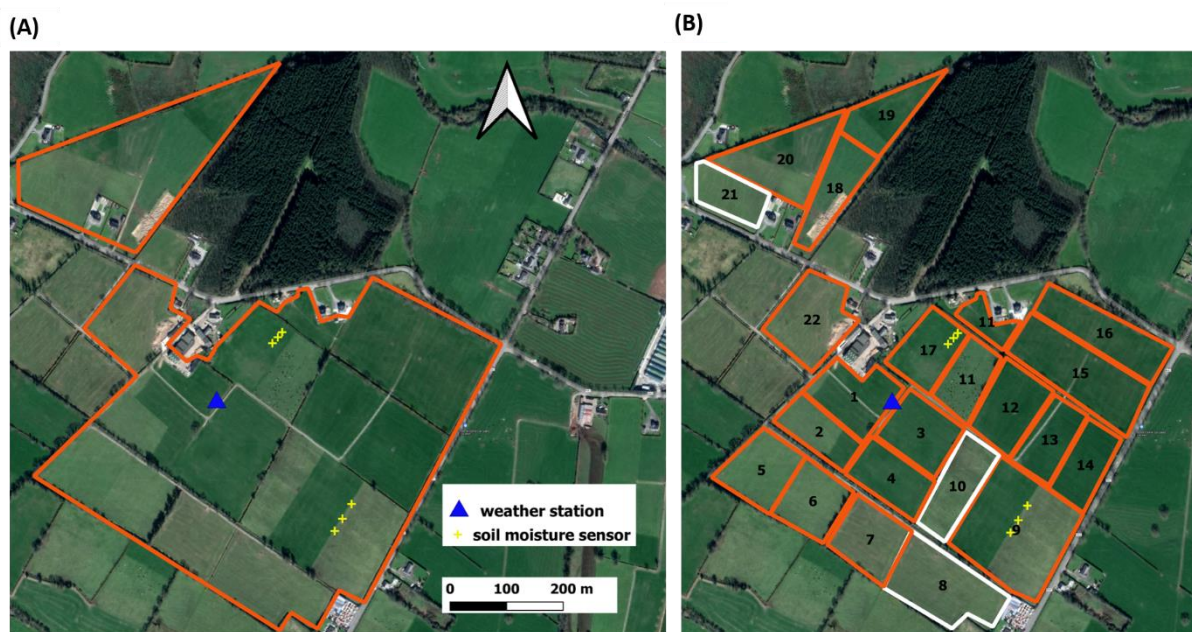


Figure 3.3. 1: (A) Study area is within the orange polygon (B) paddock boundaries and paddock drainage class distribution in the study area i.e. orange paddocks are poorly drained and white paddocks are well drained

3.3.2 Satellite and in-situ data for estimation and validation of normalised surface soil moisture (nSSM)

Optical data from Sentinel-2 (S-2) is used in an Optical Trapezoid Model (OPTRAM) to estimate normalised surface soil moisture (nSSM) for the study area. The farm is equipped with in-situ soil moisture sensors, installed at a depth of 15cm, providing daily estimates of

volumetric soil moisture (VSM), based on soil resistivity and capacitance (Sensoterra, 2022), used for validation of OPTRAM. S-2 level 1 C product (ESA, 2013) was downloaded from the United States Geological Survey (USGS) Earth Explorer website (“USGS Earth Explorer,” n.d.). The level 1C products comprise of ortho-rectified, Top of Atmosphere (TOA) reflectances, based on a UTM/WGS 84 projection reference system (Baillarin et al., 2012). The images were selected based on an initial visual interpretation of cloud cover and through an analysis of daily rainfall and Evapotranspiration (ET) data available from weather stations installed on the study area so as to ensure that the data represented all weather conditions for the study area, covering both wet and dry periods. A total of 30 S-2 images were downloaded from 2017-2021, that included cloudy and cloud-free data.

All the S-2 level 1C products were atmospherically corrected in QGIS using the Semi-automatic Classification Plugin and the Dark Object Subtraction (DOS) algorithm (Chavez, 1988; Gilmore et al., 2015). The cloudy Sentinel-2 data were masked using a cloud mask available with the Sentinel 1 C product as part of the quality information (Coluzzi et al., 2018).

3.3.3 OPTRAM

OPTRAM was developed to estimate soil moisture using satellite data. OPTRAM (Sadeghi et al., 2017a) is an improvement over the Thermal-Optical Trapezoid Model (TOTRAM), which is one of the most popular approaches to mapping soil moisture using remote sensing. OPTRAM improved TOTRAM by replacing Land Surface Temperature (LST) in TOTRAM with the short wave infrared band as a measure of soil moisture, thereby, eliminating the need for calibration of each satellite observation since LST depends on parameters such as surface air temperature, wind speed and relative humidity (Mallick et al., 2009). This modification makes OPTRAM suitable to be used even with those satellites that do not have a thermal band (Sadeghi et al., 2017a). OPTRAM has been found to perform better than TOTRAM (Burdun

et al. 2020) with the former reaching positive pearson's correlation values of upto 0.8 and the latter with low negative correlation values with water table depth. This model uses vegetation index (VI) and the Shortwave Transformed Infrared Reflectance (STR), calculated from short wave infrared (SWIR) band to map soil moisture in the STR-VI space., STR has been tested successfully for its sensitivity to soil moisture over vegetated surfaces, assuming a linear relationship between soil and vegetation water content. Though, originally developed over arid and semi-arid climatic conditions, in recent years, OPTRAM has been successfully applied over a variety of land cover including wetlands and peatlands (Mokhtari et al. 2023; Burdun et al. 2020; Burdun et al. 2023). Similarly, Basu et al. 2024 also applied OPTRAM to estimate soil moisture in the same study site as in this paper, which is also dominated by wet conditions.

Studies have shown that the VI-STR relation for high vegetation cover may be non-linear (Hassanpour et al., 2020; Stańczyk et al., 2023) and that non-linear parametrization of OPTRAM lead to better accuracies in soil moisture estimates as compared to linear parametrization (Ambrosone et al., 2020). Following from such studies, this study also modified OPTRAM by using a non-linear double logistic function instead of a linear function to determine the wet and dry edges in the STR-VI space. In this study, S-2 band 12 (i.e., SWIR band centred at 2190 nm) has been used to compute STR. The normalised surface soil moisture (nSSM) for each pixel is calculated as a linear distance between the dry edge and the wet edge as:

$$nSSM = (X - d) / (w - d) \quad \text{Equation 17}$$

where, X is the STR of the pixel for which nSSM is to be calculated, d is the STR on the dry edge curve and w is the STR on the wet edge curve. All other pixels would thus, have nSSM values between 0 and 1, with the assumption that pixels on the dry edge would correspond to a value of 0 and those on the wet edge would correspond to a value of 1 and that oversaturated pixels are not considered.

Additionally, another modification made to OPTRAM in this study is the use of the Enhanced Vegetation index (EVI) instead of the Normalised Difference Vegetation Index (NDVI) as used originally in OPTRAM. EVI has several advantages over NDVI especially with respect to saturation issues over vegetated lands, where its sensitivity decreases with increasing biomass (Antunes Daldegan et al., 2020; Ojha et al., 2021; Rocha and Shaver, 2009) and based on class separability, it has also been shown to be an optimum VI for studying Irish grassland using S-2 data (Saadeldin et al., 2022). nSSM maps for the farm were obtained at a spatial resolution of 10m (Figure 3.4.2). The model has been validated using volumetric soil moisture data from in-situ soil moisture sensors installed on the farm. There are 6 in situ soil moisture sensors installed on the farm at a depth of 15cm, providing daily estimates of volumetric soil moisture. An RMSE of 0.05 and a correlation of 0.4 was obtained between modelled nSSM and in situ volumetric soil moisture (Basu et al., 2024a). The range of volumetric soil moisture is between 0.1-0.6 m³/m³. Further details about the methods and validation of OPTRAM used in this study area is available in Basu et al. 2024.

3.3.4 Soil Moisture Deficit (SMD)

SMD is calculated using the grassland hybrid model of Schulte et al.,(2005,2015) using site specific data from the meteorological weather station on the farm i.e. daily max and min temperature, rainfall, wind speed and solar radiation. It is a water mass balance model that calculates SMD from a cumulative balance of rainfall, evapotranspiration and drainage:

$$SMD_t = SMD_{t-1} - Rain_t + ET_t + Drain_t \quad \text{Equation 18}$$

Where, , SMD_t and SMD_{t-1} are SMDs on day t and t-1 respectively in mm. $Rain_t$ is the daily rainfall (mm/hr) , ET_t is daily actual evapotranspiration (mm/hr) and $Drain_t$ is the water that is drained daily through percolation and/or surface flow. Daily estimates of rainfall and ET from the weather station on the farm is used in this model that enable daily SMD to be calculated

for individual paddocks on the farm for three drainage classes: well-drained, moderately-drained and poorly-drained. For a well-drained soil/paddock, SMD would never exceed the field capacity (SMD = 0 mm), a moderately drained paddock takes 24 hours after a rainfall event to reach field capacity and a poorly-drained paddock can take up to days to achieve the same (Schulte et al. 2005).

As paddocks on the farm are either poorly or well-drained (Figure 3.3.1(B)), the SMD model was run for these two drainage classes for the years 2017-2021, co-incident with the time period of S-2 data. The SMD time series for the farm represents temporal information where each value in the time series is a value/point in time and does not have a spatial component. SMD values in general can be interpreted as follows: negative SMD represents wet soils/ wet conditions on the farm, 0 or nearly 0 SMD represents field capacity (FC) i.e., the maximum amount of water a soil can hold against gravity and positive SMD represents dry soil/ dry conditions on the farm. More specifically, at an SMD of -10mm, the soil is considered saturated, percolation commences at 0mm, and the hydraulic conductivity increases from 0 SMD to a maximum value (soil saturation) which is specific to a drainage class (Schulte et al., 2005,2012).

3.3.5 Development of optimal thresholds using nSSM and SMD

To develop a relationship between nSSM and SMD, firstly, a cumulative sum of 7-day SMD prior to the date of each S-2 image collected in the period from 2017- 2021 was calculated. This helped in selecting specific S-2 dates from the time series which corresponded to negative, 0 and positive SMD values, covering the entire range of SMD conditions on the farm for the study period. 11 such S-2 images were finally selected out of the 30 available S-2 images that represented very wet to very dry conditions of soil moisture on the farm. To calculate a relationship between SMD and nSSM, two linear regression models were developed between

mean nSSM for the 11 selected S-2 images for the farm and the corresponding SMD estimates on those 11 dates for poorly and well drained soils, respectively. This model was run using the `lm` function from the `stats` package in R (The R Foundation, 2018). The mean nSSM was calculated as a spatial average of all the pixels on a particular day covering the farm. This enabled direct comparisons between the time series of SMD and mean nSSM.

As discussed previously, values in literature suggest that 10 mm and 50 mm are the thresholds that represent conditions of restricted trafficability on soils (Vero et al. 2014; Schulte et al. 2012) and grass growth, respectively (Teagasc, 2021c). Any SMD value between these two thresholds should be considered an optimum “window of opportunity” for both soil and crop. Therefore, SMD thresholds of 10 and 50 were applied to each of the two regression models to arrive at corresponding nSSM thresholds of 0.235 and 0.315 respectively. Thus, three categories (i.e., <0.235 , $0.235-0.315$ and >0.315) of nSSM were obtained corresponding to “excessively dry”, “optimum” and “excessively wet” conditions respectively. Proportions of farm area falling under each of these nSSM categories were calculated. The middle category of nSSM ($0.235-0.315$) represents the optimum “window of opportunity” in terms of safe soil and crop utilisation on the farm and will be referred to as the “optimum” category in this study henceforth. The optimum nSSM category represents general favourable conditions for trafficability and grass growth in the study area. A flowchart of the methodology is presented in Appendix (Figure A1).

The patterns of soil moisture in the optimum nSSM category as well as in the other categories are shown in Figure 3.4.2. These results have been validated using expert knowledge about the drainage and soil characteristics of the farm as well as by interaction with farmers. Since the farm is part of the Teagasc Heavy Soils Programme, there is complete access to and detailed knowledge about farm conditions and data such as SMD, weather, and farm management activities. These farms have been visited multiple times throughout the year during the study

period and have been visually assessed for soil moisture conditions during those times which confirm to their respective drainage classes at that time. This fine scale knowledge and data was used to validate the results.

3.3.6 Calculation of proportion of farm area within the optimum category at a daily time step

To examine the proportion of farm area within the optimum nSSM category, a piecewise linear regression function (from segmented package in R) (Muggeo, 2008) was fitted between the proportion of farm area in the optimum category of nSSM for the 11 selected S-2 images (as obtained in section 2.5) and the corresponding SMD on these dates. Using this function, the proportion of farm area falling within the optimum category was predicted at daily time steps from the daily SMD estimates. The daily values were averaged into monthly values for the time series to identify trends of trafficability and grass growth for the farm across the time series (Figure 3.4.5).

3.4 Results

3.4.1 Optimal threshold range for nSSM

3.4.1.1 Regression between SMD and nSSM

Figure 3.4.1 ((A) and (B)) show the linear regression models between mean nSSM of the 11 selected S-2 images and the corresponding SMD for both poorly and well drained soils, respectively. The slopes for both soil types is identical (0.002) and the intercept is similar with minimal difference. The co-efficient of regression is highly significant for both soil types. However, since most of the paddocks on the farm are poorly drained (Figure 3.3.1(B)), the regression model for the poorly drained soil type was finally selected for all subsequent analysis and this model was used to calculate thresholds for soil moisture regime based on SMD thresholds of 10 mm and 50 mm.

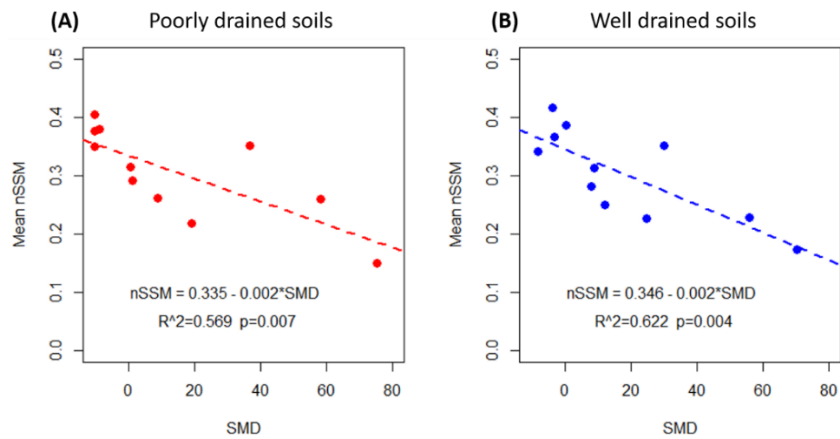


Figure 3.4. 1: Linear regression between SMD and mean nSSM for (A) poorly drained and (B) well drained soils.

Three categories of nSSM values .i.e., “Excessively Dry” (<0.235), “Optimum” ($0.235-0.315$) and “Excessively Wet” (>0.315) were obtained from the regression model between mean nSSM and SMD. For each of these categories, the proportion of farm area falling within the particular category was calculated as shown in Table 3.4.1. The optimum category of nSSM ($0.235-0.315$) corresponding to SMD between 10mm and 50mm represents the moisture range for optimum soil and crop conditions on the farm.

3.4.2 Spatial and temporal patterns of nSSM on the farm

Examples of nSSM maps for negative, ~ 0 , within the optimum range and maximum SMDs in the time series are shown in Figure 3.4.2. The maps show spatial variability of nSSM in the farm for different SMD conditions. It is important to note that this spatial variability is not paddock specific and shows a spatial continuum. The optimum category of nSSM ($0.235-0.315$), is coloured in low to high shades of green. As can be seen from the figure, this green region is spatially variable across the farm under different conditions of SMD and merges across paddocks. Blue areas on the farm represent wetter than the optimum condition and red areas correspond to drier than optimum conditions. Specifically, the soils in the blue regions on the farm would be susceptible to poaching/surface damage in case of trafficking by animals

or machinery while those in the red region are mostly limited by grass growth potential with trafficability not being a key constraint (although compaction may remain a risk to soil health).. It is interesting to note that even on the day of highest SMD (75.4 mm), which represents very dry conditions and in this case, almost a drought situation, there is still a small proportion of the farm where the soil moisture status is such that grass growth is not restricted. Similarly, on a relatively wet day (SMD -10 mm), small patches of green and red areas can be seen. Most of the red regions on this image correspond to man-made features such as the fringes of the farm yard or farm roads, while the green regions represent soil within the optimum category. It is also important to understand that on the ground, the green region representing ideal soil conditions is not a rigid boundary and would merge with other classes of nSSM preceding and following it.

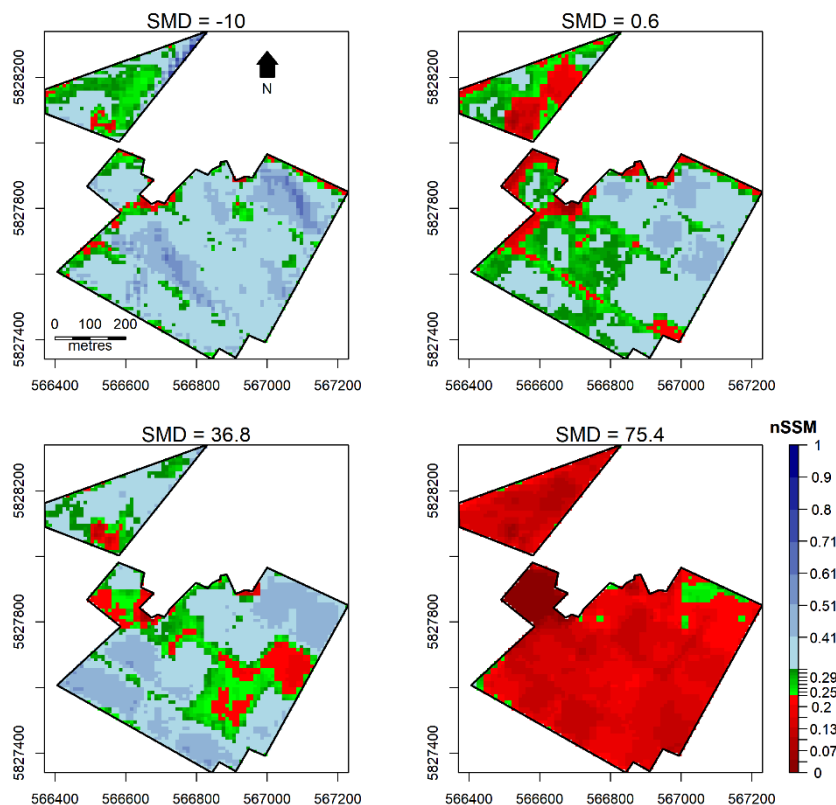


Figure 3.4. 2: Example of nSSM maps for negative, ~0, optimum category and positive SMD. Green regions represent soil in the “optimum” category, blue regions represent wetter than optimum conditions and red region represent drier than optimum conditions. Units of SMD are in mm.

3.4.3 Relationship between proportion of farm area in the optimum category and SMD

Figure 3.4.3 (A and B) shows the piecewise regression between proportion of farm area in the optimum, and drier and wetter than optimum category of nSSM, respectively, for the 11 selected S-2 images and the corresponding SMD on these dates. In the absence of a daily S-2 time series, this model was used for predicting daily farm area proportions in the optimum nSSM category. This ensured that the temporal scale of SMD and nSSM time series matches, necessary for identifying trends of trafficability and grass growth (Figure 3.4.4). The variability in scatter in Figure 3.4.3 is evident, with SMD values greater than 0 showing an almost linear relationship with optimum farm area proportions. We, however, retain all observations to not further limit the data points and also to avoid introducing any bias in the model. The model was able to explain 76% (R^2) of the observed variability. The residual standard error of the model was 9.125 on 7 degrees of freedom. The Cook's distances (Martín and Pardo, 2009) were less than 1 and hence individual observations did not unduly influence the model fit.

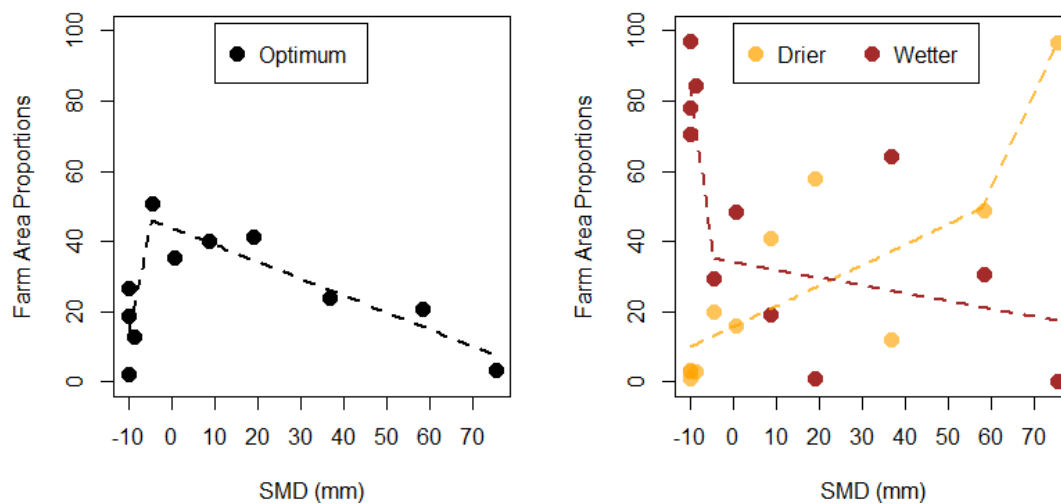


Figure 3.4. 3: (A) Proportion of farm area in the optimum category of nSSM.(B) Proportion of farm area in the drier and wetter than optimum category. Note: Dashed lines are the piecewise regression model between the variables.

Figure 3.4.4 shows the time series of the daily estimates of farm area proportions in the optimum nSSM category predicted using the piecewise regression model (Figure 3.4.3). This proportion ranges from 20 to 50 % during the study period. Generally, the proportion of area deemed optimum peaked between the months of April- October, with up to ~ 50% of the farm area being within the optimum category of nSSM in these months across the study period. In other words, up to half of the farm would have been optimal for carrying out farm management operations safely for both soil and crop in this period. This proportion is relatively low for the year 2018 in these months (between 10 to 40% vs ~ 50% in the other years) as expected since this was a year of extreme weather variability in Ireland when persistent rain in spring and early summer gave way to drought conditions by mid-summer. As such soil moisture conditions fluctuated towards the extremes more commonly than in other years.

Figure 3.4.5(A) and 3.4.5(B) show the monthly mean proportions of farm area in the optimum nSSM category for the time series for the months of January-June and July-December respectively. In the study period, the months April, May, August and September typically saw the best conditions where soil moisture was at an optimum level over a wider area and excessively wet or excessively dry conditions are avoided. In these months, approximately 35% of the farm area was in the optimum nSSM category at all times during the period of analysis. This percentage is slightly less for the year 2018, especially for August (Figure 3.4.5(C)) due to the extreme conditions as mentioned earlier. Typically, the months of October to March are limited by excessively wet conditions while June and July have seen severe moisture deficits. Increasing variability in climate and localised weather imposes extremes in the typical soil moisture regimes in a given year.

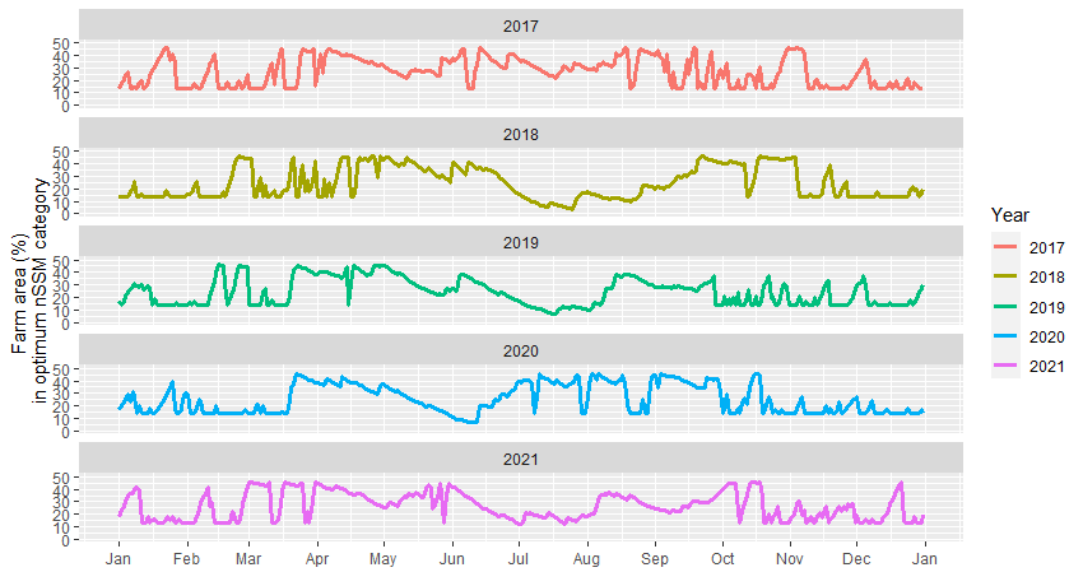


Figure 3.4. 4: Daily estimates of farm area proportions (%) in the optimum nSSM category between 2017 and 2021, calculated using the piecewise regression function between nSSM and SMD.

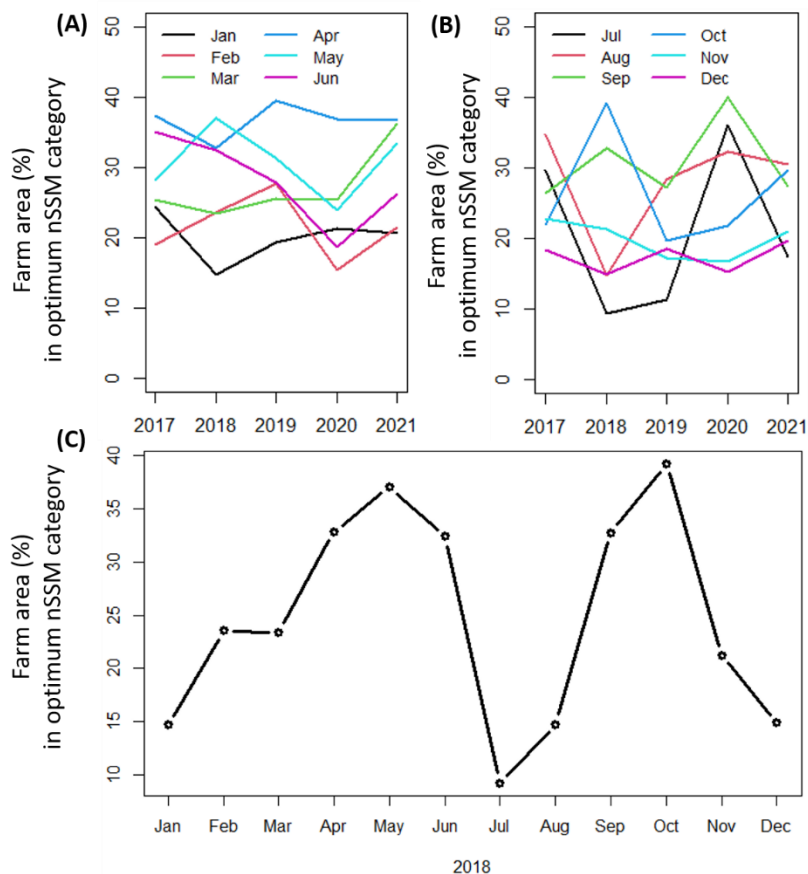


Figure 3.4. 5: (A) Monthly mean proportions of farm area in the optimum nSSM category from January-June of the time-series, (B) Monthly mean proportions of farm area in the optimum nSSM category from July-December of the time-series (C) Monthly mean proportions of farm area in the optimum nSSM category for the year 2018.

3.5 Discussion

3.5.1 Overall advantage of using optimal nSSM thresholds ranges over SMD alone

SMD based decision support tools are valuable for aiding decision making, where the farmer has knowledge of the drainage class of individual paddocks. Examples of where the SMD tool was used include Piwowarczyk et al. (2011) who used this model to predict the risk of damage from animal grazing on grassland soils and Vero et al. (2014) used this model to determine SMD thresholds, incorporating it into a decision support tool for trafficability and slurry spreading on farms. This model has also been used to monitor nitrous oxide emissions from grassland sites in Ireland, showing that higher soil moisture on the day of fertiliser application tends to increase average annual emissions (Hawkins et al., 2007). Estimates of SMD obtained from this model has also been used to identify opportunity for spring application of slurry in Ireland (Lalor and Schulte, 2008). A study in Ireland confirmed the effectiveness of such a decision support system which when combined with farmers' local knowledge about drainage conditions of paddocks on their farms helped in reducing nutrient losses and managing slurry spread so as to increase nutrient uptake by plants (Kerebel et al., 2013). However, as discussed previously, current decision support tools based on SMD alone have a temporal component only. This is a crucial knowledge gap because information on spatial variability of soil moisture conditions is also important for effective farm management. Figure 3.4.2 also confirms that on a particular day for a single value of SMD, the patterns in nSSM are not same and vary through the spatial extent of the farm. This means that it is prudent to use the SMD model within the current methodology and to combine it with soil moisture content information as shown in this study to produce the nSSM categorisation for optimal operational conditions, and produce both temporal and spatial information. This new technique as proposed in this study moves beyond the physical boundaries of paddocks and displays data at a higher resolution in space and time, and would thus help in taking more informed decisions for farm management.

By including high resolution soil moisture data, this study showed that moisture regimes are not paddock specific. The national advisory in Ireland that generates valuable advice for safe farm management issues one set of rules/advice at a regional scale based on SMD values. However, Figure 3.4.2 shows that for a single value of SMD which is specific to a particular drainage class, the soil moisture regime within the same drainage class also varies in space, and exhibits a continuum, i.e., not following paddock boundaries. Therefore, management decisions should also vary within a paddock depending on the soil conditions and such information could guide farmers in devising farm management strategies on their farms. Decision support systems based on SMD alone, though useful, may not always suffice because not all areas on the farm behave uniformly at a given day/time and can sometimes lead to under-utilisation of resources. This study shows that across the time-series, most of the years had around 50% of farm area with soil conditions that were at a lower risk of compaction as compared to very wet conditions. Thus, these areas could have been accessed safely, providing optimal management conditions. Using this improved decision support system which uses high resolution soil moisture estimates together with SMD data, farmers can ensure complete utilisation of farm resources, not having to restrict operations on the farm entirely. As shown in this study (Figure 3.4.2), even on driest days, farmers can identify certain parts of the farm that are optimum for grass growth and can for example, design targeted fertiliser applications to those areas. Similarly, on a wet day (SMD = -10 mm), the green regions represent soil within the optimum category probably due to topographical features, which are at a higher elevation than the surroundings and slope to either sides. This would minimise usage of excessive chemical fertilisers, thereby reducing emissions from the farm, particularly with respect to chemical nitrogen (N) fertilisers. This has important implications for Ireland to meet the Government's Climate Action plan that aims to reduce chemical N fertilisers. As other information is available on soil moisture through the use of remote sensing techniques this

offers finer scale possibilities i.e. moving away from paddock specific outcomes to those that may change for the same paddock over time and space. Increasing variability in climate and localised weather imposes extremes in the typical soil moisture regime in a given year. This offers challenges to standard farm management practices and results in increased volatility, which impose significant stresses on the farm system. Soil moisture data can help us understand recovery rates of farms to get back within the “optimum window of opportunity” after a stress event, such as a drought, as was the case in 2018. This information can also help improve existing decision support tools, such that, depending on recovery rates of different areas on farms, targeted actions could be taken for farm management and precision farming such as grazing management, fertiliser applications, etc. Farmers can adopt a number of strategies to cope with sub-optimal conditions, which at either extreme (wet or dry) require supplementary feed and additional labour. However, further support in decision making would ensure optimisation of management to increase overall system sustainability, efficiency and profitability. This is particularly important in light of efforts to mitigate the environmental impacts of agriculture in line with agreed targets and as weather extremes (saturated soils and drought) are likely to occur with greater frequency in coming years. This model would be most effective in designing precision agriculture strategies across the world and when tested across study sites, it would be able to reveal influence of local climatic conditions or management regimes such as irrigation.

3.5.2 Future Research

The first step would be to test this improved decision support tool on other farms in Ireland, especially those dominated by poorly draining soils and then expand this methodology to similar farms across the world. The thresholds of nSSM obtained in this study could be tested on other farms of the Teagasc HSP sites to ascertain if the same moisture conditions are valid across the farms for trafficability and grass growth. Since, all HSP sites have similar soil and

drainage characteristics, this would help improve the model if needed and make it more robust. A study similar to Kerebel et al. (2013) could be designed where farmers' knowledge about drainage conditions on these farms could be used to validate the results from this tool. It would also be interesting to test "before and after" scenarios to understand if the farmers were able to utilise their farm resources more optimally after using this tool and not having to restrict operations on the farm during certain times of the year. It would be hugely beneficial if the farmers could practically use spatial maps as generated in Figure 3.4.2 to identify optimum areas on their farm for crop growth and trafficability. The next step in the development of this tool would be to use daily high-resolution images such that a daily high resolution trafficability and productivity map can be made available to farmers. This could be achieved using drones and would be especially helpful in countries like Ireland where persistent cloud cover makes it difficult to obtain long time series of optical remote sensing data. Daily images would help match the temporal scale of SMD data, ensuring better comparison between the two variables (SMD and nSSM) and would, thus, help improve the accuracy of the model. This is a subject of further research and could lead to the development of a predictive decision support tool for farmers not just in Ireland but across the world, especially in regions where targeted irrigation (precision agriculture) is essential for achieving food security. Similarly, a comparison of Figure 3.4.3 across different farms over time could reveal management differences, and it would be worthwhile to check if such information could help tackle extreme events such as droughts. Additionally, this study acknowledges that even in Atlantic climates like Ireland, droughts are becoming a recurrent phenomenon (Antwi et al., 2022), which would result in soil compaction in dry soils. Thus, the model would have to be updated to account for such conditions and new thresholds might need to be defined for favourable trafficability and grass growth conditions. Along with trafficability, it would also be important to assess risk of compaction in soils even under trafficable conditions, with the help of available tools like

Terranimo (“Terranimo,” n.d.) which helps assess soil compaction by agricultural vehicles, taking into account soil and vehicle properties such as clay content, tyre pressure, etc. Such decision support tools could be improved even further if local meteorological data is available for the farm representing accurate local weather conditions, improving predictions. To test this new decision support system, it would be important to test this model on a subset of farms to test different scenarios a) how well farmers local knowledge of their farms matches with the predictions from the existing SMD model with regards to accessibility of the farms b) if the predictions from the new model that also combines estimates of soil moisture with SMD can help in achieving higher productivity from their farms.

A major threat to soil quality on farms in Ireland is from trafficking by machinery and grazing by animals. Most of the damage happens in the form of short-term compaction of top soil or long-term depth compaction. Bondi et al. (2021) developed a national Soil Trafficking Intensity Index in Ireland for Compaction (STIC) which is a sum of compaction from machinery and grazing to identify which management regime poses more threat to soil structure and also the levels of such management intensities that “soil can cope with” based on soil conditions. In general, it was found that grazing management has much lower risk of soil compaction because though the pressure by animals is greater on soil as compared to machinery, the pressure is evenly distributed on the farm as opposed to localised pressure by heavy machinery. Farmers also thus follow grazing management regime in Ireland. However, for poorly drained soils as in this study, a closer investigation is required because such soils are in particular more impacted by trafficking from both management operations. Combining this index with the proposed decision support tool could be especially valuable for managing soil and crop health on poorly drained soils. This could provide support to different stakeholders such as farmers, contractors and policy makers by providing high resolution spatial information on soil condition on farms to develop tailored management response within farms. Alternatively, since

the reliability of STIC depends on field scale data, a high resolution soil moisture estimate could help improve this index.

3.6 Conclusion

This study presents one of the first attempts to assess optimised management capabilities at the farm level and is a proof of concept for improving existing decision support tools for farm management applications using estimates of both SMD and soil moisture regimes. This study focusses on a site dominated by “heavy” or wet soils, however, previous studies have shown that varying levels of compaction can occur across a range of moisture conditions, including dry soils (Keller et al., 2019). The validation of this study is based on expert knowledge about paddock soil and drainage conditions and continuous monitoring of the farms which gives information at very fine scales both spatially and temporally. While this study acknowledges the effectiveness of existing decision support systems, it also addresses the knowledge gap of a missing threshold for soil moisture regimes by developing an index for soil moisture for optimum trafficability and grass growth on farms, equivalent to SMD thresholds for same. This makes it more practically applicable on farms, given the limitations associated with a single value of used at farm scale. It is also essential to capture such differences to ensure complete utilisation of resources, where a part of the farm, which is most susceptible to damage to soil or cannot support grass growth can be closed for activities, while some areas could still be used for crop production etc. This decision support tool also highlights specific months where maximum usage of the farm can be made with minimum damage to the soil and optimal production conditions.

Table 3.4. 1: SMD values and farm area proportions (%) within the identified nSSM categories.

	Saturated					FC					Drought
SMD (mm)	-10	-10	-10	-8.7	-4.6	0.6	8.9	19.1	36.8	58.3	75.4
Month /Year*	Jan/17	Jan/19	Mar/20	Nov/21	Oct/18	Apr/18	Apr/20	Jun/17	Sep/19	Jul/21	Jul/18
nSSM categories :	Farm Area Proportions (%)										
Excessively Dry (<0.235)	3	3	1	3	20	16	41	58	12	49	97
Optimum (0.235-0.315)	19	27	2	13	51	35	40	41	24	21	3
Excessively Wet (>0.315)	78	70	97	84	29	49	19	1	64	31	0

Abbreviations used in the table : SMD=Soil Moisture Deficit ; FC=Field Capacity of nSSM map that matches SMD condition.

Chapter 4: Retrospective examination of fertilizer application decisions on a heavy textured dairy farm using paddock specific management records, in-situ weather and soil moisture threshold maps

Rumia Basu^{a,c}, Owen Fenton^b, Eve Daly^c, Patrick Tuohy^{a*}

^a *Vista Milk SFI Research Centre, Teagasc, Moorepark, Fermoy, Co. Cork, Ireland*

^b *Environmental Research Centre, Teagasc, Johnstown Castle, Wexford, Co. Wexford, Ireland*

^c *Earth and Ocean Sciences, School of Natural Sciences, University of Galway, Ireland*

** Corresponding author:*

Patrick Tuohy

VistaMilk SFI Research Centre,

Teagasc, Moorepark,

Fermoy, Co. Cork P61 C996

Email: patrick.tuohy@teagasc.ie

Under Review

4.1 Abstract

In the European Union (EU), the objective of the Nitrates Directive (ND) is the reduction of water pollution caused or induced by nitrates from agricultural sources. In Ireland, the Nitrates Action Plan states that nitrogen (N) fertilizers should not be applied to waterlogged soils or when heavy rainfall is expected within 48 hours of application. In Ireland, a daily agri-meteorological forecast is available which gives: a) soil moisture deficit (SMD) information at regional scale to enable a farmer or contractor to assess soil moisture status b) predicted hourly rainfall to inform a farmer or contractor if heavy rainfall is forecast within the 48-hour period. The objectives of the present study were to assess soil moisture and rainfall status at and in the 48 hours after N fertilizer applications for two paddocks on a heavy textured intensive dairy farm in Ireland for the period 2017-2021. In addition, a combined normalised surface soil moisture (nSSM) (from satellite imagery) and SMD approach was implemented for the farm to map and identify the soil moisture conditions during and after fertilizer applications. Results showed that the amount of N applied to the two paddocks was generally high in the beginning

of the year (on an average around 60 kg/ha of fertiliser amounting to 30% of the total for that year) and there was variation in the total amount of N applied across the years. The total rainfall received on the days of application for the two paddocks also varied across the years. The average N applied in the time period was 283 kg/ha for paddock 9 and 252 kg/ha for paddock 10. N application followed the open and closed periods as per the ND. Additionally, for both paddocks a variation in soil moisture conditions was observed every year, with the most favourable conditions peaking between April and October, coinciding with the grass growing season in Ireland. In future, this type of analysis can be made possible in real-time by using daily satellite/drone images to produce daily soil moisture maps, which will help identify favourable conditions of fertiliser application in space and time.

Keywords: Grassland; Fertiliser; Remote Sensing; Agriculture

4.2 Introduction

Globally, nitrogen (N) is the most widely used fertilizer in agricultural systems (Govindasamy et al., 2023). Recent decades have seen an increasing demand globally for food, including dairy products and this has called for intensification of agricultural systems especially grasslands, resulting in an increase in N use (Cardenas et al., 2019; Ruelle et al., 2018). This is especially true in Europe where 35% of the agricultural area is covered by permanent grasslands which is an important resource supporting livestock production (Hopkins and Holz, 2006; King et al., 2012). In temperate regions, such as Ireland, chemical N fertilisers greatly support grass-based livestock systems (Ryan et al., 2011) and inorganic N fertilisers have been widely used to improve yields (King et al., 2012). While the benefits of adding N fertilisers in agricultural management is significant, N is an expensive fertiliser which can impose increased financial and environmental cost due to over application as not all N that is applied is used efficiently

(Buckley et al., 2016; Buckley and Carney, 2013). The current average Nitrogen Use Efficiency (NUE) on dairy farms in Ireland is estimated to be ~25% (Teagasc, 2021d).

Soil moisture is one of the many environmental factors that governs the uptake of N by plants and the form in which it is absorbed (Ding et al., 2021; Flynn et al., 2023; Liang et al., 2022). Apart from nitrogen uptake, soil moisture is also a major factor governing N₂O emissions (Bracken et al., 2021, 2020). Soil moisture has also been shown to affect pasture responses to N fertiliser (Pembleton et al., 2013).

To minimise nutrient losses to water and air, the ND, which promotes good agricultural practices in the EU, obliges member states to set out regulations pertaining to fertilizer usage. In Ireland, the Nitrates Action Programme (NAP) aims to reduce potential water pollution caused or induced by nitrates from agricultural sources. The major focus of Ireland's 5th NAP ("gov.ie - Nitrates Directive," 2020) that runs from 2022-2025 is on reducing chemical N fertiliser use to a maximum of 325000 tonnes by 2030 and increasing Nitrogen Use Efficiency (NUE) to 35%. NUE is a measure of how much of the nitrogen supplied to the crops through fertilisers is used by the crop and ultimately how much of it is recovered in the end product such as meat or dairy products (Teagasc, 2021d). Critical to the success of these goals will be adherence to regulations pertaining to application of N fertilizers. For example, guidelines within the NAP states that N fertilisers should not be applied on waterlogged soils (indicated in Ireland with daily Soil Moisture Deficit (SMD) information for well, moderate and poorly draining soils (Schulte et al., 2015)) or when heavy rainfall (heavy is not defined in the NAP, rainfall is measured in Ireland by the national meteorological service) is predicted in 48 hours. Basu et al. (2024a) estimated normalised surface soil moisture (nSSM) for two dairy farms in Ireland, dominated by poorly draining (Tuohy et al., 2015) or wet soils, using Sentinel-2 data. This gives soil moisture status at the paddock level for the farms at a high spatial resolution of

10m and reveals spatial and temporal trends in the soil moisture regime. The nSSM estimates were used in a recent study by Basu et al. (2024b), where a combined nSSM and SMD approach was used to identify an optimum range of soil moisture conditions on poorly draining soils on dairy farms. The combined nSSM and SMD approach identifies, and maps “soil moisture thresholds (SMT) within which, soil can be protected against traffic induced damage and within which, grass can grow and not wilt. These maps showed high variability in soil moisture conditions (on any given day) and highlighted areas of paddocks that fell within or outside of these thresholds. Beyond decisions regarding if a soil is waterlogged or if rainfall is heavy, a more holistic approach should also consider if spreading fertilizer will damage the soil, and whether the crop can grow on the application date. Currently, if a soil is not waterlogged with no heavy rainfall occurring in the next 48-hour period, a farmer can spread fertiliser but compact the soil in the process.

The objective of this study is to retrospectively analyse decisions regarding N application on two paddocks on a dairy farm in Ireland through the lens of NAP, whilst also considering other decisions such as soil and crop needs using SMT maps. This was achieved using paddock based N application data along with rainfall, SMD and soil moisture status data for the paddocks and creation of SMT maps for the farm. This study provides a proof of concept and can, thus, be used to develop a real-time decision support system for farmers targeting sustainable fertiliser applications.

4.3 Materials and Methods

4.3.1 Study Area

The study farm is located in, Co. Tipperary ($52^{\circ} 36'N$, $8^{\circ} 01'W$). The farm is approximately 40 Ha in size, has flat terrain and receives approximately 980 mm of rainfall annually. The farm is equipped with a weather station and in-situ soil moisture sensors.

A soil survey at paddock scale was conducted on the farm in 2015, according to the protocols developed for the Irish Soil Information System (ISIS) project to assign soil subgroups and drainage classes to the paddocks on the farm. All the soils are classified as belonging to one of the 11 soil Great Groups and further into sub-groups (Environmental Protection Agency, 2014; Simo et al., 2008). An auger and test pit survey was also carried out on the farm for mapping the soil type for each paddock. This was done by driving an auger bore into the soil to a depth of 1m, every Ha. Additionally, 3-4 soil pits, each at depth of 1-2m were dug on the farm to analyse the dominant soil type (Teagasc, 2021b). Based on this assessment, soil type and drainage class (as shown in Figure 4.3.1) were assigned to each of the paddocks. The soil texture on the farm is mostly sandy loam and the dominant soil subgroup is Surface-Water Gley, which are characterised as being wet and acidic with gleying within 40cm (Teagasc, 2014). The majority of the paddocks (Figure 4.3.1) are poorly drained (i.e., those that become saturated during a rainfall event and continue to hold excess water for several days thereafter), except for paddocks 8,10 and 21 which are well drained (they reach saturation during a rainfall event but do not remain excessively wet thereafter) (Schulte et al. 2015; Tuohy et al. 2018).

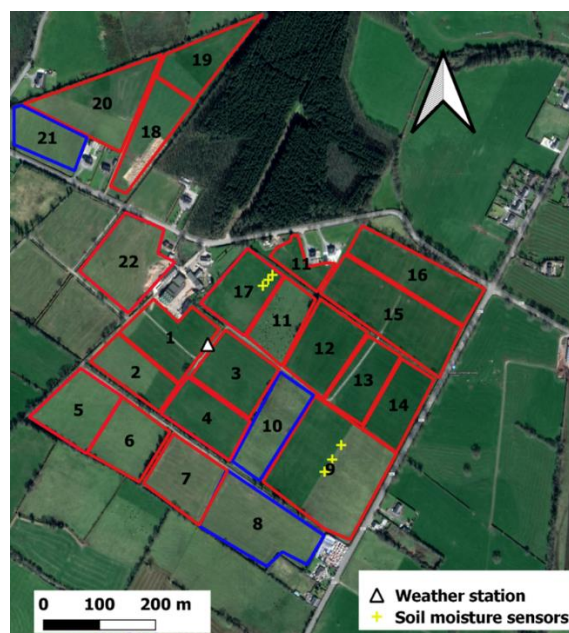


Figure 4.3. 1: Paddocks on the study farm with locations of the weather station and soil moisture sensors. Red paddocks are poorly drained and blue paddocks are well drained. The white triangle shows

the weather station on the farm and yellow crosses are the in-situ soil moisture sensors. Paddocks 9 and 10 are the focus of this study.

4.3.2 Data collation for fertiliser application, associated moisture status of the soil and rainfall

To examine decisions around the timing of fertilizer applications between 2017 and 2021 for paddocks 9 and 10 (Figure 4.3.1) data related to: fertilizer application (paddock specific) date and amount; daily SMD and daily rainfall (cumulative rainfall in the 48 hour period between 5 and 10 mm) were collated as follows:.

- N fertiliser application data was obtained from Pasture Base Ireland (Teagasc, 2021e) which consists of a dated entry of the amount of N fertiliser (kg/ha) applied to each paddock on the farm.
- Daily SMD for the farm was calculated using the grassland hybrid model of Schulte et al. (2015) for the time period 2017-2021. This model uses daily rainfall and evapotranspiration (ET) data from the weather station on the farm (Figure 4.3.1).
- A cumulative rainfall was calculated for a 48-hour window after the application of N, including the day of application. This helps identify presence/absence of rainfall around the date of N application. No fertiliser should be applied if heavy rainfall is forecast in the 48-hour window after fertiliser application. This is in accordance with the ND which suggest restricting fertiliser application if heavy rainfall is predicted in the 48-hour period after fertiliser application. (Teagasc, 2021f). However, the amount of rainfall that constitutes as “heavy” is not defined. We define 5 mm and 10 mm as two indicative thresholds for rainfall in the 48-hour period of fertilizer application.

4.3.3 Development of SMT maps

Basu et al. (2024a) estimated nSSM for the present study farm using Sentinel-2 data and the Enhanced Vegetation Index (EVI) in a modified OPTRAM approach. The nSSM helps

understand the temporal and spatial variations of soil moisture at the paddock scale for the farm. Information on soil moisture at this resolution is important to assess decisions about N application with respect to moisture status (and therefore risk of soil compaction) and crop growth conditions as detailed later in the section. The modelled nSSM was validated against in-situ volumetric soil moisture data from the sensors installed on the farm, with an RMSE between 0.05-0.06 and an R^2 of 0.4.

Following from the modelled nSSM, Basu et al. (2024b) developed a methodology for establishing a relationship between SMD and nSSM for identifying conditions that minimise soil compaction potential (on a dairy farm from fertilizer applications) and represent conditions when optimum grass growth occurs (and therefore would benefit from fertilizer applications) for the farm. The nSSM and SMD relationship, therefore, also establishes a link with the consequences of N application on the farm. To obtain a relationship between nSSM and SMD, a linear regression model was applied between mean nSSM for the farm and corresponding SMD values (Figure 4.3.2). SMD thresholds of 10 mm and 50 mm (identified in Basu et al., (2024b)) were applied to the regression model to derive nSSM thresholds; 0.235 and 0.315, respectively. Three categories (i.e., <0.235 , $0.235-0.315$ and >0.315) of nSSM corresponding to “excessively dry”, “optimum/favourable” and “excessively wet” conditions were established. Along with the NAP guidelines (which focusses on water quality and aims to prevent fertiliser applications when soils are waterlogged or vulnerable to heavy rainfall), decisions to apply fertiliser must also be cognizant of soil and crop factors. Between 0-10mm SMD, soils are not waterlogged, yet damage to soil could occur during fertiliser application operations. Therefore, besides assessing daily rainfall and SMD to adhere to the NAP, decision making on poorly draining soils (that are vulnerable to soil damage by trafficking below 10mm SMD (Vero et al., 2014)), should also pertain to soil and crop. Thus, based on these nSSM thresholds, SMT maps were produced for the study farm at a high spatial resolution of 10 m,

which exhibited spatial variability in soil moisture regime on any given day on the farm. Along with NAP conditions, a separate analysis was conducted to examine if fertilizer application occurred coincident with soil conditions that protected the soil from compaction and allowed for optimum grass growth in the paddocks.

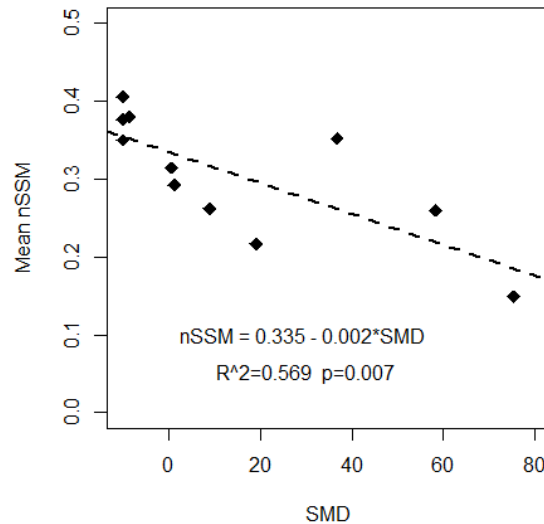


Figure 4.3. 2: Linear regression between mean normalised surface soil moisture (nSSM) and Soil Moisture Deficit (SMD) for the study farm.

4.3.4 Proportion of farm area in the favourable nSSM category

Proportion of area of each paddock on the farm falling under the “optimum” category was calculated from the SMT maps. A piecewise regression was applied between the calculated paddock area proportions and the corresponding SMD values. The model was able to explain 72% and 52% (R^2) of the observed variability for paddocks 9 and 10 respectively. Paddock area proportions were predicted at daily time steps using this regression model. Figure 4.3.3 shows the model applied for paddocks 9 and 10, which are representative of the drainage classes on the farm. Henceforth, this paper shows subsequent analysis for these two paddocks only. The proportion of paddock area in the non-optimum nSSM category can be calculated from these proportions using simple arithmetic.

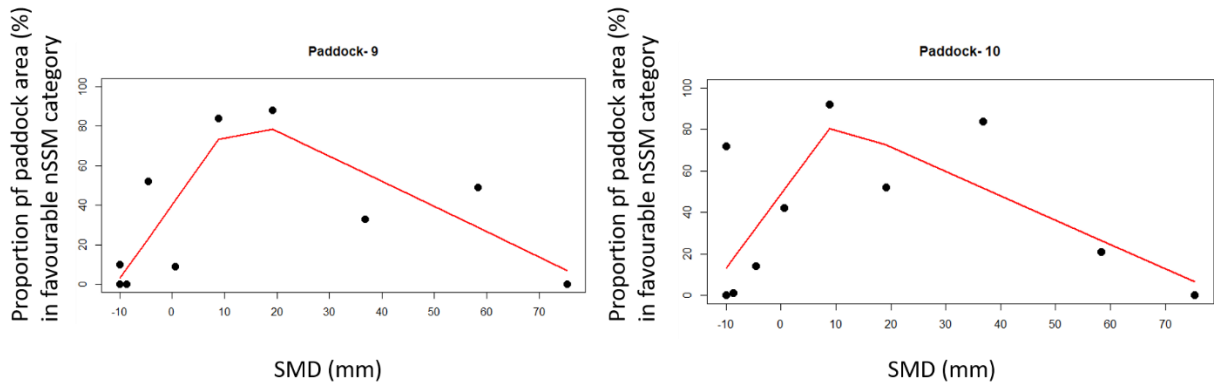


Figure 4.3. 3: Piecewise linear regression model fitted between proportions of paddock area in the optimum/favourable nSSM category and corresponding SMD values for paddocks 9 and 10.

4.3.5 Data analysis

The date of N application was analysed with respect to a) waterlogged status of the paddocks (Yes/No) based on SMD values of less than 0 mm, b) rainfall conditions around the date of application, and c) what proportion of the farm area had favourable nSSM conditions (from the regression model in section 4.3.3) when N was applied. The analysis in this study is done for two paddocks on the farm (paddocks 9 and 10) that are representative of the drainage conditions on the farm and all results confirm to these two paddocks only.

4.4 Results

4.4.1 Fertiliser application timing

As a general trend, in both paddock 9 and 10, across the years, the first application of N took place between January to March and the application period ended in September/October. The total amount of N applied (kg/ha) for paddock 9 in the year 2017 was 292.6, followed by 282.7 in 2018, 309.0 in 2019, 276.7 in 2020 and 255.3 in 2021. The total rainfall for the dates of application varied between 24.6 mm in 2017, to 15.6 mm in 2018, 11.0 mm in 2019, 9.4 mm in 2020 and 16.0 mm in 2021, with the mean rainfall on the dates of application being 15 mm across the years. Thus, the total N applied varied each year. It is interesting to note that for

paddock 9, year 2020 stands out as being the year in which the total rainfall on the dates of application was also lowest.

For paddock 10, the total amount of N applied (kg/ha) in 2017 was 192.9, followed by 282.7 in 2018, 265.4 in 2019, 264.4 in 2020 and 255.3 in 2021. Similar to paddock 9, the total N applied varied across the years. The total rainfall for the dates of application varied between 2 mm in 2017, to 15.6 mm in 2018, 7.4 mm in 2019, 9.4 mm in 2020 and 16 mm in 2021, with the highest rainfall received in 2021 and lowest in 2017. The average rainfall during the period of application was 10mm. The average N (kg/ha) applied between 2017-2021 was 283 kg/ha for paddock 9 and 252 kg/ha for paddock 10.

4.4.2 Soil and rainfall conditions for fertiliser application dates

Shapes in Figure 4.4.1 represent different cumulative rainfall conditions within 48 hours of N application. Filled circles indicate the dates when total rainfall in the 48-hour window is less than 5mm, squares indicate rainfall in the range 5-10 mm, while inverted triangles represent rainfall greater than 10mm. As can be seen from Figure 4.4.1 (a), for paddock 9, in 4 out of the 5 years, one date of application had a cumulative rainfall greater than 10mm in the 48-hour window (red dot). For paddock 10 (Figure 4.4.1 (b)), in 3 out of the 5 years, one N application date had rainfall greater than 10mm.

Tables 4.4.1 and 4.4.2 show comparison between the rate and timing of N application with SMD on that day and cumulative rainfall for the 48-hour period following application for paddocks 9 and 10 respectively, through 2017-2021 for specific dates discussed here. The SMD values are colour coded such that values in blue represent waterlogged conditions (SMD less than 0 mm), those in yellow are within the SMD range 0-10mm, green represents the favourable SMT range (SMD 10-50 mm) and red represents very dry conditions (SMD greater than 50mm).

As can be seen from Table 4.4.1, For paddock 9, in January 2017 (28/01/2017), the highest amount of N (60kg/ha) for that year was applied, when only around 3% of the paddock was in the favourable nSSM category. The SMD for the same date was at its lowest (-10mm) indicating that the soil was waterlogged and too wet for fertiliser application. The soil would have been at a considerable risk of compaction by machinery and uptake of N by the crop would also be low. Additionally, 9.8 mm of rain was received in the 48-hour period following N application, which is fairly high for poorly draining soils.

During favourable SMD conditions for the farm (between 10 mm and 50mm, shown in green) in terms of both trafficability and crop growth, the rate of N application was not as high. For example, on 08/08/2017 (Table 4.4.1) the proportion of farm area within the favourable nSSM condition was quite high (78%) and around 7mm of rainfall was received in the 48-hour window. However, only 34 kg/ha (11% of the total fertiliser applied) of N was applied on this day as opposed to 60 kg/ha in January. On the contrary, on 05/06/2017, 34.4 kg/ha of N was applied amounting to 12% of the total fertiliser for that year. The soil and rainfall conditions on this day were not very conducive for fertiliser application. Total rainfall in the 48 hour period was 16.8 mm and the soil was waterlogged with an SMD of -3.4 mm .

Similarly, on certain days, when the SMD went beyond 50mm (shown in red) and the soil was very dry, N was still applied. Particular examples include two days (15/07/2018 and 12/06/2020) when the proportion of the paddock in the optimum nSSM category was also very low (4-10%) and drought like conditions were reached (SMD greater than 70mm), yet more than 30 kg/ha of N was applied, amounting to 12% of the total N applied. It is important to note that on 12/06/2020, the total rainfall in the 48 hour period after N application was 28.8 mm, yet the soil would have remained very dry for a short period with respect to N application. It is possible then that N utilisation would have been low and the soil was at a significant risk of compaction.

On certain dates (eg.10/05/2018, 25/07/2020.), the rainfall in the 48 hour period was able to bring back the SMD in the optimum range of 10 to 50 mm and around 80% of the paddock 9 had optimal nSSM conditions. This presented a good opportunity for N application with respect to soil conditions. However, these dates also received significant rainfall in the 48-hour window after application of fertiliser. A notable example is that for 12/05/2021, which represented ideal conditions for N application and probable uptake by crops. 82% of the paddock on this day was within the optimum SMT range, the SMD value being 16, around 8mm of rain was received in the 48 hour window and 61 kg/ha of N was applied, amounting to 24% of the fertiliser for that year. The farmer was in compliance with all regulations and the environmental conditions also seem conducive for fertiliser utilisation.

Similar trends can be seen for paddock 10 (Table 4.4.2), where at the start of the year (28/01/2017), 30% of the total fertiliser for that year was applied on a single day even though soils were waterlogged. The SMD on that day was -10 mm, suggesting very wet soils, the proportion of paddock within the optimum category was only 13% and 9.8 mm of rain was received in the 48-hour period after fertiliser application (therefore sub-optimum conditions prevailed with trafficking causing compaction and the crop not able to use the fertilizer to grow). The year 2020 was most anomalous in terms of N application such that on a very dry day i.e., on 12/06/2020, when the SMD was 77.7 mm, pointing towards drought like conditions, 33 kg/ha of N (12% of the total) was applied. Almost the entire paddock on that day was under sub-optimal conditions in terms of crop growth (i.e., wilting conditions) and a very high amount of rainfall (28.8 mm) was recorded in the 48-hour window after application.

Another example is the month of May 2018 (10/05/2018), when 82% of the paddock was under favourable SMT conditions and 33.4 kg/ha of N was applied. The farmer was in compliance with government directives. However, the total rain in the 48 hour window was quite high (16 mm).

However, on 29/03/2019, a good outcome of N application can be expected as there was no rain on the day and in the 48 hour period of application. SMD was 7.4 mm, though outside of SMT thresholds as defined in this study, yet within the guidelines as defined by the government and 44.5 kg/ha of N (17% of total) was applied.

Table 4.4. 1: Date of N application and associated soil and rainfall conditions for paddock 9. Blue colour represents waterlogged conditions (SMD less than 0 mm), green colour represents SMD between 10-50 mm and red colour represents SMD greater than 50 mm.

Date of N application (DD/MM/YYYY)	Total N applied(kg/ha)	SMD on date of application (mm)	Rainfall received on date of application(mm)	Total Rainfall received in the 48 hour window (mm)	Proportion of paddock area (%) in SMD 0-10mm	Proportion of paddock area (%) in SMD 10-50mm
28/01/2017	60.2	-10	1.8	9.8	6.0	3.0
08/08/2017	34.2	19.5	6.7	6.8	6.5	78.0
05/06/2017	34.4	-3.4	15.2	16.8	8.03	27.4
15/07/2018	33.4	72.9	8.0	8.0	0.0	10.1
10/05/2018	33.3	10.7	0.8	16.2	7.8	80.0
12/06/2020	33.0	77.7	0.0	28.8	0.0	4.02
25/07/2020	25.3	11.3	2.8	5.8	7.7	82.0
12/05/2021	61.0	16	7.4	8.0	7.0	82.4

Table 4.4. 2: Date of N application and associated soil and rainfall conditions for paddock 10. Blue colour represents waterlogged conditions (SMD <0mm), green colour represents SMD between 10-50mm, yellow colour represents SMD between 0-10mm and red colour represents SMD greater than 50 mm.

Date of N application (DD/MM/YYYY)	Total N applied(kg/ha)	SMD on date of application (mm)	Rainfall received on date of application(mm)	Total Rainfall received in the 48 hour window (mm)	Proportion of paddock area (%) in SMD 0-10mm	Proportion of paddock area (%) in SMD 10-50mm
28/01/2017	60.3	-10	1.8	9.8	7.0	13.1

10/05/2018	33.4	10.7	0.8	16.2	7.4	82.4
29/03/2019	44.5	7.4	0.0	0.0	8.0	75.2
12/06/2020	33.0	77.7	0.0	28.8	0.0	4.0

4.4.3 Fertiliser application dates with respect to favourable soil and crop conditions

The SMT thresholds give detailed insights into N application and its utilisation with respect to soil and crop conditions during fertiliser application. Figure 4.4.1 (a and b) show the proportion of paddocks in the favourable nSSM (0.235-0.315) category compared to the total N applied on the paddocks. The blue line in Figure 4.4.1 shows the farm area proportion in the optimum nSSM category across the year and the shapes (according to amount of rainfall in the 48 hour window) represent the date on which N was applied to the paddocks. It can be observed from the figures that the proportion of farm area in the optimum category of nSSM varies highly throughout the year. The optimum proportion peaks between April-August, sometimes extending up to October. This also coincides with the main growing season that runs from March to November. As a general trend in both paddocks, it can be seen that that for any particular year, the amount of first application of N was mostly higher than at other times. Year 2017 stands out for both paddocks, since at the beginning of the year (January), when a very small proportion of the paddock had optimal nSSM conditions, maximum amount of fertiliser (60.25 kg/ha) for that year was applied in both paddocks. This amounted to 20% of the total fertiliser in 2017 for paddock 9 and 30% for paddock 10. It is also interesting to note that for paddock 10, in year 2017, more than half of the total fertiliser applied in the year was spread over only two days in January and May. The total amount of fertiliser applied annually, also varied across the years for both paddocks as also discussed in section 4.4.1. It is interesting to note that even though favourable soil and crop conditions for the paddocks peaked between April-August, this was necessarily not the time when N application also peaked.

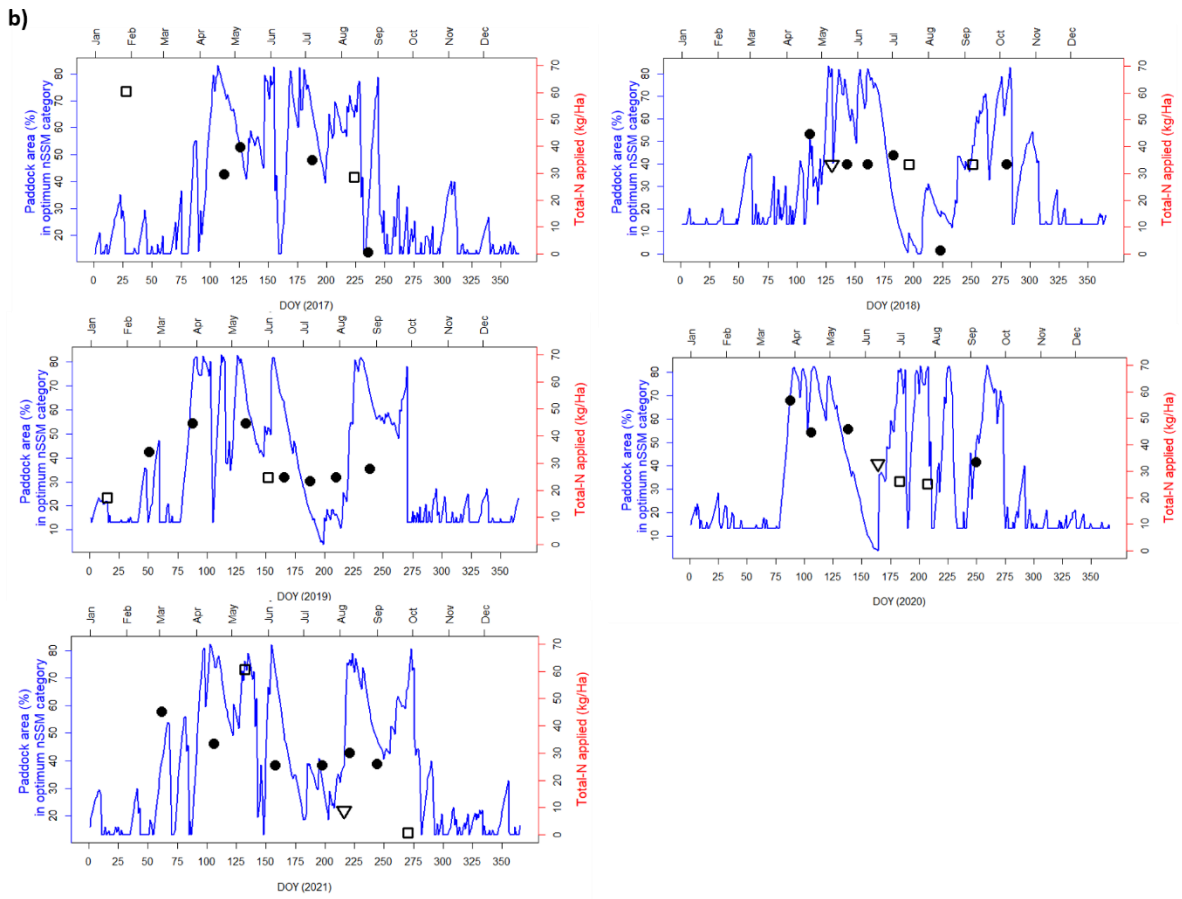
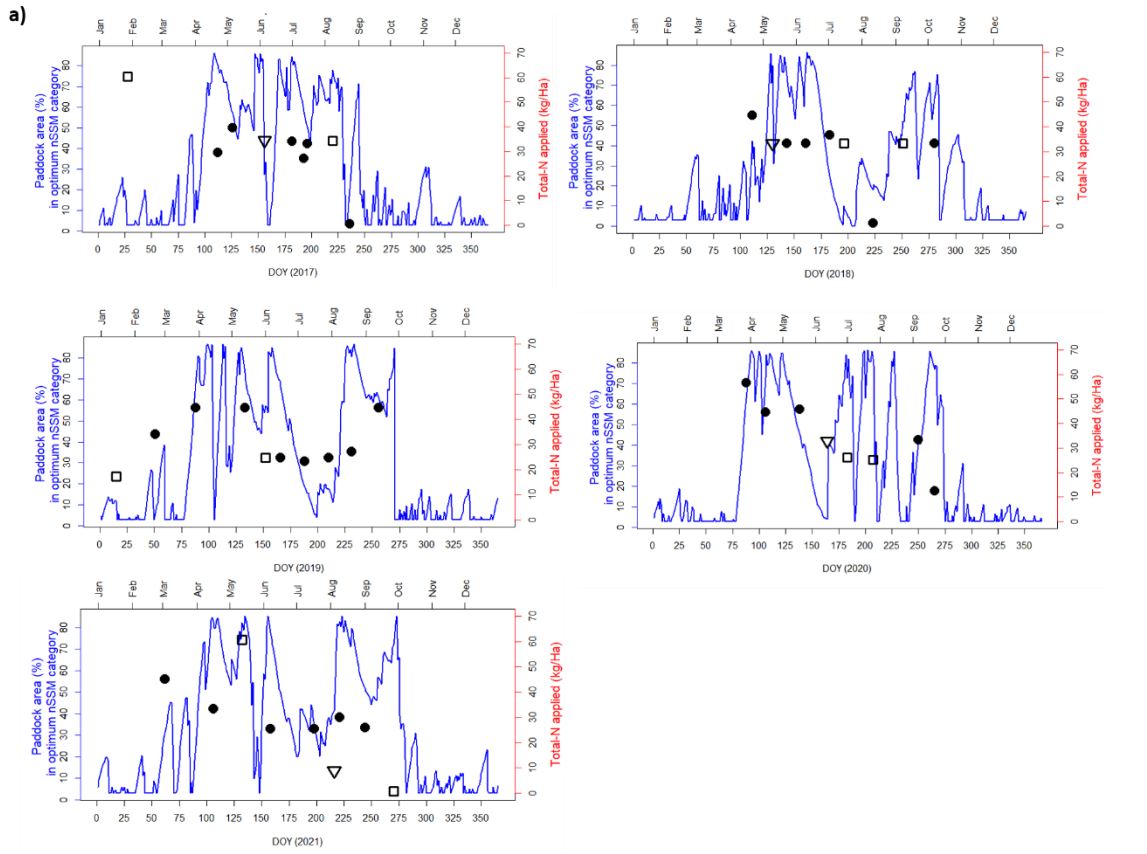


Figure 4.4. 1: Paddock area proportions in the favourable nSSM category compared with N applied for a) paddock 9 and b) paddock 10. Filled circles represent dates when rainfall for the 48-hour period after N application was less than 5 mm, squares represent rainfall between 5-10mm and inverted triangles represent rainfall greater than 10 mm.

4.5 Discussion

4.5.1 Insights into N application and probable consequences

Ireland is primarily a grass based economy with 80% of the agricultural area being permanent grassland which is the major feed source for livestock (Higgins et al., 2019). Productivity of Irish grasslands depends on the availability of N to plants and sources of N include chemical and organic N fertiliser, mineralisation of N from soil organic matter and nitrogen fixing legumes such as white clover (O'Donovan et al., 2021). At the same time, the main limiting factors towards grass production also include N, temperature, soil moisture and drainage, and pH among others (Government, 2019). These are some of the factors that are particularly relevant to this study especially soil moisture and drainage. Additionally, the guidelines as set by NAP form the background for N application on the farm. The study farm receives high annual rainfall and the soil is mostly poorly drained, thereby, remains saturated for large parts of the year. Thus, any N, applied during wet periods, can contribute to significant losses of N to the environment. Specific examples of such soil, crop and rainfall conditions have been outlined in section 3. N applied during non-optimal conditions (defined by SMT in this study) could lead to potential losses of fertiliser. In Ireland, there is risk of nitrate leaching from grassland fields in early spring and in autumn and winter of a particular year. This is because of high rainfall and low grass growth rates during this time (Teagasc, 2021g).

Rainfall intensity and volume both show an increasing trend in Ireland (Tuohy et al., 2018). A 30 year analysis of rainfall trends for Ireland between 1991-2020 reveals an increase in average annual rainfall by 7%, with the greatest increase observed in summer ("Met Éireann," 2023). This would result in even lesser area on the farm falling within optimal soil moisture conditions

in general throughout the year. Additionally, high rainfall during summer would mean more pressure in terms of water logging in the later months, increasing the probability of nutrient losses. Thus, any amount of fertiliser applied during August-September could result in more losses than uptake. In general, the actual evapotranspiration rates are lower than the rainfall received in the winter months as compared to summer, and therefore would result in more saturated soils in the beginning of the year. Any N applied during this time would result in more losses.

This study highlights that farmers follow the open and closed period government directives with respect to fertiliser application. However, sometimes the weather may result in poor N uptake especially, if there was a sudden rainfall event which was not forecast. Interestingly, a general trend of applying high N in the beginning of the year was observed, especially in 2017 for both paddocks 9 and 10 under waterlogged soil conditions. Additionally, on certain days such as 10/05/2018 (Table 4.4.1), soil moisture conditions presented ideal conditions for fertiliser application, yet a very high amount of rainfall received in the 48-hour window might have resulted in losses of N to the environment. This highlights a typical case, where there might have been a mismatch in the weather forecast vs actual weather conditions on that day. In England, which has a similar climate to that of Ireland and where water is not the limiting factor for crop growth, it has been found that higher the rainfall, lower is the NUE (Powlson et al., 1992). Additionally, it is also advisable that fertilisers be applied only when the soil conditions are conducive for trafficking by tractors (Teagasc, 2021g). Under waterlogged conditions (SMD <0), the soil structure is destroyed by machinery and needs re-development (Lepore et al., 2023; Teagasc, 2022). N applied on waterlogged soils could also leach to the environment, adding to the challenges that Ireland already faces in terms of meeting targets regarding water quality, greenhouse gas emissions and reducing the use of N fertiliser by 14% between 2018-2025 (O'Donovan et al., 2021). Thus, fertiliser application during waterlogged

conditions would not only lead to nutrient leaching, but also cause irreversible damage to soil. Soil moisture status, therefore, emerges as the major governing factor for decisions on fertiliser application.

4.5.2 Future work

Enhanced grazing management and adoption of precision agriculture technologies can help achieve higher nutrient utilisation on Irish farms (Higgins et al., 2019; O'Donovan et al., 2021). However, adoption of precision agriculture technology is low in Ireland (Higgins et al., 2019). Based on weather and farm conditions, farmers often have to make decisions on their farm on a daily basis. There are also policy initiatives and government directives that aid farmers in taking decisions about fertiliser application. However, Daxini et al. (2019) found that adoption of such policy advices by farmers is not uniform and that farmer typology should be considered while framing such policies and directives. Policies and advisory regarding fertiliser application could be made more effective if the farmers have access to near-real time information about the farm conditions, especially with respect to soil moisture conditions, enabling them to visualise ground situations. A recent study by Murphy et al. (2024) also highlights the need for a farm level focus and calls for “precision grassland management systems” to reduce N leaching especially under severe weather conditions. By providing a farm level SMT information and a paddock level analysis for N application, this study paves the way for developing focussed decision support systems, using high-resolution remote and other farm level data. In order to achieve maximum utilisation of N fertilisers, it would be best to apply fertilisers when soil moisture conditions lie in the “optimum/favourable” category as defined by this study. This would ensure that fertiliser is available to the crop and there is least damage to soil by compaction from machinery. The proof of concept presented in this study could be improved by using daily high resolution optical images from drones to produce daily “SMT” maps at the farm/ paddock level. Additionally, daily crop condition maps could also be

produced using vegetation indices such as the Normalised Difference Vegetation Index (NDVI) or the Enhanced Vegetation Index (EVI). This information when combined with meteorological forecasts and government directives that are already in place, has the potential to develop a near real-time decision support tools for farmers that can improve N utilisation on Irish farms. High-resolution temporal and spatial information in the form of SMT maps would enable farmers to know exactly when and where to apply fertiliser. Hackett, 2017 also suggests use of drone/satellite images for N status of cereal crops in Ireland, at high spatial resolutions which would help determine fertiliser application rates based on current crop growth status as opposed to historical growth rates. Such targeted applications would pave way for adoption of precision agriculture practices, reducing both environmental and financial losses.

4.6 Conclusion

Hackett (2017) report that it is extremely difficult to determine the exact amount of N that should be applied in order to maximise returns and this presents one of the biggest challenges in N management on farms. This study critically analyses various factors governing N application and recommends that in addition to weather conditions and forecasts, SMT be considered a major governing factor regarding N application. Optimal soil moisture conditions prove to be beneficial for both soil and crop such that the N applied could be effectively utilised. Through a retrospective analysis of decisions regarding N application, this study analyses trends of N applications for two paddocks on a dairy farm in Ireland. It is clear that farmers tend to apply a large amount of fertiliser at the beginning of the year. Though farmers follow government directives regarding N application, a near-real time spatial and temporal information about on-farm conditions could enable better farm management practices, especially if there are sudden changes in weather conditions. Though retrospective in nature, this study presents important aspects of N application by dairy farmers in Ireland and highlights the need for a real time decision support tool for farmers in both space and time..

Thus, it provides for an essential starting point to improve future decisions. The approach used in this study could be applied to scenarios where water is not the limiting factor and where soils tend to remain saturated for longer periods of time.

Chapter 5: Discussion and Conclusion

5.1 Discussion

This thesis demonstrates the potential of high-resolution Sentinel-2 data in estimating surface soil moisture at the paddock level for two dairy farms in Ireland and two applications governing farm management (Basu et al., 2024a, 2024b). A modification was made to the OPTRAM model (Sadeghi et al., 2017a) for estimating nSSM, tailored to the characteristics of the study sites (Chapter 2). A suite of vegetation indices were tested for their sensitivity towards surface soil moisture. The methodology developed in Chapter 2 was used to develop a proof of concept for farm management using a combined SMD and high-resolution nSSM (Chapter 3) that defined threshold in nSSM for safeguarding both soil and crop health. This concept was further used in Chapter 4 to analyse nutrient management on the farm, demonstrating that soil moisture should be considered a governing factor for framing rules and policies around nutrient application in Ireland. Chapters 2, 3 and 4 together provide an end-to-end framework involving use of remotely sensed data for developing a decision support system for farm management. The thresholds of soil moisture calculated in Chapter 3 help identify areas of the farm which could be safely trafficked and managed even when other areas of the farm may be inaccessible due to waterlogged and /or very dry soils. This would help enable better utilisation of farm resources. Chapter 4 identifies individual N application events which could have led to under-utilisation or poor uptake of nutrients by crops when applied on very wet or very dry soils or when environmental conditions were not conducive. Thus, information on farm-level soil moisture conditions in decision support systems could not only guide decisions regarding trafficability and compaction, rather also provide guidelines for efficient fertiliser application.

5.2 Highlights

5.2.1. Optical Trapezoid Model

The use of OPTRAM has limitations as discussed in Chapter 2 especially with regards to mismatch between the actual VSM vs that recorded at the satellite due to the temporal resolution of the satellite and visual estimation of the wet and dry edges (Stańczyk et al., 2023). Fitting of the dry and wet edges in the OPTRAM model is also subjective as it uses visual estimation of parameters such as lowest VI value, highest STR value etc. for fitting the edges. A review of previous studies and experiments carried out in this thesis demonstrate that scenarios beyond linear wet and dry edges including edges being negatively sloped are possible. There is a possibility of overestimation of dry and wet edges and studies have corrected for it either by downscaling of satellite data (Sadeghi et al., 2017a) or through site-specific calibrations (Ambrosone et al., 2020). However, downscaling has its own challenges starting with the decision regarding the degree of downscaling and the loss of information that entails from this process. Therefore, this thesis addresses this issue through masking of problematic land cover classes like water bodies and trees and removing the top and bottom 1% of STR data points. However, OPTRAM remains a valuable and one of the most popularly used methods for estimating soil moisture because of its universal parametrisation and its effectiveness in estimating near surface soil moisture over vegetated surfaces (Sadeghi et al., 2017a). This thesis demonstrated that OPTRAM has the potential for functioning well on poorly draining / wet soils under gradually wet climatic conditions. OPTRAM has also been successfully used to study dynamics of water table depth in peatlands with a high correlation of 0.7 between in-situ and OPTRAM estimates (Burdun et al., 2020b). This method could be extended to estimate nSSM for peat soils which are a major land cover category in Ireland, spanning across 1.46 m ha (14600 km²), covering nearly 21% of the land surface (Tuohy et al., 2023). However, a longer time series of satellite data and a denser network of in-situ soil moisture sensors would be needed to increase the confidence in the methodology. Networks like ISMON could aid such efforts in future studies.

5.2.2. Temporal Stability of soil moisture

TS has been used as a statistical concept to study time-varying properties mostly in the field of hydrology as detailed in Chapter 2. Recently, this concept has been used to study spatial and temporal patterns in soil moisture across a variety of land cover types and from catchment to plot scale, using in-situ data (Dari et al., 2019; de Queiroz et al., 2020; Zhao et al., 2020). However, this thesis was one of the first to demonstrate the ability of TS metrics in analysing maps of satellite derived soil moisture at the farm scale.

This thesis used median based metrics instead of the popular mean-based metrics (Brocca et al., 2007; Martínez-Fernández and Ceballos, 2003; Vanderlinden et al., 2012) for studying such behaviour, showing that time-varying farm management practices could also be responsible for the patterns in TS, apart from factors such as soil properties and weather. The farms in this study are well-monitored throughout the year and data for farm dynamics such as grazing, fertilizer applications, grass cutting etc. (Teagasc, n.d.) along with information on weather are regularly recorded. Thus, the patterns observed in the TS and nSSM maps could be well explained and verified against farm management practice, soil and terrain properties.

It is worthwhile to investigate if the ISMON network of in-situ sensors can further improve confidence in the estimation of soil moisture at the catchment scale. Additionally, the availability of low cost sensors (Briciu-Burghina et al., 2022) and the regular record of farm management practices by farmers holds exciting potential for future studies.

5.2.3. Farm and nutrient management using the concept of nSSM and SMD

Information on soil moisture and its spatio-temporal variation is crucial for effective farm management such as planning for nutrient application, irrigation scheduling or drainage management. Satellite soil moisture data can help improve efficiencies of agriculture management practices (Modanesi et al., 2020). SMD, though a useful concept, suffers from

limitations such as containing only a temporal estimate of soil moisture and is not a gridded dataset that can provide information on spatial variability of soil moisture. Since soil moisture is known to be highly variable in space and time (Li et al., 2021) and as also discussed in Chapter 3, SMD is a single value for any given day across a spatial region, failing to capture the intricacies associated with spatial variability of soil moisture. This could be problematic leading to under-utilisation of resources. This thesis addresses this gap by developing a relationship between nSSM and SMD to calculate corresponding soil moisture thresholds (Basu et al., 2024b) and producing maps depicting spatial variability in soil moisture on any particular day. These thresholds were used to develop a proof of concept for an improved farm management decision support system, safeguarding both soil and crop health, wherein farm areas were identified supporting optimum crop growth. Thus, fertiliser application in these areas could be optimised, resulting in reduced air and water pollution caused through run-off and emissions. This concept was further developed for analysing nutrient management on an Irish dairy farm, suggesting that soil moisture should be considered as a major factor while framing policies and directives governing nutrient management.

5.3 Future work

The findings of this thesis can pave the way for the following future research topics:

- The modified OPTRAM model should be tested across more sites in Ireland including peatlands which cover nearly 21% of the land surface or 1.46 million ha (Tuohy et al., 2023).
- High resolution radar data such as Sentinel-1 could be used for estimating surface soil moisture to solve the problems in obtaining longer time series of satellite data due to persistent cloud cover. Studies have shown encouraging results for VSM estimation from Sentinel-1 using a combination of Dubois model (for estimating relative soil

permittivity) and Topp's model (empirical model for relating soil permittivity and soil moisture) (Singh et al., 2020).

- The use of multispectral data from Sentinel-2 and the polarisation bands from Sentinel-1 could be used in conjunction with in-situ VSM data to train machine learning models for estimating surface soil moisture (Nativel et al., 2022). This thesis could not test this idea due to the lack of a dense network of in-situ sensors.
- The proof of concepts developed for farm and nutrient management should be tested across other sites to improve confidence.

5.4 Conclusion

This thesis addresses two important objectives. Firstly, a methodology was developed for estimating surface soil moisture using Sentinel-2 data at the farm level for Irish farms that are dominated by soils with low hydraulic conductivity. Since, the soils on these farms reach saturation during rainfall events and tend to remain wet thereafter for long periods of time, it negatively affects crop productivity and farm management. Therefore, the other objective of this thesis was to develop proof of concept tools for an improved decision support system for farm and nutrient management. The study area is unique because Ireland remains cloud covered for a significant portion of the year, thereby making it difficult to obtain longer time-series of optical satellite data. The concept of surface soil moisture thresholds in developing a farm-management decision support system is novel and important because soils on the study farm are at a risk of compaction by heavy machinery in the SMD range of 0-50mm. Additionally, nutrients can be most effectively utilised if both the soil and crop are at an optimum condition and the surface soil moisture thresholds can help farmers take better decisions for overall farm management. This thesis takes a step further by determining soil moisture thresholds corresponding to existing SMD thresholds, adding a spatial dimension to existing decision

support tools which was otherwise missing. This novel concept highlight areas where farm management could be applied safely leading to optimum utilisation of resources and efficient usage of fertilisers. The methodology and applications developed in this thesis can be applied globally for precision agriculture applications, especially in regions where water is not the limiting factor for crop growth.

List of References

- Abdu, H., Robinson, D.A., Boettinger, J., Jones, S.B., 2017. Electromagnetic induction mapping at varied soil moisture reveals field-scale soil textural patterns and gravel lenses. *Front. Agric. Sci. Eng.* 4, 135–145. <https://doi.org/10.15302/J-FASE-2017143>
- Acharya, U., Daigh, A.L.M., Oduor, P.G., 2022. Soil Moisture Mapping with Moisture-Related Indices, OPTRAM, and an Integrated Random Forest-OPTRAM Algorithm from Landsat 8 Images. *Remote Sens.* 14, 3801. <https://doi.org/10.3390/rs14153801>
- Al-Yaari, A., Wigneron, J.P., Dorigo, W., Colliander, A., Pellarin, T., Hahn, S., Mialon, A., Richaume, P., Fernandez-Moran, R., Fan, L., Kerr, Y.H., De Lannoy, G., 2019. Assessment and inter-comparison of recently developed/reprocessed microwave satellite soil moisture products using ISMN ground-based measurements. *Remote Sens. Environ.* 224, 289–303. <https://doi.org/10.1016/j.rse.2019.02.008>
- Ambrosone, M., Matese, A., Di Gennaro, S.F., Gioli, B., Tudoroiu, M., Genesio, L., Miglietta, F., Baronti, S., Maienza, A., Ungaro, F., Toscano, P., 2020. Retrieving soil moisture in rainfed and irrigated fields using Sentinel-2 observations and a modified OPTRAM approach. *Int. J. Appl. Earth Obs. Geoinf.* 89, 102113. <https://doi.org/10.1016/j.jag.2020.102113>
- Antunes Daldegan, G., Gonzalez-Roglich, M., Noon, M., Zvolef, A.I., 2020. Assessing the performance of NDVI, 2-band EVI and MSAVI vegetation indices for land degradation monitoring across variable biomass cover at global scale. - NASA/ADS.
- Antwi, S.H., Rolston, A., Linnane, S., Getty, D., 2022. Communicating water availability to improve awareness and implementation of water conservation: A study of the 2018 and 2020 drought events in the Republic of Ireland. *Sci. Total Environ.* 807, 150865. <https://doi.org/10.1016/j.scitotenv.2021.150865>
- Anwar, M.R., Liu, D.L., Macadam, I., Kelly, G., 2013. Adapting agriculture to climate change: A review. *Theor. Appl. Climatol.* 113, 225–245. <https://doi.org/10.1007/s00704-012-0780-1>
- Asam, S., Gessner, U., González, R.A., Wenzl, M., Kriese, J., Kuenzer, C., 2022. Mapping Crop Types of Germany by Combining Temporal Statistical Metrics of Sentinel-1 and Sentinel-2 Time Series with LPIS Data. *Remote Sens.* 14, 2981. <https://doi.org/10.3390/rs14132981>
- Attarzadeh, R., Amini, J., Notarnicola, C., Greifeneder, F., 2018. Synergetic use of Sentinel-1 and Sentinel-2 data for soil moisture mapping at plot scale. *Remote Sens.* 10, 1285. <https://doi.org/10.3390/rs10081285>
- Babaeian, E., Sadeghi, M., Franz, T.E., Jones, S., Tuller, M., 2018. Mapping soil moisture with the OPtical TRapezoid Model (OPTRAM) based on long-term MODIS observations. *Remote Sens. Environ.* 211, 425–440. <https://doi.org/10.1016/j.rse.2018.04.029>
- Babaeian, E., Sadeghi, M., Jones, S.B., Montzka, C., Vereecken, H., Tuller, M., 2019a. Ground, Proximal, and Satellite Remote Sensing of Soil Moisture. *Rev. Geophys.* <https://doi.org/10.1029/2018RG000618>
- Babaeian, E., Sidike, P., Newcomb, M.S., Maimaitijiang, M., White, S.A., Demieville, J., Ward, R.W., Sadeghi, M., LeBauer, D.S., Jones, S.B., Sagan, V., Tuller, M., 2019b. A New Optical Remote Sensing Technique for High-Resolution Mapping of Soil Moisture. *Front. Big Data* 2, 37. <https://doi.org/10.3389/fdata.2019.00037>
- Baillarin, S.J., Meygret, A., Dechoz, C., Petrucci, B., Lacherade, S., Tremas, T., Isola, C., Martimort, P.,

- Spoto, F., 2012. Sentinel-2 level 1 products and image processing performances, in: International Geoscience and Remote Sensing Symposium (IGARSS). pp. 7003–7006. <https://doi.org/10.1109/IGARSS.2012.6351959>
- Baroni, G., Ortuani, B., Facchi, A., Gandolfi, C., 2013. The role of vegetation and soil properties on the spatio-temporal variability of the surface soil moisture in a maize-cropped field. *J. Hydrol.* 489, 148–159. <https://doi.org/10.1016/j.jhydrol.2013.03.007>
- Basu, R., Daly, E., Brown, C., Shnel, A., Tuohy, P., 2024a. Temporal Stability of Grassland Soil Moisture Utilising Sentinel-2 Satellites and Sparse Ground-Based Sensor Networks. *Remote Sens.* 16, 220. <https://doi.org/10.3390/RS16020220>
- Basu, R., Fenton, O., Daly, E., Tuohy, P., 2024b. Identifying favourable conditions for farm scale trafficability and grass growth using a combined Sentinel-2 and soil moisture deficit approach. *Front. Environ. Sci.* 12, 1–13. <https://doi.org/10.3389/fenvs.2024.1331659>
- Bauer-Marschallinger, B., Freeman, V., Cao, S., Paulik, C., Schaufler, S., Stachl, T., Modanesi, S., Massari, C., Ciabatta, L., Brocca, L., Wagner, W., 2019. Toward Global Soil Moisture Monitoring with Sentinel-1: Harnessing Assets and Overcoming Obstacles. *IEEE Trans. Geosci. Remote Sens.* 57, 520–539. <https://doi.org/10.1109/TGRS.2018.2858004>
- Benegas, L., Hasselquist, N., Bargaés-Tobella, A., Malmer, A., Ilstedt, U., 2021. Positive Effects of Scattered Trees on Soil Water Dynamics in a Pasture Landscape in the Tropics. *Front. Water* 3. <https://doi.org/10.3389/frwa.2021.736824>
- Bengtsson, J., Bullock, J.M., Egoh, B., Everson, C., Everson, T., O’Connor, T., O’Farrell, P.J., Smith, H.G., Lindborg, R., 2019. Grasslands—more important for ecosystem services than you might think. *Ecosphere* 10, e02582. <https://doi.org/10.1002/ecs2.2582>
- Berg, A., Sheffield, J., 2018. Climate Change and Drought: the Soil Moisture Perspective. *Curr. Clim. Chang. Reports.* <https://doi.org/10.1007/s40641-018-0095-0>
- Bhogapurapu, N., Dey, S., Homayouni, S., Bhattacharya, A., Rao, Y.S., 2022. Field-scale soil moisture estimation using sentinel-1 GRD SAR data. *Adv. Sp. Res.* 70, 3845–3858. <https://doi.org/10.1016/j.asr.2022.03.019>
- Bhuyan, H., Scheuermann, A., Bodin, D., Becker, R., 2020. Soil moisture and density monitoring methodology using TDR measurements. *Int. J. Pavement Eng.* 21, 1263–1274. <https://doi.org/10.1080/10298436.2018.1537491>
- Blüthgen, N., Dormann, C.F., Prati, D., Klaus, V.H., Kleinebecker, T., Hölzel, N., Alt, F., Boch, S., Gockel, S., Hemp, A., Müller, J., Nieschulze, J., Renner, S.C., Schöning, I., Schumacher, U., Socher, S.A., Wells, K., Birkhofer, K., Buscot, F., Oelmann, Y., Rothenwöhrer, C., Scherber, C., Tscharrntke, T., Weiner, C.N., Fischer, M., Kalko, E.K.V., Linsenmair, K.E., Schulze, E.D., Weisser, W.W., 2012. A quantitative index of land-use intensity in grasslands: Integrating mowing, grazing and fertilization. *Basic Appl. Ecol.* 13, 207–220. <https://doi.org/10.1016/j.baae.2012.04.001>
- Bogena, H.R., Huisman, J.A., Baatz, R., Hendricks Franssen, H.J., Vereecken, H., 2013. Accuracy of the cosmic-ray soil water content probe in humid forest ecosystems: The worst case scenario. *Water Resour. Res.* 49, 5778–5791. <https://doi.org/10.1002/wrcr.20463>
- Bogena, H.R., Huisman, J.A., Güntner, A., Hübner, C., Kusche, J., Jonard, F., Vey, S., Vereecken, H., 2015. Emerging methods for noninvasive sensing of soil moisture dynamics from field to catchment scale: a review. *Wiley Interdiscip. Rev. Water.* <https://doi.org/10.1002/WAT2.1097>
- Bondi, G., O’Sullivan, L., Fenton, O., Creamer, R., Marongiu, I., Wall, D.P., 2021. Trafficking intensity

- index for soil compaction management in grasslands. *Soil Use Manag.* 37, 504–518. <https://doi.org/10.1111/sum.12586>
- Bousbih, S., Zribi, M., Hajj, M. El, Baghdadi, N., Lili-Chabaane, Z., Gao, Q., Fanise, P., 2018. Soil moisture and irrigation mapping in a semi-arid region, based on the synergetic use of Sentinel-1 and Sentinel-2 data. *Remote Sens.* 10, 1953. <https://doi.org/10.3390/rs10121953>
- Bracken, C.J., Lanigan, G.J., Richards, K.G., Müller, C., Tracy, S.R., Grant, J., Krol, D.J., Sheridan, H., Lynch, M.B., Grace, C., Fritch, R., Murphy, P.N.C., 2021. Source partitioning using N₂O isotopomers and soil WFPS to establish dominant N₂O production pathways from different pasture sward compositions. *Sci. Total Environ.* 781, 146515. <https://doi.org/10.1016/j.scitotenv.2021.146515>
- Bracken, C.J., Lanigan, G.J., Richards, K.G., Müller, C., Tracy, S.R., Grant, J., Krol, D.J., Sheridan, H., Lynch, M.B., Grace, C., Fritch, R., Murphy, P.N.C., 2020. Sward composition and soil moisture conditions affect nitrous oxide emissions and soil nitrogen dynamics following urea-nitrogen application. *Sci. Total Environ.* 722, 137780. <https://doi.org/10.1016/j.scitotenv.2020.137780>
- Briciu-Burghina, C., Zhou, J., Ali, M.I., Regan, F., 2022. Demonstrating the Potential of a Low-Cost Soil Moisture Sensor Network. *Sensors* 22, 987. <https://doi.org/10.3390/s22030987>
- Brocca, L., Morbidelli, R., Melone, F., Moramarco, T., 2007. Soil moisture spatial variability in experimental areas of central Italy. *J. Hydrol.* 333, 356–373. <https://doi.org/10.1016/j.jhydrol.2006.09.004>
- Brunner, E., Mardock, E.S., 1946. A Neutron Method for Measuring Saturations in Laboratory Flow Experiments. *Trans. AIME* 165, 133–143. <https://doi.org/10.2118/946133-g>
- Brutsaert, W., 2014. The daily mean zero-flux plane during soil-controlled evaporation: A Green's function approach. *Water Resour. Res.* 50, 9405–9413. <https://doi.org/10.1002/2014WR016111>
- Buckley, C., Carney, P., 2013. The potential to reduce the risk of diffuse pollution from agriculture while improving economic performance at farm level. *Environ. Sci. Policy* 25, 118–126. <https://doi.org/10.1016/j.envsci.2012.10.002>
- Buckley, C., Wall, D.P., Moran, B., O'Neill, S., Murphy, P.N.C., 2016. Farm gate level nitrogen balance and use efficiency changes post implementation of the EU Nitrates Directive. *Nutr. Cycl. Agroecosystems* 104, 1–13. <https://doi.org/10.1007/S10705-015-9753-Y/TABLES/4>
- Burdun, I., Bechtold, M., Aurela, M., De Lannoy, G., Desai, A.R., Humphreys, E., Kareksela, S., Komisarenko, V., Liimatainen, M., Marttila, H., Minkkinen, K., Nilsson, M.B., Ojanen, P., Salko, S.S., Tuittila, E.S., Uuemaa, E., Rautiainen, M., 2023. Hidden becomes clear: Optical remote sensing of vegetation reveals water table dynamics in northern peatlands. *Remote Sens. Environ.* 296, 113736. <https://doi.org/10.1016/j.rse.2023.113736>
- Burdun, I., Bechtold, M., Sagris, V., Komisarenko, V., Lannoy, G. De, Mander, Ü., 2020a. A comparison of three trapezoid models using optical and thermal satellite imagery for water table depth monitoring in Estonian Bogs. *Remote Sens.* 12, 1980. <https://doi.org/10.3390/rs12121980>
- Burdun, I., Bechtold, M., Sagris, V., Lohila, A., Humphreys, E., Desai, A.R., Nilsson, M.B., De Lannoy, G., Mander, Ü., 2020b. Satellite determination of peatland water table temporal dynamics by localizing representative pixels of A SWIR-Based Moisture Index. *Remote Sens.* 12, 2936. <https://doi.org/10.3390/RS12182936>
- Campbell, G., 2015. Plant Available Water: How Do I Determine Field Capacity and Permanent

Wilting Point? [WWW Document]. M. Gr. URL <https://metergroup.com/measurement-insights/plant-available-water-how-do-i-determine-field-capacity-and-permanent-wilting-point/> (accessed 5.14.24).

- Cardenas, L.M., Bhogal, A., Chadwick, D.R., McGeough, K., Misselbrook, T., Rees, R.M., Thorman, R.E., Watson, C.J., Williams, J.R., Smith, K.A., Calvet, S., 2019. Nitrogen use efficiency and nitrous oxide emissions from five UK fertilised grasslands. *Sci. Total Environ.* 661, 696–710. <https://doi.org/10.1016/j.scitotenv.2019.01.082>
- Champagne, C., White, J., Berg, A., Belair, S., Carrera, M., 2019. Impact of soil moisture data characteristics on the sensitivity to crop yields under drought and excess moisture conditions. *Remote Sens.* 11, 372. <https://doi.org/10.3390/rs11040372>
- Chaudhary, S.K., Srivastava, P.K., Gupta, D.K., Kumar, P., Prasad, R., Pandey, D.K., Das, A.K., Gupta, M., 2022. Machine learning algorithms for soil moisture estimation using Sentinel-1: Model development and implementation. *Adv. Sp. Res.* 69, 1799–1812. <https://doi.org/10.1016/j.asr.2021.08.022>
- Chavez, P.S., 1988. An improved dark-object subtraction technique for atmospheric scattering correction of multispectral data. *Remote Sens. Environ.* 24, 459–479. [https://doi.org/10.1016/0034-4257\(88\)90019-3](https://doi.org/10.1016/0034-4257(88)90019-3)
- Chen, L., Zhangzhong, L., Zheng, W., Yu, J., Wang, Z., Wang, L., Huang, C., 2019. Data-driven calibration of soil moisture sensor considering impacts of temperature: A case study on FDR sensors. *Sensors (Switzerland)* 19, 4381. <https://doi.org/10.3390/s19204381>
- Chen, M., Zhang, Y., Yao, Y., Lu, J., Pu, X., Hu, T., Wang, P., 2020. Evaluation of the OPTRAM Model to Retrieve Soil Moisture in the Sanjiang Plain of Northeast China. *Earth Sp. Sci.* 7, e2020EA001108. <https://doi.org/10.1029/2020EA001108>
- Chtouki, M., Laaziz, F., Naciri, R., Garré, S., Nguyen, F., Oukarroum, A., 2022. Interactive effect of soil moisture content and phosphorus fertilizer form on chickpea growth, photosynthesis, and nutrient uptake. *Sci. Rep.* 12, 1–13. <https://doi.org/10.1038/s41598-022-10703-0>
- Collow, T.W., Robock, A., Basara, J.B., Illston, B.G., 2012. Evaluation of SMOS retrievals of soil moisture over the central United States with currently available in situ observations. *J. Geophys. Res. Atmos.* 117. <https://doi.org/10.1029/2011JD017095>
- Coluzzi, R., Imbrenda, V., Lanfredi, M., Simoniello, T., 2018. A first assessment of the Sentinel-2 Level 1-C cloud mask product to support informed surface analyses. *Remote Sens. Environ.* 217, 426–443. <https://doi.org/10.1016/j.rse.2018.08.009>
- Congedo, L., 2021. Semi-Automatic Classification Plugin: A Python tool for the download and processing of remote sensing images in QGIS. *J. Open Source Softw.* 6, 3172. <https://doi.org/10.21105/joss.03172>
- Cosh, M.H., Caldwell, T.G., Baker, C.B., Bolten, J.D., Edwards, N., Goble, P., Hofman, H., Ochsner, T.E., Quiring, S., Schalk, C., Skumanich, M., Svoboda, M., Woloszyn, M.E., 2021. Developing a strategy for the national coordinated soil moisture monitoring network. *Vadose Zo. J.* 20, e20139. <https://doi.org/10.1002/vzj2.20139>
- Cui, D., Liang, S., Wang, D., 2021. Observed and projected changes in global climate zones based on Köppen climate classification. *Wiley Interdiscip. Rev. Clim. Chang.* <https://doi.org/10.1002/wcc.701>
- D’Odorico, P., Caylor, K., Okin, G.S., Scanlon, T.M., 2007. On soil moisture-vegetation feedbacks and their possible effects on the dynamics of dryland ecosystems. *J. Geophys. Res. Biogeosciences*

112. <https://doi.org/10.1029/2006JG000379>

- da Silva Cardoso, A., Junqueira, J.B., Reis, R.A., Ruggieri, A.C., 2020. How do greenhouse gas emissions vary with biofertilizer type and soil temperature and moisture in a tropical grassland? *Pedosphere* 30, 607–617. [https://doi.org/10.1016/S1002-0160\(20\)60025-X](https://doi.org/10.1016/S1002-0160(20)60025-X)
- Dari, J., Morbidelli, R., Saltalippi, C., Massari, C., Brocca, L., 2019. Spatial-temporal variability of soil moisture: Addressing the monitoring at the catchment scale. *J. Hydrol.* 570, 436–444. <https://doi.org/10.1016/j.jhydrol.2019.01.014>
- Das, N.N., Entekhabi, D., Dunbar, R.S., Chaubell, M.J., Colliander, A., Yueh, S., Jagdhuber, T., Chen, F., Crow, W., O'Neill, P.E., Walker, J.P., Berg, A., Bosch, D.D., Caldwell, T., Cosh, M.H., Collins, C.H., Lopez-Baeza, E., Thibeault, M., 2019. The SMAP and Copernicus Sentinel 1A/B microwave active-passive high resolution surface soil moisture product. *Remote Sens. Environ.* 233, 111380. <https://doi.org/10.1016/j.rse.2019.111380>
- Daxini, A., Ryan, M., O'Donoghue, C., Barnes, A.P., Buckley, C., 2019. Using a typology to understand farmers' intentions towards following a nutrient management plan. *Resour. Conserv. Recycl.* 146, 280–290. <https://doi.org/10.1016/j.resconrec.2019.03.027>
- de Queiroz, M.G., da Silva, T.G.F., Zolnier, S., Jardim, A.M. da R.F., de Souza, C.A.A., Araújo Júnior, G. do N., de Moraes, J.E.F., de Souza, L.S.B., 2020. Spatial and temporal dynamics of soil moisture for surfaces with a change in land use in the semi-arid region of Brazil. *Catena* 188, 104457. <https://doi.org/10.1016/j.catena.2020.104457>
- Devine, S., O'Geen, A., 2019. Climate-smart management of soil water storage: Statewide analysis of California perennial crops. *Environ. Res. Lett.* 14, 044021. <https://doi.org/10.1088/1748-9326/ab058c>
- Ding, J., Li, F., Le, T., Xu, D., Zhu, M., Li, C., Zhu, X., Guo, W., 2021. Tillage and seeding strategies for wheat optimizing production in harvested rice fields with high soil moisture. *Sci. Rep.* 11, 1–12. <https://doi.org/10.1038/s41598-020-80256-7>
- Dorigo, W., Himmelbauer, I., Aberer, D., Schremmer, L., Petrakovic, I., Zappa, L., Preimesberger, W., Xaver, A., Annor, F., Ardö, J., Baldocchi, D., Bitelli, M., Blöschl, G., Boga, H., Brocca, L., Calvet, J.C., Camarero, J.J., Capello, G., Choi, M., Cosh, M.C., van de Giesen, N., Hajdu, I., Ikonen, J., Jensen, K.H., Kanniah, K.D., de Kat, I., Kirchengast, G., Rai, P.K., Kyrouac, J., Larson, K., Liu, S., Loew, A., Moghaddam, M., Fernández, J.M., Bader, C.M., Morbidelli, R., Musial, J.P., Osenga, E., Palecki, M.A., Pellarin, T., Petropoulos, G.P., Pfeil, I., Powers, J., Robock, A., Rüdiger, C., Rummel, U., Strobel, M., Su, Z., Sullivan, R., Tagesson, T., Varlagin, A., Vreugdenhil, M., Walker, J., Wen, J., Wenger, F., Wigneron, J.P., Woods, M., Yang, K., Zeng, Y., Zhang, X., Zreda, M., Dietrich, S., Gruber, A., van Oevelen, P., Wagner, W., Scipal, K., Drusch, M., Sabia, R., 2021. The International Soil Moisture Network: Serving Earth system science for over a decade. *Hydrol. Earth Syst. Sci.* <https://doi.org/10.5194/hess-25-5749-2021>
- Edokossi, K., Calabria, A., Jin, S., Molina, I., 2020. GNSS-reflectometry and remote sensing of soil moisture: A review of measurement techniques, methods, and applications. *Remote Sens.* <https://doi.org/10.3390/rs12040614>
- Entekhabi, D., Njoku, E.G., O'Neill, P.E., Kellogg, K.H., Crow, W.T., Edelstein, W.N., Entin, J.K., Goodman, S.D., Jackson, T.J., Johnson, J., Kimball, J., Piepmeier, J.R., Koster, R.D., Martin, N., McDonald, K.C., Moghaddam, M., Moran, S., Reichle, R., Shi, J.C., Spencer, M.W., Thurman, S.W., Tsang, L., Van Zyl, J., 2010. The soil moisture active passive (SMAP) mission. *Proc. IEEE* 98, 704–716. <https://doi.org/10.1109/JPROC.2010.2043918>
- Environmental Protection Agency, 2014. Irish Soil Information System Synthesis Report.

<https://doi.org/10.4135/9781483346526.n193>

Environmental Protection Agency Ireland, 2014. Interactions of Soil Hydrology , Land Use and Climate Change and their Impact on Soil Quality (SoilH).

EPA, 2018. Current trends: Land and soil | Environmental Protection Agency [WWW Document]. EPA Irel. URL <https://www.epa.ie/our-services/monitoring--assessment/assessment/irelands-environment/land--soil/current-trends-land-and-soil/> (accessed 1.5.23).

ESA, 2013. User Guides - Sentinel-2 MSI [WWW Document]. Sentinels.copernicus.eu. URL <https://sentinels.copernicus.eu/web/sentinel/user-guides/sentinel-2-msi/product-types/level-1c> (accessed 10.25.22).

ESA, 2010. About the Soil Moisture CCI project [WWW Document]. URL <https://climate.esa.int/en/projects/soil-moisture/about/> (accessed 11.14.23).

EU, 2022. The EU NatureRestoration Law [WWW Document]. Eur. Comm. URL https://environment.ec.europa.eu/topics/nature-and-biodiversity/nature-restoration-law_en#documents (accessed 3.31.23).

Farthing, M.W., Ogden, F.L., 2017. Numerical Solution of Richards' Equation: A Review of Advances and Challenges. *Soil Sci. Soc. Am. J.* 81, 1257–1269. <https://doi.org/10.2136/sssaj2017.02.0058>

Feng, H., Zhang, M., 2015. Global land moisture trends: Drier in dry and wetter in wet over land. *Sci. Rep.* 5, 1–6. <https://doi.org/10.1038/srep18018>

Filippucci, P., Tarpanelli, A., Massari, C., Serafini, A., Strati, V., Alberi, M., Raptis, K.G.C., Mantovani, F., Brocca, L., 2020. Soil moisture as a potential variable for tracking and quantifying irrigation: A case study with proximal gamma-ray spectroscopy data. *Adv. Water Resour.* 136, 103502. <https://doi.org/10.1016/j.advwatres.2019.103502>

Finkele, K., Hochstrasser, T., Murphy, P.N.C., Daly, E., Jarmain, C., Richards, K., Fenton, O., Cummins, T., Saunders, M., Johnston, P.M., Bruen, M., Byrne, K.A., Delaney, D.T., Fealy, R., Green, S., Higgins, S., Williams, N.H., Lanigan, G., McCarthy, T., McCormack, T., Mellander, P.-E., Nicholson, O., Nugent, C., O'Loughlin, F., Tobin, B., Tuohy, P., Whetton, R., 2022. The new Irish Soil Moisture Observation Network- ISMON: an Umbrella for Integrating Several Recent Soil Moisture Measurements Initiatives, in: EMS Annual Meeting 2022. Copernicus Meetings. <https://doi.org/10.5194/EMS2022-273>

Fluet-Chouinard, E., Stocker, B.D., Zhang, Z., Malhotra, A., Melton, J.R., Poulter, B., Kaplan, J.O., Goldewijk, K.K., Siebert, S., Minayeva, T., Hugelius, G., Joosten, H., Barthelmes, A., Prigent, C., Aires, F., Hoyt, A.M., Davidson, N., Finlayson, C.M., Lehner, B., Jackson, R.B., McIntyre, P.B., 2023. Extensive global wetland loss over the past three centuries. *Nature* 614, 281–286. <https://doi.org/10.1038/s41586-022-05572-6>

Flynn, N.E., Comas, L.H., Stewart, C.E., Fonte, S.J., 2023. High N availability decreases N uptake and yield under limited water availability in maize. *Sci. Rep.* 13, 1–12. <https://doi.org/10.1038/s41598-023-40459-0>

Foroughi, H., Naseri, A.A., Boroomand Nasab, S., Hamzeh, S., Sadeghi, M., Tuller, M., Jones, S.B., 2020. A new mathematical formulation for remote sensing of soil moisture based on the Red-NIR space. *Int. J. Remote Sens.* 41, 8034–8047. <https://doi.org/10.1080/01431161.2020.1770365>

Franz, T.E., Zreda, M., Ferre, T.P.A., Rosolem, R., Zweck, C., Stillman, S., Zeng, X., Shuttleworth, W.J., 2012a. Measurement depth of the cosmic ray soil moisture probe affected by hydrogen from various sources. *Water Resour. Res.* 48. <https://doi.org/10.1029/2012WR011871>

- Franz, T.E., Zreda, M., Ferre, T.P.A., Rosolem, R., Zweck, C., Stillman, S., Zeng, X., Shuttleworth, W.J., 2012b. Measurement depth of the cosmic ray soil moisture probe affected by hydrogen from various sources. *Water Resour. Res.* 48. <https://doi.org/10.1029/2012WR011871>
- Fry, J.E., Guber, A.K., 2020. Temporal stability of field-scale patterns in soil water content across topographically diverse agricultural landscapes. *J. Hydrol.* 580, 124260. <https://doi.org/10.1016/j.jhydrol.2019.124260>
- Gaddikeri, V., Hasan, M., Kumar, D., Sarangi, A., Alam, W., 2022. Performance Analysis and Measurement of Soil Moisture Content by Piezoresistive Sensor. *Mapan - J. Metrol. Soc. India* 37, 149–160. <https://doi.org/10.1007/s12647-021-00512-7>
- Gałęzewski, L., Jaskulska, I., Jaskulski, D., Lewandowski, A., Szyptowska, A., Wilczek, A., Szczepańczyk, M., 2021. Analysis of the need for soil moisture, salinity and temperature sensing in agriculture: a case study in Poland. *Sci. Rep.* 11, 1–14. <https://doi.org/10.1038/s41598-021-96182-1>
- Gao, B.C., 1996. NDWI - A normalized difference water index for remote sensing of vegetation liquid water from space. *Remote Sens. Environ.* 58, 257–266. [https://doi.org/10.1016/S0034-4257\(96\)00067-3](https://doi.org/10.1016/S0034-4257(96)00067-3)
- GCOS, 2020. Gcos | Wmo [WWW Document]. URL <https://gcos.wmo.int/en/essential-climate-variables/soil-moisture> (accessed 11.14.23).
- Gilmore, S., Saleem, A., Dewan, A., 2015. Effectiveness of DOS (Dark-Object Subtraction) method and water index techniques to map wetlands in a rapidly urbanising megacity with Landsat 8 data, in: CEUR Workshop Proceedings. <http://SunSITE.Informatik.RWTH-Aachen.DE/Publications/CEUR-WS/>, pp. 100–108.
- Global Climate Observing System, (GCOS), 2020. Gcos | Wmo [WWW Document]. URL <https://gcos.wmo.int/en/essential-climate-variables/soil-moisture> (accessed 10.20.22).
- gov.ie - Nitrates Directive [WWW Document], 2020. . Dep. Housing, Local Gov. Herit. URL <https://www.gov.ie/en/publication/b87ad-nitrates-directive/> (accessed 10.17.23).
- Government, S., 2019. Fertiliser recommendations for grassland.
- Govindasamy, P., Muthusamy, S.K., Bagavathiannan, M., Mowrer, J., Jagannadham, P.T.K., Maity, A., Halli, H.M., G. K, S., Vadivel, R., T. K, D., Raj, R., Pooniya, V., Babu, S., Rathore, S.S., L, M., Tiwari, G., 2023. Nitrogen use efficiency—a key to enhance crop productivity under a changing climate. *Front. Plant Sci.* <https://doi.org/10.3389/fpls.2023.1121073>
- Gruber, A., De Lannoy, G., Albergel, C., Al-Yaari, A., Brocca, L., Calvet, J.C., Colliander, A., Cosh, M., Crow, W., Dorigo, W., Draper, C., Hirschi, M., Kerr, Y., Konings, A., Lahoz, W., McColl, K., Montzka, C., Muñoz-Sabater, J., Peng, J., Reichle, R., Richaume, P., Rüdiger, C., Scanlon, T., van der Schalie, R., Wigneron, J.P., Wagner, W., 2020. Validation practices for satellite soil moisture retrievals: What are (the) errors? *Remote Sens. Environ.* <https://doi.org/10.1016/j.rse.2020.111806>
- Guadalupe Ramos Hernández, J., Gracia-Sánchez, J., Patricia Rodríguez-Martínez, T., Adalberto Zuñiga-Morales, J., 2019. Correlation between TDR and FDR Soil Moisture Measurements at Different Scales to Establish Water Availability at the South of the Yucatan Peninsula, in: *Soil Moisture*. IntechOpen. <https://doi.org/10.5772/intechopen.81477>
- Habel, J.C., Dengler, J., Janišová, M., Török, P., Wellstein, C., Wiezik, M., 2013. European grassland ecosystems: Threatened hotspots of biodiversity. *Biodivers. Conserv.* <https://doi.org/10.1007/s10531-013-0537-x>

- Hackett, R., 2017. Optimising Nitrogen Input for Cereals, in: Proceedings of the Fertiliser Association of Ireland, 52. pp. 17–31.
- Hanson, B.R., Orloff, S., Peters, D., 2000. Monitoring soil moisture helps refine irrigation management. *Calif. Agric.* 54, 38–42. <https://doi.org/10.3733/ca.v054n03p38>
- Hardie, M., 2020. Review of novel and emerging proximal soil moisture sensors for use in agriculture. *Sensors (Switzerland)* 20, 1–23. <https://doi.org/10.3390/s20236934>
- Hassanpour, R., Zarehaghi, D., Neyshabouri, M.R., Feizizadeh, B., Rahmati, M., 2020. Modification on optical trapezoid model for accurate estimation of soil moisture content in a maize growing field. *J. Appl. Remote Sens.* 14, 034519. <https://doi.org/10.1117/1.jrs.14.034519>
- Hawkins, M.J., Hyde, B.P., Ryan, M., Schulte, R.P.O., Connolly, J., 2007. An empirical model and scenario analysis of nitrous oxide emissions from a fertilised and grazed grassland site in Ireland. *Nutr. Cycl. Agroecosystems* 79, 93–101. <https://doi.org/10.1007/s10705-007-9099-1>
- Hejcman, M., Hejcmanová, P., Pavlů, V., Beneš, J., 2013. Origin and history of grasslands in central Europe - A review. *Grass Forage Sci.* <https://doi.org/10.1111/gfs.12066>
- Herbin, T., Hennessy, D., Richards, K.G., Piwowarczyk, A., Murphy, J.J., Holden, N.M., 2011. The effects of dairy cow weight on selected soil physical properties indicative of compaction. *Soil Use Manag.* 27, 36–44. <https://doi.org/10.1111/j.1475-2743.2010.00309.x>
- Higgins, S., Schellberg, J., Bailey, J.S., 2019. Improving productivity and increasing the efficiency of soil nutrient management on grassland farms in the UK and Ireland using precision agriculture technology. *Eur. J. Agron.* <https://doi.org/10.1016/j.eja.2019.04.001>
- Hopkins, A., Holz, B., 2006. Grassland for agriculture and nature conservation: production, quality and multi-functionality. *Agron. Res.* 4, 3–20.
- Hupet, F., Vanclooster, M., 2002. Intraseasonal dynamics of soil moisture variability within a small agricultural maize cropped field. *J. Hydrol.* 261, 86–101. [https://doi.org/10.1016/S0022-1694\(02\)00016-1](https://doi.org/10.1016/S0022-1694(02)00016-1)
- Insam, H., Seewald, M.S.A., 2010. Volatile organic compounds (VOCs) in soils. *Biol. Fertil. Soils.* <https://doi.org/10.1007/s00374-010-0442-3>
- IPCC 6th Assessment report, 2023. Water, IPCC. Cambridge University Press. <https://doi.org/10.1017/9781009325844.006>
- Ireland Central Statistics Office, 2022. South-East Region Regional Accounts for Agriculture 2022 - Central Statistics Office [WWW Document]. URL <https://www.cso.ie/en/releasesandpublications/ep/p-raa/regionalaccountsforagriculture2022/south-eastregion/> (accessed 2.17.24).
- Kashyap, B., Kumar, R., 2021. Sensing Methodologies in Agriculture for Soil Moisture and Nutrient Monitoring. *IEEE Access* 9, 14095–14121. <https://doi.org/10.1109/ACCESS.2021.3052478>
- Keller, T., Sandin, M., Colombi, T., Horn, R., Or, D., 2019. Historical increase in agricultural machinery weights enhanced soil stress levels and adversely affected soil functioning. *Soil Tillage Res.* 194, 104293. <https://doi.org/10.1016/j.still.2019.104293>
- Kerebel, A., Cassidy, R., Jordan, P., Holden, N.M., 2013. Farmer perception of suitable conditions for slurry application compared with decision support system recommendations. *Agric. Syst.* 120, 49–60. <https://doi.org/10.1016/j.agry.2013.05.007>
- Kerr, Y.H., Waldteufel, P., Wigneron, J.P., Delwart, S., Cabot, F., Boutin, J., Escorihuela, M.J., Font, J.,

- Reul, N., Gruhier, C., Juglea, S.E., Drinkwater, M.R., Hahne, A., Martin-Neira, M., Mecklenburg, S., 2010. The SMOS L: New tool for monitoring key elements of the global water cycle. *Proc. IEEE* 98, 666–687. <https://doi.org/10.1109/JPROC.2010.2043032>
- Khellouk, R., Barakat, A., Boudhar, A., Hadria, R., Lionboui, H., El Jazouli, A., Rais, J., El Baghdadi, M., Benabdelouahab, T., 2020. Spatiotemporal monitoring of surface soil moisture using optical remote sensing data: a case study in a semi-arid area. *J. Spat. Sci.* <https://doi.org/10.1080/14498596.2018.1499559>
- Khellouk, R., Barakat, A., Jazouli, A. El, Boudhar, A., Lionboui, H., Rais, J., Benabdelouahab, T., 2021. An integrated methodology for surface soil moisture estimating using remote sensing data approach. *Geocarto Int.* 36, 1443–1458. <https://doi.org/10.1080/10106049.2019.1655797>
- King, C., McEniry, J., Richardson, M., O’Kiely, P., 2012. Yield and chemical composition of five common grassland species in response to nitrogen fertiliser application and phenological growth stage. *Acta Agric. Scand. Sect. B Soil Plant Sci.* 62, 644–658. <https://doi.org/10.1080/09064710.2012.687055>
- Kirkham, M.B., 2014. Field Capacity, Wilting Point, Available Water, and the Nonlimiting Water Range, in: *Principles of Soil and Plant Water Relations*. Academic Press, pp. 153–170. <https://doi.org/10.1016/b978-0-12-420022-7.00010-0>
- Kirkham, M.B., 2005. Field Capacity, Wilting Point, Available Water, and the Nonlimiting Water Range, in: *Principles of Soil and Plant Water Relations*. Elsevier, pp. 153–170. <https://doi.org/10.1016/b978-0-12-420022-7.00010-0>
- Krishnan, S., Indu, J., 2023. Assessing the potential of temperature/vegetation index space to infer soil moisture over Ganga Basin. *J. Hydrol.* 621, 129611. <https://doi.org/10.1016/j.jhydrol.2023.129611>
- Krueger, E.S., Ochsner, T.E., Levi, M.R., Basara, J.B., Snitker, G.J., Wyatt, B.M., 2021. Grassland productivity estimates informed by soil moisture measurements: Statistical and mechanistic approaches. *Agron. J.* 113, 3498–3517. <https://doi.org/10.1002/agj2.20709>
- Lalor, S.T.J., Schulte, R.P.O., 2008. Low-ammonia-emission application methods can increase the opportunity for application of cattle slurry to grassland in spring in Ireland. *Grass Forage Sci.* 63, 531–544. <https://doi.org/10.1111/j.1365-2494.2008.00657.x>
- Lange, M., Feilhauer, H., Kühn, I., Doktor, D., 2022. Mapping land-use intensity of grasslands in Germany with machine learning and Sentinel-2 time series. *Remote Sens. Environ.* 277, 112888. <https://doi.org/10.1016/j.rse.2022.112888>
- Lemaire, G., Hodgson, J., Chabbi, A., 2011. Grassland productivity and ecosystems services, *Grassland Productivity and Ecosystems Services*. <https://doi.org/10.2989/10220119.2014.955878>
- Lepore, E., Schmidt, O., Fenton, O., Tracy, S., Bondi, G., Wall, D., 2023. Moisture limits for grassland soil to avoid structural damage due to machine trafficking, in: *EGU23. Copernicus Meetings*. <https://doi.org/10.5194/EGUSPHERE-EGU23-3137>
- Li, Z.L., Leng, P., Zhou, C., Chen, K.S., Zhou, F.C., Shang, G.F., 2021. Soil moisture retrieval from remote sensing measurements: Current knowledge and directions for the future. *Earth-Science Rev.* <https://doi.org/10.1016/j.earscirev.2021.103673>
- Liang, C., Yue, Y., Gao, J.Q., Zhang, X.Y., Li, Q.W., Yu, F.H., 2022. Effects of soil moisture on organic and inorganic nitrogen uptake by dominant plant species in Zoigê alpine wetlands. *Ecol. Indic.* 141, 109087. <https://doi.org/10.1016/j.ecolind.2022.109087>

- Lipovetsky, S., 2010. Double logistic curve in regression modeling. *J. Appl. Stat.* 37, 1785–1793. <https://doi.org/10.1080/02664760903093633>
- Liu, R., Shang, R., Liu, Y., Lu, X., 2017. Global evaluation of gap-filling approaches for seasonal NDVI with considering vegetation growth trajectory, protection of key point, noise resistance and curve stability. *Remote Sens. Environ.* 189, 164–179. <https://doi.org/10.1016/j.rse.2016.11.023>
- Lobell, D.B., Asner, G.P., 2002. Moisture Effects on Soil Reflectance. *Soil Sci. Soc. Am. J.* 66, 722–727. <https://doi.org/10.2136/sssaj2002.7220>
- Lv, L., Franz, T.E., Robinson, D.A., Jones, S.B., 2014. Measured and Modeled Soil Moisture Compared with Cosmic-Ray Neutron Probe Estimates in a Mixed Forest. *Vadose Zo. J.* 13, 1–13. <https://doi.org/10.2136/vzj2014.06.0077>
- Mallick, K., Bhattacharya, B.K., Patel, N.K., 2009. Estimating volumetric surface moisture content for cropped soils using a soil wetness index based on surface temperature and NDVI. *Agric. For. Meteorol.* 149, 1327–1342. <https://doi.org/10.1016/j.agrformet.2009.03.004>
- Mananze, S., Pôças, I., 2019. Agricultural drought monitoring based on soil moisture derived from the optical trapezoid model in Mozambique. *J. Appl. Remote Sens.* 13, 1. <https://doi.org/10.1117/1.jrs.13.024519>
- Martín, N., Pardo, L., 2009. On the asymptotic distribution of Cook's distance in logistic regression models. *J. Appl. Stat.* 36, 1119–1146. <https://doi.org/10.1080/02664760802562498>
- Martínez-Fernández, J., Ceballos, A., 2003. Temporal Stability of Soil Moisture in a Large-Field Experiment in Spain. *Soil Sci. Soc. Am. J.* 67, 1647–1656. <https://doi.org/10.2136/sssaj2003.1647>
- McGrath, T., McKeown, M., O'Loughlin, F., 2023. Climate Change Impacts on Ireland's Water Resources.
- Met Eireann, 2023. Latest Farming Commentary - Met Éireann - The Irish Meteorological Service.
- Met Eireann, 2020. Drought Summary - Met Éireann - The Irish Meteorological Service [WWW Document]. URL <https://www.met.ie/drought-summary> (accessed 5.15.24).
- Met Éireann [WWW Document], 2023. . Met Eireann. URL <https://www.met.ie/july-2023-provisionally-irelands-wettest-july-on-record> (accessed 1.11.24).
- MetEireann, 2022. Rain - Met Éireann - The Irish Meteorological Service [WWW Document]. URL <https://www.met.ie/climate/what-we-measure/rainfall> (accessed 10.20.22).
- Meurer, K., Barron, J., Chenu, C., Coucheney, E., Fielding, M., Hallett, P., Herrmann, A.M., Keller, T., Koestel, J., Larsbo, M., Lewan, E., Or, D., Parsons, D., Parvin, N., Taylor, A., Vereecken, H., Jarvis, N., 2020. A framework for modelling soil structure dynamics induced by biological activity. *Glob. Chang. Biol.* <https://doi.org/10.1111/gcb.15289>
- Mimeau, L., Trambly, Y., Brocca, L., Massari, C., Camici, S., Finaud-Guyot, P., 2021. Modeling the response of soil moisture to climate variability in the Mediterranean region. *Hydrol. Earth Syst. Sci.* 25, 653–669. <https://doi.org/10.5194/hess-25-653-2021>
- Modanesi, S., Massari, C., Camici, S., Brocca, L., Amarnath, G., 2020. Do Satellite Surface Soil Moisture Observations Better Retain Information About Crop-Yield Variability in Drought Conditions? *Water Resour. Res.* 56. <https://doi.org/10.1029/2019WR025855>
- Mohanty, B.P., Cosh, M.H., Lakshmi, V., Montzka, C., 2017. Soil Moisture Remote Sensing: State-of-the-Science. *Vadose Zo. J.* 16, vzj2016.10.0105. <https://doi.org/10.2136/vzj2016.10.0105>

- Mohanty, B.P., Skaggs, T.H., 2001. Spatio-temporal evolution and time-stable characteristics of soil moisture within remote sensing footprints with varying soil, slope, and vegetation. *Adv. Water Resour.* 24, 1051–1067. [https://doi.org/10.1016/S0309-1708\(01\)00034-3](https://doi.org/10.1016/S0309-1708(01)00034-3)
- Mokhtari, A., Sadeghi, M., Afrasiabian, Y., Yu, K., 2023. OPTRAM-ET: A novel approach to remote sensing of actual evapotranspiration applied to Sentinel-2 and Landsat-8 observations. *Remote Sens. Environ.* 286, 113443. <https://doi.org/10.1016/j.rse.2022.113443>
- Mueller, B., Seneviratne, S.I., 2012. Hot days induced by precipitation deficits at the global scale. *Proc. Natl. Acad. Sci. U. S. A.* 109, 12398–12403. <https://doi.org/10.1073/pnas.1204330109>
- Muggeo, V.M., 2008. segmented: an R Package to Fit Regression Models with Broken-Line Relationships. *R news* 8, 20–25.
- Mukhlisin, M., Astuti, H.W., Wardihani, E.D., Matlan, S.J., 2021. Techniques for ground-based soil moisture measurement: a detailed overview. *Arab. J. Geosci.* <https://doi.org/10.1007/s12517-021-08263-0>
- Murphy, D.J., Dillon, P., O’ Donovan, M., Shalloo, L., Ruelle, E., 2024. Nitrate leaching on Irish grassland dairy farms: A review. *Eur. J. Agron.* 153, 127042. <https://doi.org/10.1016/j.eja.2023.127042>
- Naranjo-Lucena, A., Munita Corbalán, M.P., Martínez-Ibeas, A.M., McGrath, G., Murray, G., Casey, M., Good, B., Sayers, R., Mulcahy, G., Zintl, A., 2018. Spatial patterns of *Fasciola hepatica* and *Calicophoron daubneyi* infections in ruminants in Ireland and modelling of *C. daubneyi* infection. *Medical and Health Sciences* 1108 *Medical Microbiology* 07 *Agricultural and Veterinary Sciences* 0707 *Veterinary Science. Parasites and Vectors* 11, 1–13. <https://doi.org/10.1186/s13071-018-3114-z>
- Nativel, S., Ayari, E., Rodriguez-Fernandez, N., Baghdadi, N., Madelon, R., Albergel, C., Zribi, M., 2022. Hybrid Methodology Using Sentinel-1/Sentinel-2 for Soil Moisture Estimation. *Remote Sens.* 14, 2434. <https://doi.org/10.3390/rs14102434>
- Newell-Price, J.P., Whittingham, M.J., Chambers, B.J., Peel, S., 2013. Visual soil evaluation in relation to measured soil physical properties in a survey of grassland soil compaction in England and Wales. *Soil Tillage Res.* 127, 65–73. <https://doi.org/10.1016/j.still.2012.03.003>
- Nguyen, T.T., Ngo, H.H., Guo, W., Chang, S.W., Nguyen, D.D., Nguyen, C.T., Zhang, J., Liang, S., Bui, X.T., Hoang, N.B., 2022. A low-cost approach for soil moisture prediction using multi-sensor data and machine learning algorithm. *Sci. Total Environ.* 833, 155066. <https://doi.org/10.1016/j.scitotenv.2022.155066>
- O’ donovan, M., Ruelle, E., Egan, M., 2021. Grazing management to increase N use efficiency, Teagasc.
- Ojanen, P., Minkkinen, K., 2020. Rewetting Offers Rapid Climate Benefits for Tropical and Agricultural Peatlands But Not for Forestry-Drained Peatlands. *Global Biogeochem. Cycles* 34, e2019GB006503. <https://doi.org/10.1029/2019GB006503>
- Ojha, N., Merlin, O., Suere, C., Escorihuela, M.J., 2021. Extending the Spatio-Temporal Applicability of DISPATCH Soil Moisture Downscaling Algorithm: A Study Case Using SMAP, MODIS and Sentinel-3 Data. *Front. Environ. Sci.* 9, 40. <https://doi.org/10.3389/fenvs.2021.555216>
- Pandey, D.K., Putrevu, D., Misra, A., 2020. Large-scale soil moisture mapping using Earth observation data and its validation at selected agricultural sites over Indian region, in: *Agricultural Water Management: Theories and Practices*. Academic Press, pp. 185–207. <https://doi.org/10.1016/B978-0-12-812362-1.00010-2>

- Paul, C., Fealy, R., Fenton, O., Lanigan, G., O'Sullivan, L., Schulte, R.P.O., 2018. Assessing the role of artificially drained agricultural land for climate change mitigation in Ireland. *Environ. Sci. Policy* 80, 95–104. <https://doi.org/10.1016/j.envsci.2017.11.004>
- Pembleton, K.G., Rawnsley, R.P., Burkitt, L.L., 2013. Environmental influences on optimum nitrogen fertiliser rates for temperate dairy pastures. *Eur. J. Agron.* 45, 132–141. <https://doi.org/10.1016/j.eja.2012.09.006>
- Peng, J., Albergel, C., Balenzano, A., Brocca, L., Cartus, O., Cosh, M.H., Crow, W.T., Dabrowska-Zielinska, K., Dadson, S., Davidson, M.W.J., de Rosnay, P., Dorigo, W., Gruber, A., Hagemann, S., Hirschi, M., Kerr, Y.H., Lovergine, F., Mahecha, M.D., Marzahn, P., Mattia, F., Musial, J.P., Preuschmann, S., Reichle, R.H., Satalino, G., Silgram, M., van Bodegom, P.M., Verhoest, N.E.C., Wagner, W., Walker, J.P., Wegmüller, U., Loew, A., 2021. A roadmap for high-resolution satellite soil moisture applications – confronting product characteristics with user requirements. *Remote Sens. Environ.* <https://doi.org/10.1016/j.rse.2020.112162>
- Petropoulos, G.P., Griffiths, H.M., Dorigo, W., Xaver, A., Gruber, A., 2013. Surface Soil Moisture Estimation: Significance, Controls, and Conventional Measurement Techniques, in: *Remote Sensing of Energy Fluxes and Soil Moisture Content*. CRC Press, pp. 29–48. <https://doi.org/10.1201/b15610-7>
- Petropoulos, G.P., Ireland, G., Barrett, B., 2015. Surface soil moisture retrievals from remote sensing: Current status, products & future trends. *Phys. Chem. Earth.* <https://doi.org/10.1016/j.pce.2015.02.009>
- Pires, L.F., 2018. Soil analysis using nuclear techniques: A literature review of the gamma ray attenuation method. *Soil Tillage Res.* <https://doi.org/10.1016/j.still.2018.07.015>
- Piowarczyk, A., Giuliani, G., Holden, N.M., 2011. Can soil moisture deficit be used to forecast when soils are at high risk of damage owing to grazing animals? *Soil Use Manag.* 27, 255–263. <https://doi.org/10.1111/j.1475-2743.2011.00339.x>
- Powlson, D.S., Hart, P.B.S., Poulton, P.R., Johnston, A.E., Jenkinson, D.S., 1992. Influence of soil type, crop management and weather on the recovery of 15 N-labelled fertilizer applied to winter wheat in spring. *J. Agric. Sci.* 118, 83–100. <https://doi.org/10.1017/S0021859600068040>
- Qing, Y., Wang, S., Yang, Z.L., Gentile, P., 2023. Soil moisture–atmosphere feedbacks have triggered the shifts from drought to pluvial conditions since 1980. *Commun. Earth Environ.* 4, 1–10. <https://doi.org/10.1038/s43247-023-00922-2>
- Qiu, J., Crow, W.T., Wagner, W., Zhao, T., 2019. Effect of vegetation index choice on soil moisture retrievals via the synergistic use of synthetic aperture radar and optical remote sensing. *Int. J. Appl. Earth Obs. Geoinf.* 80, 47–57. <https://doi.org/10.1016/j.jag.2019.03.015>
- Rai, R.K., Singh, V.P., Upadhyay, A., 2017. Irrigation Scheduling, in: *Planning and Evaluation of Irrigation Projects*. pp. 385–412.
- Rasheed, M.W., Tang, J., Sarwar, A., Shah, S., Saddique, N., Khan, M.U., Imran Khan, M., Nawaz, S., Shamshiri, R.R., Aziz, M., Sultan, M., 2022. Soil Moisture Measuring Techniques and Factors Affecting the Moisture Dynamics: A Comprehensive Review. *Sustain.* <https://doi.org/10.3390/su141811538>
- Reinermann, S., Asam, S., Kuenzer, C., 2020. Remote sensing of grassland production and management-A review. *Remote Sens.* <https://doi.org/10.3390/rs12121949>
- Ribeiro, F.L., Guevara, M., Vázquez-Lule, A., Paula Cunha, A., Zeri, M., Vargas, R., 2021. The impact of drought on soil moisture trends across Brazilian biomes. *Nat. Hazards Earth Syst. Sci.* 21, 879–

892. <https://doi.org/10.5194/nhess-21-879-2021>

- Roberts, T.M., Colwell, I., Chew, C., Lowe, S., Shah, R., 2022. A Deep-Learning Approach to Soil Moisture Estimation with GNSS-R. *Remote Sens.* 14, 3299. <https://doi.org/10.3390/rs14143299>
- Robinson, D.A., Campbell, C.S., Hopmans, J.W., Hornbuckle, B.K., Jones, S.B., Knight, R., Ogden, F., Selker, J., Wendroth, O., 2008. Soil Moisture Measurement for Ecological and Hydrological Watershed-Scale Observatories: A Review. *Vadose Zo. J.* 7, 358–389. <https://doi.org/10.2136/vzj2007.0143>
- Robock, A., Vinnikov, K.Y., Srinivasan, G., Entin, J.K., Hollinger, S.E., Speranskaya, N.A., Liu, S., Namkhai, A., 2000. The Global Soil Moisture Data Bank. *Bull. Am. Meteorol. Soc.* 81, 1281–1299. [https://doi.org/10.1175/1520-0477\(2000\)081<1281:TGSMDB>2.3.CO;2](https://doi.org/10.1175/1520-0477(2000)081<1281:TGSMDB>2.3.CO;2)
- Rocha, A. V, Shaver, G.R., 2009. Advantages of a two band EVI calculated from solar and photosynthetically active radiation fluxes. *Agric. For. Meteorol.* 149, 1560–1563. <https://doi.org/10.1016/j.agrformet.2009.03.016>
- Rodrigues, C.I.D., Brito, L.M., Nunes, L.J.R., 2023. Soil Carbon Sequestration in the Context of Climate Change Mitigation: A Review. *Soil Syst.* <https://doi.org/10.3390/soilsystems7030064>
- Rosenbaum, U., Bogena, H.R., Herbst, M., Huisman, J.A., Peterson, T.J., Weuthen, A., Western, A.W., Vereecken, H., 2012. Seasonal and event dynamics of spatial soil moisture patterns at the small catchment scale. *Water Resour. Res.* 48. <https://doi.org/10.1029/2011WR011518>
- Rötzer, K., Montzka, C., Bogena, H., Wagner, W., Kerr, Y.H., Kidd, R., Vereecken, H., 2014. Catchment scale validation of SMOS and ASCAT soil moisture products using hydrological modeling and temporal stability analysis. *J. Hydrol.* 519, 934–946. <https://doi.org/10.1016/j.jhydrol.2014.07.065>
- Ruelle, E., Hennessy, D., Delaby, L., 2018. Development of the Moorepark St Gilles grass growth model (MoSt GG model): A predictive model for grass growth for pasture based systems. *Eur. J. Agron.* 99, 80–91. <https://doi.org/10.1016/j.eja.2018.06.010>
- Ryan, W., Hennessy, D., Murphy, J.J., Boland, T.M., Shalloo, L., 2011. A model of nitrogen efficiency in contrasting grass-based dairy systems. *J. Dairy Sci.* 94, 1032–1044. <https://doi.org/10.3168/jds.2010-3294>
- Saadeldin, M., O’Hara, R., Zimmermann, J., Mac Namee, B., Green, S., 2022. Using deep learning to classify grassland management intensity in ground-level photographs for more automated production of satellite land use maps. *Remote Sens. Appl. Soc. Environ.* 26, 100741. <https://doi.org/10.1016/j.rsase.2022.100741>
- Sadeghi, M., Babaeian, E., Tuller, M., Jones, S.B., 2017a. The optical trapezoid model: A novel approach to remote sensing of soil moisture applied to Sentinel-2 and Landsat-8 observations. *Remote Sens. Environ.* 198, 52–68. <https://doi.org/10.1016/j.rse.2017.05.041>
- Sadeghi, M., Jones, S.B., Philpot, W.D., 2015. A linear physically-based model for remote sensing of soil moisture using short wave infrared bands. *Remote Sens. Environ.* 164, 66–76. <https://doi.org/10.1016/j.rse.2015.04.007>
- Sadeghi, M., Tabatabaenejad, A., Tuller, M., Moghaddam, M., Jones, S.B., 2017b. Advancing NASA’s AirMOSS p-band radar root zone soil moisture retrieval algorithm via incorporation of richards’ equation. *Remote Sens.* 9, 17. <https://doi.org/10.3390/rs9010017>
- Salvucci, G.D., Entekhabi, D., 1994. Equivalent steady soil moisture profile and the time compression approximation in water balance modeling. *Water Resour. Res.* 30, 2737–2749.

<https://doi.org/10.1029/94WR00948>

- Santos, W.J.R., Silva, B.M., Oliveira, G.C., Volpato, M.M.L., Lima, J.M., Curi, N., Marques, J.J., 2014. Soil moisture in the root zone and its relation to plant vigor assessed by remote sensing at management scale. *Geoderma* 221–222, 91–95. <https://doi.org/10.1016/j.geoderma.2014.01.006>
- Schaap, M.G., Leij, F.J., 2000. Improved Prediction of Unsaturated Hydraulic Conductivity with the Mualem-van Genuchten Model. *Soil Sci. Soc. Am. J.* 64, 843–851. <https://doi.org/10.2136/sssaj2000.643843x>
- Schils, R.L.M., Bufe, C., Rhymer, C.M., Francksen, R.M., Klaus, V.H., Abdalla, M., Milazzo, F., Lellei-Kovács, E., Berge, H. ten, Bertora, C., Chodkiewicz, A., Dămătîrcă, C., Feigenwinter, I., Fernández-Rebollo, P., Ghiasi, S., Hejduk, S., Hiron, M., Janicka, M., Pellaton, R., Smith, K.E., Thorman, R., Vanwallegghem, T., Williams, J., Zavattaro, L., Kampen, J., Derkx, R., Smith, P., Whittingham, M.J., Buchmann, N., Price, J.P.N., 2022. Permanent grasslands in Europe: Land use change and intensification decrease their multifunctionality. *Agric. Ecosyst. Environ.* 330, 107891. <https://doi.org/10.1016/j.agee.2022.107891>
- Schulte, R.P.O., Diamond, J., Finkle, K., Holden, N.M., Brereton, A.J., 2005. Predicting the soil moisture conditions of Irish grasslands. *Irish J. Agric. Food Res.* 44, 95–110.
- Schulte, R.P.O., Fealy, R., Creamer, R.E., Towers, W., Harty, T., Jones, R.J.A., 2012. A review of the role of excess soil moisture conditions in constraining farm practices under Atlantic conditions. *Soil Use Manag.* <https://doi.org/10.1111/j.1475-2743.2012.00437.x>
- Schulte, R.P.O., Simo, I., Creamer, R.E., Holden, N.M., 2015. A note on the hybrid soil moisture deficit model v2.0. *Irish J. Agric. Food Res.* 54, 128–131. <https://doi.org/10.1515/ijafr-2015-0014>
- Schwen, A., Zimmermann, M., Bodner, G., 2014. Vertical variations of soil hydraulic properties within two soil profiles and its relevance for soil water simulations. *J. Hydrol.* 516, 169–181. <https://doi.org/10.1016/j.jhydrol.2014.01.042>
- Schwieger, S., Kreyling, J., Couwenberg, J., Smiljanić, M., Weigel, R., Wilmking, M., Blume-Werry, G., 2021. Wetter is Better: Rewetting of Minerotrophic Peatlands Increases Plant Production and Moves Them Towards Carbon Sinks in a Dry Year. *Ecosystems* 24, 1093–1109. <https://doi.org/10.1007/s10021-020-00570-z>
- Seneviratne, S.I., Corti, T., Davin, E.L., Hirschi, M., Jaeger, E.B., Lehner, I., Orlowsky, B., Teuling, A.J., 2010. Investigating soil moisture-climate interactions in a changing climate: A review. *Earth-Science Rev.* <https://doi.org/10.1016/j.earscirev.2010.02.004>
- Sensoterra, n.d. Single Depth Sensor | Sensoterra [WWW Document]. URL <https://www.sensoterra.com/en/product/single-depth-sensor/> (accessed 10.13.22).
- Shafian, S., Maas, S.J., 2015. Index of soil moisture using raw Landsat image digital count data in Texas High Plains. *Remote Sens.* 7, 2352–2372. <https://doi.org/10.3390/rs70302352>
- Sheng, W., Zhou, R., Sadeghi, M., Babaeian, E., Robinson, D.A., Tuller, M., Jones, S.B., 2017. A TDR Array Probe for Monitoring Near-Surface Soil Moisture Distribution. *Vadose Zo. J.* 16, 1–8. <https://doi.org/10.2136/vzj2016.11.0112>
- Simo, I., Creamer, R.E., Reidy, B., Jahns, G., Massey, P., Hamilton, B., Hannam, J.A., McDonald, E., Sills, P., Spaargaren, O., 2008. Irish Soil Information System.
- Singh, A., Gaurav, K., Meena, G.K., Kumar, S., 2020. Estimation of soil moisture applying modified Dubois model to Sentinel-1; A regional study from Central India. *Remote Sens.* 12, 2266.

<https://doi.org/10.3390/rs12142266>

- Sollenberger, L.E., Kohmann, M.M., Dubeux, J.C.B., Silveira, M.L., 2019. Grassland management affects delivery of regulating and supporting ecosystem services. *Crop Sci.*
<https://doi.org/10.2135/cropsci2018.09.0594>
- Stańczyk, T., Kasperska-Wołowicz, W., Szatyłowicz, J., Gnatowski, T., Papierowska, E., 2023. Surface Soil Moisture Determination of Irrigated and Drained Agricultural Lands with the OPTRAM Method and Sentinel-2 Observations. *Remote Sens.* 15, 5576.
<https://doi.org/10.3390/rs15235576>
- Stevanato, L., Baroni, G., Cohen, Y., Lino, F.C., Gatto, S., Lunardon, M., Marinello, F., Moretto, S., Morselli, L., 2019. A novel cosmic-ray neutron sensor for soil moisture estimation over large areas. *Agric.* 9, 202. <https://doi.org/10.3390/agriculture9090202>
- Sun, H., Liu, H., Ma, Y., Xia, Q., 2021. Optical remote sensing indexes of soil moisture: Evaluation and improvement based on aircraft experiment observations. *Remote Sens.* 13, 4638.
<https://doi.org/10.3390/rs13224638>
- Susha Lekshmi, S.U., Singh, D.N., Shojaei Baghini, M., 2014. A critical review of soil moisture measurement. *Meas. J. Int. Meas. Confed.*
<https://doi.org/10.1016/j.measurement.2014.04.007>
- Teagasc, 2022. Environment - Finding a suitable soil moisture range for safe field operations in grassland - Teagasc | Agriculture and Food Development Authority [WWW Document]. Teagasc. URL <https://www.teagasc.ie/news--events/daily/environment/finding-a-suitable-soil-moisture-range-for-safe-field-operations-in-grassland.php> (accessed 11.21.23).
- Teagasc, 2021a. Teagasc Heavy Soils Programme – Lessons Learned - Teagasc | Agriculture and Food Development Authority.
- Teagasc, 2021b. Moorepark Dairy Levy Research Update Teagasc heavy soils programme – lessons learned - A guide to the key findings of the Teagasc Heavy Soils Programme to-date, Teagasc.
- Teagasc, 2021c. Environment - Fertiliser advice under prolonged dry soil conditions - Teagasc | Agriculture and Food Development Authority [WWW Document]. URL <https://www.teagasc.ie/news--events/daily/environment/fertiliser-advice-under-prolonged-dry-soil-conditions.php> (accessed 6.19.23).
- Teagasc, 2021d. Environment - Nitrogen Use Efficiency = Cleaner Water - Teagasc | Agriculture and Food Development Authority [WWW Document]. Teagasc. URL <https://www.teagasc.ie/news--events/daily/environment/nitrogen-use-efficiency--cleaner-water.php> (accessed 12.21.23).
- Teagasc, 2021e. PastureBase Ireland [WWW Document]. URL <https://pasturebase.teagasc.ie/V2/login.aspx> (accessed 11.6.23).
- Teagasc, 2021f. Teagasc | Agriculture and Food Development Authority [WWW Document]. Teagasc. URL <https://www.teagasc.ie/news--events/daily/environment/agriculture-and-water.php> (accessed 12.7.23).
- Teagasc, 2021g. Factsheet No 2 [WWW Document]. Teagasc. URL <https://www.teagasc.ie/media/website/publications/2021/Early-Nitrogen-for-Spring-Grassland.pdf> (accessed 12.25.23).
- Teagasc, 2019. Teagasc (Irish Agriculture and Food Development Authority) [WWW Document]. Teagasc. https://doi.org/10.1007/978-1-349-95810-8_1128
- Teagasc, 2017. Teagasc - Agriculture in Ireland [WWW Document]. Teagasc. URL

- <https://www.teagasc.ie/rural-economy/rural-economy/agri-food-business/agriculture-in-ireland/> (accessed 2.17.24).
- Teagasc, 2014. Soil Associations [WWW Document]. EPA. URL <http://gis.teagasc.ie/soils/soilguide.php> (accessed 10.28.23).
- Teagasc, n.d. Pasture Base Ireland [WWW Document]. URL <https://pasturebase.teagasc.ie/>
- Terranimo [WWW Document], n.d. URL <https://terranimo.world/choose-a-region> (accessed 1.17.24).
- The R Foundation, 2018. R: The R Project for Statistical Computing [WWW Document]. URL <https://www.r-project.org/> (accessed 1.3.24).
- Topp, G.C., Davis, J.L., Annan, A.P., 1980. Electromagnetic determination of soil water content: Measurements in coaxial transmission lines. *Water Resour. Res.* 16, 574–582. <https://doi.org/10.1029/WR016i003p00574>
- Tripathi, A., Tiwari, R.K., 2022. Synergetic utilization of sentinel-1 SAR and sentinel-2 optical remote sensing data for surface soil moisture estimation for Rupnagar, Punjab, India. *Geocarto Int.* 37, 2215–2236. <https://doi.org/10.1080/10106049.2020.1815865>
- Tuohy, P., Fenton, O., Holden, N.M., Humphreys, J., 2015. The effects of treading by two breeds of dairy cow with different live weights on soil physical properties, poaching damage and herbage production on a poorly drained clay-loam soil. *J. Agric. Sci.* 153, 1424–1436. <https://doi.org/10.1017/S0021859614001099>
- Tuohy, P., O’ Loughlin, J., Peyton, D., Fenton, O., 2018. The performance and behavior of land drainage systems and their impact on field scale hydrology in an increasingly volatile climate. *Agric. Water Manag.* 210, 96–107. <https://doi.org/10.1016/j.agwat.2018.07.033>
- Tuohy, P., O’ Sullivan, L., Bracken, C.J., Fenton, O., 2023. Drainage status of grassland peat soils in Ireland: Extent, efficacy and implications for GHG emissions and rewetting efforts. *J. Environ. Manage.* 344, 118391. <https://doi.org/10.1016/j.jenvman.2023.118391>
- UN Water, 2022. Water, Food and Energy | UN-Water. UN Water.
- University of Minnesota Extension, 2021. Basics of irrigation scheduling | UMN Extension [WWW Document]. URL <https://extension.umn.edu/irrigation/basics-irrigation-scheduling#table-1-available-water-capacity-%28awc%29-by-soil-texture-1846610> (accessed 5.15.24).
- Urban, M., Berger, C., Mudau, T.E., Heckel, K., Truckenbrodt, J., Odipo, V.O., Smit, I.P.J., Schullius, C., 2018. Surface moisture and vegetation cover analysis for drought monitoring in the southern Kruger National Park using Sentinel-1, Sentinel-2, and Landsat-8. *Remote Sens.* 10, 1482. <https://doi.org/10.3390/rs10091482>
- Urraca, R., Gracia-Amillo, A.M., Koubli, E., Huld, T., Trentmann, J., Riihelä, A., Lindfors, A. V., Palmer, D., Gottschalg, R., Antonanzas-Torres, F., 2017. Extensive validation of CM SAF surface radiation products over Europe. *Remote Sens. Environ.* 199, 171–186. <https://doi.org/10.1016/j.rse.2017.07.013>
- USGS Earth Explorer [WWW Document], n.d. URL <https://earthexplorer.usgs.gov/>
- Vachaud, G., Passerat De Silans, A., Balabanis, P., Vauclin, M., 1985. Temporal Stability of Spatially Measured Soil Water Probability Density Function. *Soil Sci. Soc. Am. J.* 49, 822–828. <https://doi.org/10.2136/sssaj1985.03615995004900040006x>
- Vanderlinden, K., Vereecken, H., Hardelauf, H., Herbst, M., Martínez, G., Cosh, M.H., Pachepsky, Y.A.,

2012. Temporal Stability of Soil Water Contents: A Review of Data and Analyses. *Vadose Zo. J.* 11, vzj2011.0178. <https://doi.org/10.2136/vzj2011.0178>
- Vereecken, H., Huisman, J.A., Pachepsky, Y., Montzka, C., van der Kruk, J., Bogaen, H., Weihermüller, L., Herbst, M., Martinez, G., Vanderborght, J., 2014. On the spatio-temporal dynamics of soil moisture at the field scale. *J. Hydrol.* 516, 76–96. <https://doi.org/10.1016/j.jhydrol.2013.11.061>
- Vero, S.E., Antille, D.L., Lalor, S.T.J., Holden, N.M., 2014. Field evaluation of soil moisture deficit thresholds for limits to trafficability with slurry spreading equipment on grassland. *Soil Use Manag.* 30, 69–77. <https://doi.org/10.1111/sum.12093>
- Verrot, L., Geris, J., Gao, L., Peng, X., Oyesiku-Blakemore, J., Smith, J.U., Hodson, M.E., Zhang, G., Hallett, P.D., 2019. A simple modelling framework for shallow subsurface water storage and flow. *Water (Switzerland)* 11, 1725. <https://doi.org/10.3390/w11081725>
- Wagner, W., Hahn, S., Kidd, R., Melzer, T., Bartalis, Z., Hasenauer, S., Figa-Saldaña, J., De Rosnay, P., Jann, A., Schneider, S., Komma, J., Kubu, G., Brugger, K., Aubrecht, C., Züger, J., Gangkofner, U., Kienberger, S., Brocca, L., Wang, Y., Blöschl, G., Eitzinger, J., Steinnocher, K., Zeil, P., Rubel, F., 2013. The ASCAT soil moisture product: A review of its specifications, validation results, and emerging applications. *Meteorol. Zeitschrift.* <https://doi.org/10.1127/0941-2948/2013/0399>
- Wagner, W., Lemoine, G., Rott, H., 1999. A method for estimating soil moisture from ERS Scatterometer and soil data. *Remote Sens. Environ.* 70, 191–207. [https://doi.org/10.1016/S0034-4257\(99\)00036-X](https://doi.org/10.1016/S0034-4257(99)00036-X)
- Wagner, W., Pathe, C., Doubkova, M., Säbel, D., Bartsch, A., Hasenauer, S., Blöschl, G., Scipal, K., Martínez-Fernández, J., Löw, A., 2008. Temporal stability of soil moisture and radar backscatter observed by the Advanced Synthetic Aperture Radar (ASAR). *Sensors* 8, 1174–1197. <https://doi.org/10.3390/s80201174>
- Walker, J.P., Willgoose, G.R., Kalma, J.D., 2004. In situ measurement of soil moisture: A comparison of techniques. *J. Hydrol.* 293, 85–99. <https://doi.org/10.1016/j.jhydrol.2004.01.008>
- Wang, A., Lettenmaier, D.P., Sheffield, J., 2011. Soil moisture drought in China, 1950–2006. *J. Clim.* 24, 3257–3271. <https://doi.org/10.1175/2011JCLI3733.1>
- Wang, Q., Li, J., Jin, T., Chang, X., Zhu, Y., Li, Y., Sun, J., Li, D., 2020. Comparative analysis of Landsat-8, Sentinel-2, and GF-1 data for retrieving soil moisture over wheat farmlands. *Remote Sens.* 12, 2708. <https://doi.org/10.3390/RS12172708>
- Wang, S., Fu, G., 2023. Modelling soil moisture using climate data and normalized difference vegetation index based on nine algorithms in alpine grasslands. *Front. Environ. Sci.* 11, 1130448. <https://doi.org/10.3389/fenvs.2023.1130448>
- West, H., Quinn, N., Horswell, M., White, P., 2018. Assessing vegetation response to soil moisture fluctuation under extreme drought using sentinel-2. *Water (Switzerland)* 10, 838. <https://doi.org/10.3390/w10070838>
- World Meteorological Organisation, 2024. Drought [WWW Document]. URL <https://wmo.int/topics/drought> (accessed 5.15.24).
- Wu, X., Ma, W., Xia, J., Bai, W., Jin, S., Calabria, A., 2021. Spaceborne gnss-r soil moisture retrieval: Status, development opportunities, and challenges. *Remote Sens.* 13, 1–24. <https://doi.org/10.3390/rs13010045>
- Xu, C., Qu, J.J., Hao, X., Cosh, M.H., Prueger, J.H., Zhu, Z., Gutenberg, L., 2018. Downscaling of surface soil moisture retrieval by combining MODIS/Landsat and in situ measurements. *Remote Sens.*

10, 210. <https://doi.org/10.3390/rs10020210>

- Yang, P., Verhoef, W., van der Tol, C., 2017. The mSCOPE model: A simple adaptation to the SCOPE model to describe reflectance, fluorescence and photosynthesis of vertically heterogeneous canopies. *Remote Sens. Environ.* 201, 1–11. <https://doi.org/10.1016/j.rse.2017.08.029>
- Yilmaz, M.T., Hunt, E.R., Jackson, T.J., 2008. Remote sensing of vegetation water content from equivalent water thickness using satellite imagery. *Remote Sens. Environ.* 112, 2514–2522. <https://doi.org/10.1016/j.rse.2007.11.014>
- Yu, T., Ran, Q., Pan, H., Li, J., Pan, J., Ye, S., 2023. The impacts of rainfall and soil moisture to flood hazards in a humid mountainous catchment: a modeling investigation. *Front. Earth Sci.* 11, 1285766. <https://doi.org/10.3389/feart.2023.1285766>
- Zhang, D., Zhou, G., 2016. Estimation of soil moisture from optical and thermal remote sensing: A review. *Sensors (Switzerland)*. <https://doi.org/10.3390/s16081308>
- Zhang, L., Ji, L., Wylie, B.K., 2011. Response of spectral vegetation indices to soil moisture in grasslands and shrublands. *Int. J. Remote Sens.* 32, 5267–5286. <https://doi.org/10.1080/01431161.2010.496471>
- Zhang, S., Shao, M., 2017. Temporal stability of soil moisture in an oasis of northwestern China. *Hydrol. Process.* 31, 2725–2736. <https://doi.org/10.1002/hyp.11200>
- Zhang, Y., Liang, S., Zhu, Z., Ma, H., He, T., 2022. Soil moisture content retrieval from Landsat 8 data using ensemble learning. *ISPRS J. Photogramm. Remote Sens.* 185, 32–47. <https://doi.org/10.1016/j.isprsjprs.2022.01.005>
- Zhao, Z., Shen, Y., Wang, Q., Jiang, R., 2020. The temporal stability of soil moisture spatial pattern and its influencing factors in rocky environments. *Catena* 187, 104418. <https://doi.org/10.1016/j.catena.2019.104418>
- Zhou, S., Williams, A.P., Lintner, B.R., Berg, A.M., Zhang, Y., Keenan, T.F., Cook, B.I., Hagemann, S., Seneviratne, S.I., Gentile, P., 2021. Soil moisture–atmosphere feedbacks mitigate declining water availability in drylands. *Nat. Clim. Chang.* 11, 38–44. <https://doi.org/10.1038/s41558-020-00945-z>
- Zhuang, R., Manfreda, S., Zeng, Y., Su, Z., Dor, E. Ben, Petropoulos, G.P., 2023. Soil moisture monitoring using unmanned aerial system, in: *Unmanned Aerial Systems for Monitoring Soil, Vegetation, and Riverine Environments*. Elsevier, pp. 179–200. <https://doi.org/10.1016/B978-0-323-85283-8.00003-5>
- Zhuo, W., Huang, J., Li, L., Zhang, X., Ma, H., Gao, X., Huang, H., Xu, B., Xiao, X., 2019. Assimilating Soil Moisture Retrieved from Sentinel-1 and Sentinel-2 Data into WOFOST Model to Improve Winter Wheat Yield Estimation. *Remote Sens.* 11, 1618. <https://doi.org/10.3390/RS11131618>

Appendix

Table A 1: All S-2 passes for Rossmore and Stradone used in the study. Dates in bold are those used in the validation with in situ VSM sensors

Year	Rossmore Dates (DD/MM)	Stradone Dates (DD/MM)
2015		29/09
2017	01/01, 20/06, 08/09, 07/11	01/01, 20/06, 07/11, 27/12
2018	10/02, 21/04, 06/05, 16/05, 25/06, 30/06, 10/07, 18/10, 28/10, 07/12, 12/12	06/01, 20/02, 25/02, 21/04, 10/07
2019	16/01, 07/03, 18/09	10/02, 18/09, 28/10
2020	20/02, 01/03, 06/03, 15/04, 12/10	25/04, 27/09, 06/11
2021	25/01, 01/03, 26/03, 10/04, 25/04, 05/05, 29/06, 19/07, 07/09, 21/11, 26/11	16/03, 25/04, 29/06, 28/08, 07/09, 21/11
2022	16/03, 26/03, 31/03	14/02, 01/03, 21/03, 26/03, 20/04, 10/05

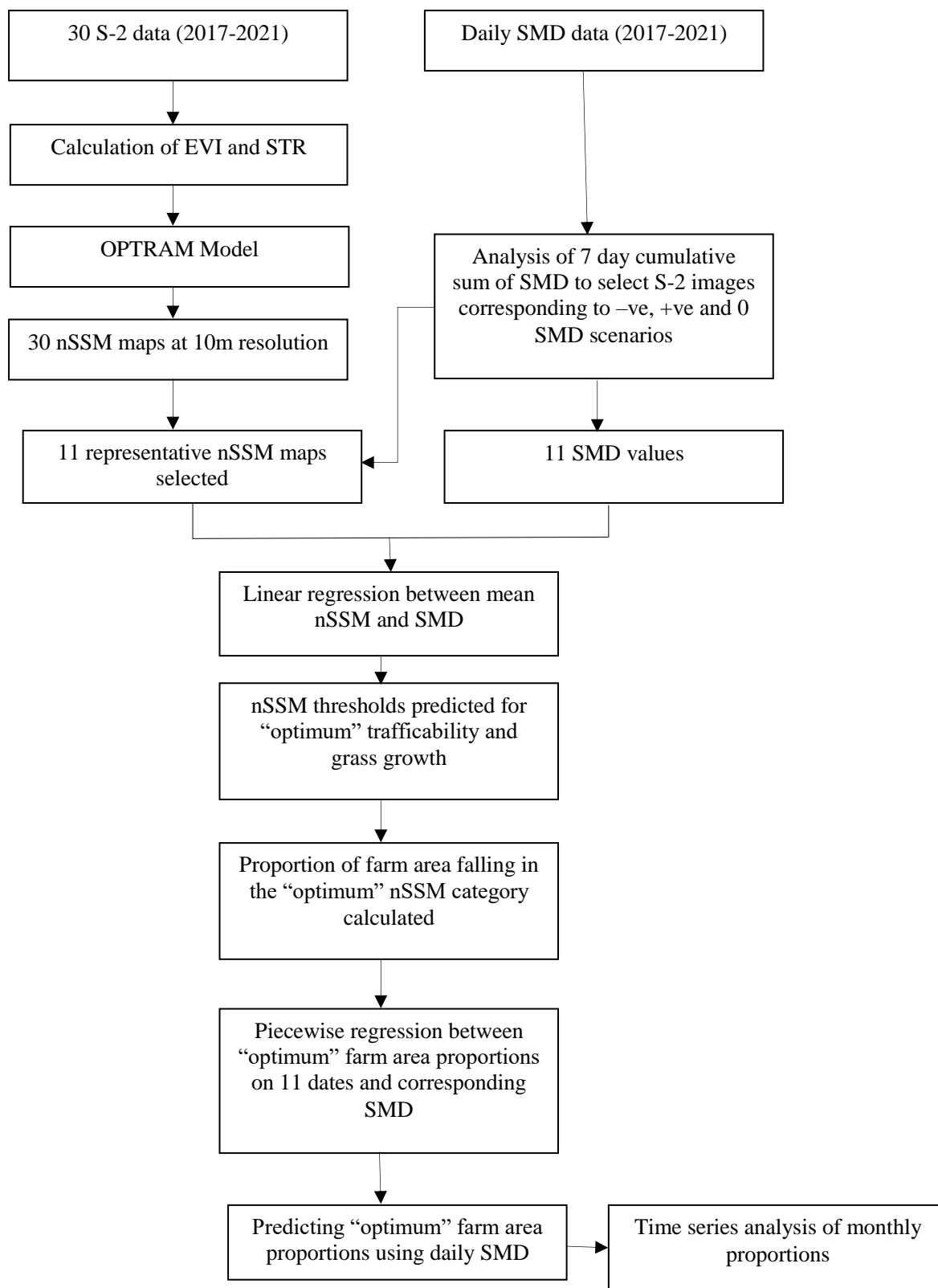


Figure A 1: Flowchart of methodology (Chapter 3)

Summary of Research Outputs

This thesis comprises of three research articles, of which two are published and one is under review.

- Chapter 2 was published in *Remote Sensing* (IF 5.0). As lead author, I wrote the original draft of the paper and contributed to review and editing of final version of the paper. I was responsible for data curation, formal analysis, investigation and visualisation.
- Chapter 3 was published in *Frontiers in Environmental Science* (IF 4.6). As lead author, I wrote the original draft of the paper and contributed to review and editing of final version of the paper. I contributed towards conceptualisation, software, data curation, formal analysis, investigation and visualisation.
- Chapter 4 is currently under review. As lead author, I wrote the original draft of the paper and contributed to review and editing of final version of the paper. I contributed towards conceptualisation, software, data curation, formal analysis, investigation and visualisation.

Journal Publications:

Basu, R., Daly, E., Brown, C., Shnel, A., Tuohy, P., 2024a. Temporal Stability of Grassland Soil Moisture Utilising Sentinel-2 Satellites and Sparse Ground-Based Sensor Networks. *Remote Sens.* 16, 220. <https://doi.org/10.3390/RS16020220>

Basu, R., Fenton, O., Daly, E., Tuohy, P., 2024b. Identifying favourable conditions for farm scale trafficability and grass growth using a combined Sentinel-2 and soil moisture deficit approach. *Front. Environ. Sci.* In press. <https://doi.org/10.3389/fenvs.2024.1331659>

Basu, R., Fenton, O., Daly, E., Tuohy, P. Retrospective examination of fertilizer application decisions on a heavy textured dairy farm using paddock specific management records, in-situ weather and soil moisture threshold maps. (under review)

Conferences:

Basu, R., Brown, C., Tuohy, P., and Daly, E., Estimating high resolution surface soil moisture using Sentinel-2 and identifying optimum conditions of trafficability and grass growth on Irish farms, AGU Fall Meeting 2023, 11-15 December 2023, (Oral presentation e lightning).

Basu, R., Brown, C., Tuohy, P., and Daly, E., Estimating surface soil moisture in Ireland at high resolution using Sentinel 2 and a modified OPTRAM model, Environ 2023, 03-05 April 2023, ATU Donegal (Oral presentation).

Basu, R., Brown, C., Tuohy, P., and Daly, E., Estimating high resolution surface soil moisture from Sentinel 2 and a modified OPTRAM model, VistaMilk Industry Day, Teagasc, 07 December 2022. (Oral presentation)

Basu, R., Brown, C., Tuohy, P., and Daly, E., Estimating high resolution surface soil moisture in Ireland using Sentinel 2 and a modified OPTRAM model, Irish Earth Observation Symposium, 03-04 November 2022, TU Dublin (Oral presentation)

Basu, R., Brown, C., Tuohy, P., and Daly, E., Estimating surface soil moisture from Sentinel 2: A modified OPTRAM approach, VistaMilk Internal Conference, Teagasc, 09-10 May 2022. (Oral presentation)

Basu, R., Brown, C., Tuohy, P., and Daly, E., Characterising soil moisture regimes on poorly drained soils in Ireland using optical satellite derived vegetation indices and the OPTRAM model, EGU General Assembly 2021, online, 19–30 April 2021, EGU21-3336, <https://doi.org/10.5194/egusphere-egu21-3336>, 2021. (vPICO presentation)

Basu, R., Brown, C., Tuohy, P., and Daly, E., A remote Sensing Approach to Characterising Soil Moisture Regimes on Poorly Drained Soils in Ireland, AGU Fall meeting 2020, online, 1–17 December 2020. (poster presentation)

Basu, R., Brown, C., Tuohy, P., and Daly, E., Characterising Soil Moisture Regimes on poorly Drained Soils in Ireland using Remote Sensing Indices, VistaMilk Internal Conference, Teagasc, 10th March 2021. (oral presentation)

Basu, R., Daly, E., Fenton, O., Tuohy, P., Remote Sensing, GIS and Machine Learning Approaches to aid Soil Characterisation and Drainage Design, 64th Irish Geological Research Meeting, Athlone, Ireland, 25-26 Feb 2020. (poster presentation)

Other science communications:

Article in RTE Brainstorm (<https://www.rte.ie/brainstorm/2022/0915/1323524-satellite-images-soil-monitoring/>)

Teagasc VistaMilk podcast “Soil from Space” (<https://www.vistamilk.ie/podcasts/>)

Paper acknowledgements

The research in this thesis and the corresponding papers/articles were financially supported by Vista Milk SFI Research Centre, Teagasc, Science Foundation Ireland (SFI) and the Department of Agriculture, Food and Marine on behalf of the Government of Ireland under Grant Number [16/RC/3835]. The authors thank the farmers involved who provided land access, time and resources for the study.